Biogeomorphological aspects within tidal sand wave fields

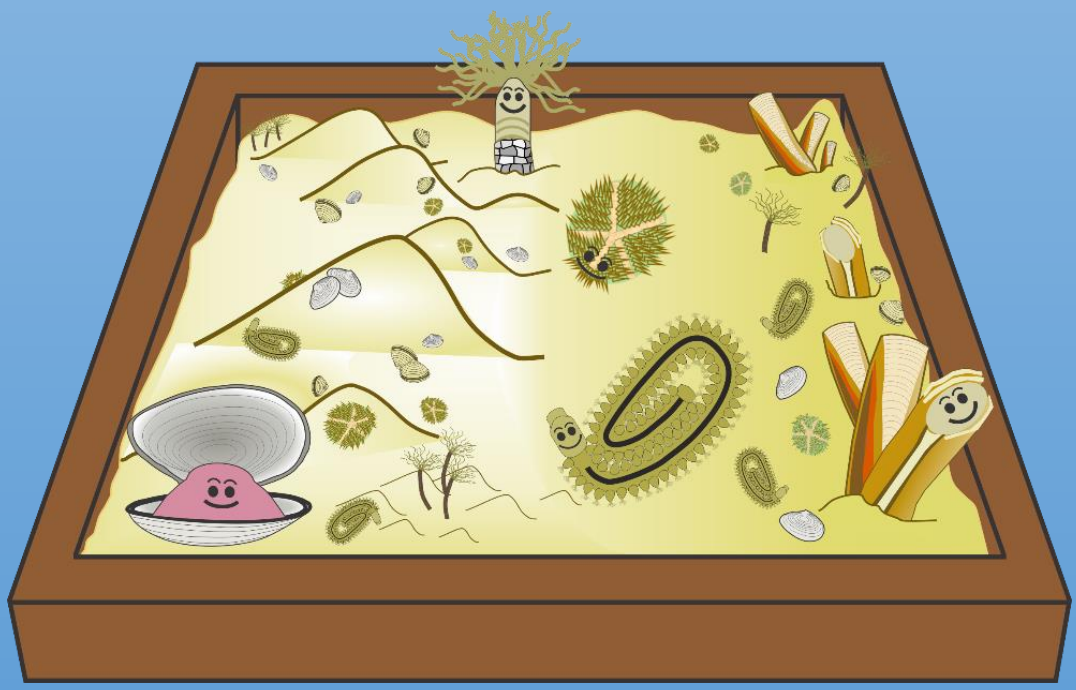

Chiu H. Cheng

Biogeomorphological aspects within tidal sand wave fields

Promoter: Karline Soetaert

Promoter: Bas. W. Borsje

Dissertation submitted in fulfillment of the requirements for the degree of Doctor (Ph.D.) in Science: Marine Sciences

By Chiu H. Cheng

Chiu H. Cheng (2021)
Title: Biogeomorphological aspects within tidal sand wave fields
PhD thesis: Ghent University

The research presented in this PhD thesis was a part of the research program SANDBOX (Smart and sustainable design for offshore operations in a sandy seabed), under the project number 871.15.011. It was partially funded by the Dutch Research Council (NWO) and Royal Boskalis Westminster N.V.

Cover design: Chiu H. Cheng
Printed by: Reproduct

Members of the examination committee

Prof. Dr. Tom Moens (Chair)
Ghent University

Prof. Dr. Karline Soetaert (Promoter)
Department of Estuarine and Delta Systems
Royal Netherlands Institute for Sea Research

Prof. Dr. ir. Bas W. Borsje (Promoter)
Water Engineering and Management
University of Twente

Dr. ir. Martin Baptist
Wageningen University & Research

Dr. Ulrike Braeckman (Secretary)
Ghent University

Prof. Dr. Steven Degraer
Royal Belgian Institute of Natural Sciences (RBINS)/Ghent University

Prof. Dr. Peter Herman
Delft University of Technology

Prof. Dr. Vera Van Lancker
Royal Belgian Institute of Natural Sciences (RBINS)/Ghent University

Table of Contents

Chapter 1 General Introduction

Photo by Chiu H. Cheng

1.1 Introduction

1.1.1 A Shallow shelf sea environment

The North Sea is a marginal body of water that is located on the European continental shelf, connecting with the Atlantic Ocean to the north, at the Norwegian Sea, and through the English Channel to the south. The surface area is approximately 575,000 km^2, with a water volume of 54,000 km^3. The mean water depth is approximately 94 m, but the range is quite variable, with areas as shallow as 20 m or less in the central part of the North Sea (e.g., Dogger Bank) to over 700 m at the Skagerrak near the Norwegian channel (OSPAR quality report 2000). Moreover, the North Sea is a highly important economic area as it is extensively utilized for activities such as fishing, recreation, shipping, oil and gas production, sand mining and offshore renewable energy production, nature conservation, among others (Bergman and Santbrink 2000; Huettel and Webster 2001; Baptist et al. 2006; Reiss et al. 2010; Jongbloed et al. 2014; de Jong et al. 2016; Schultze and Nehls 2017; de Vrees 2019).

Within this marine system, the Dutch sector of the North Sea makes up roughly a tenth of the total area, at 57,000 km^2 and with water depths ranging from 0 to 71 m (Borsje et al. 2009b). It has long been an area of high socio-economic importance for the Netherlands and, consequently, subjected to human activities. The earliest ones were particularly from fishing and shipping, but more recently, especially in the last several decades, also from dredging and disposal as well as harbor extensions. In just the Netherlands alone, 24 million m^3 of sand are extracted each year for beach nourishment and coastal protection projects. Demands are expected to rise to 40-85 million m^3 per year due to concerns about rising sea levels (Deltacommissie 2008). Thus, the amount of human activities is anticipated to further increase in the foreseeable future to address these needs (Deltacommissie 2008; Stolk and Dijkshoorn 2009; de Jong et al. 2014b, 2015b; a, 2016; ICES 2014).

Furthermore, the combination of the threats from global climate change and the huge economic expansion in the western world in general, has led to an unprecedented trend of energy expansion into the coastal seas. As a result, there has been an increasing emphasis on shifting wind energy installations (e.g., Offshore Wind Farms, OWFs) to the offshore areas (Halpern et al. 2015). Currently, sustainable energy-related activities are one of the more-important endeavors with regards to offshore construction activity (de Vrees 2019). The allocation of offshore regions to these OWFs is estimated to increase from the present 0.2 percent to anywhere from 8 to 22 percent of the total area of the Dutch sector by 2050, not to mention the additional coverage needed for the cable connections (https://www.derijkenoordzee.nl/onze-visie). Such large footprint requirements of these installations present new and additional challenges to the other offshore activities, and there are important environmental, social and economic implications (Kannen and Burkhard 2009).

1.1.2 Sediment dynamics and geomorphology

The marine seabed environments, particularly in the shallow seas, are dynamic regions. Offshore sandy environments quite often contain a variety of seabed features and bedforms, and the Dutch North Sea is no exception. Among these features are the rhythmic, sinusoidal bedforms, which are often superimposed on the bare seafloor. These structures range from small sand ripples of less than 1 m in wavelength and a height of 0.01 m to the very large tidal sandbanks which can reach several km in length and 10 m or more in height (Morelissen et al. 2003, Knaapen 2005; Table 1.1). Between these extremes are several other common micro- and meso-scale bedforms such as megaripples and sand waves. The combination between the predominant hydrodynamic

forces and the presence of these bottom protrusions will invariably cause differential sediment sorting (Venditti 2013; Lefebvre et al. 2016). The result is then, a cascading effect of sediment motion, deposition and ultimately, sorting, all of which pose significant implications for the spatio-temporal evolution of the ensuing bedforms (Blondeaux 2012), depending on the location in question. But despite the resemblance in form, not all of these bedforms are equally comparable in behavior. Ripples and sand waves, in particular, are among the more-dynamic features, commonly found in shallow seas and thus, carry important implications for the evolution of the seabed (Baas and De Koning 1995; Németh et al. 2002; Knaapen 2005; Van Oyen et al. 2011; Bartholdy et al. 2015).

Table 1.1. Dimensions of common bedforms in offshore sandy environments: L = wavelength, H = height (Knaapen 2005; Liao and Yu 2005; Barnard et al. 2006).

Bedform	***L* (m)**	***H* (m)**
Ripples	0.1 - 1	0.01 or more
Megaripples	10	0.1 or more
Sand waves	100 - 1000	1 - 10
Long bed waves	1500	5
Shoreface connected ridges	4000	5
Tidal sandbanks	5000 - 6000	10 or more

Ripples are perhaps the most ubiquitous sinusoidal features on the earth's surface, particularly in the sandy marine environment (Bartholdy et al. 2015). They form within an optimal range of sediment grain sizes (up to 0.8 mm) and at flow speeds that exceed the threshold of motion yet fall within velocities that do not completely wash out the ripples and leave a flat bed with intense sheet flow of sediment movement (Soulsby 1997; Precht and Huettel 2003). They are found in both the very shallow, coastal zones as well as in deeper waters of tens of meters or more, but are either wave-generated or current-generated (Figure 1.1). In the case of wave ripple formation, the orbital motion of the wave interacts with the seabed in areas shallow enough for it to reach the bottom, causing disturbances and subsequent movement of sand. As the surface waves induce oscillatory flows near the bottom, a steady stream of recirculating cells creates a series of symmetrical, parallel ridges perpendicular to the direction of the propagating waves (Nelson et al. 2013). In contrast, where the water motion is dominated by unidirectional flow (e.g., ocean currents, turbidity currents and rivers), the resulting separation of the boundary layer on the seabed

produces current ripples (Lapôtre et al. 2017). Here, the eroding grains are pushed up on the gentler (stoss) side of the ripple towards the crest, while the gravitational forces cause the grains to avalanche down the steeper (lee) side. The descent of the grains have a tendency to settle close to the maximum critical slope (angle of repose, typically around 32° for sand) that a given sediment grain mixture can sustain (van Rijn et al. 1993; Soulsby 1997; Betat et al. 2002; van Rijn 2007; Nelson et al. 2013). Because these ripples are mainly formed by near-bed flow in the viscous sublayer, they are far less depth-dependent compared to wave-generated ripples (Stride et al. 1982; Cheel 2005; Lapôtre et al. 2017). This ensuing roughness on the seabed is significant in enhancing sediment suspension while also affecting the turbulence within the benthic boundary layer (Grant and Madsen 1986), particularly in wave-induced ripples.

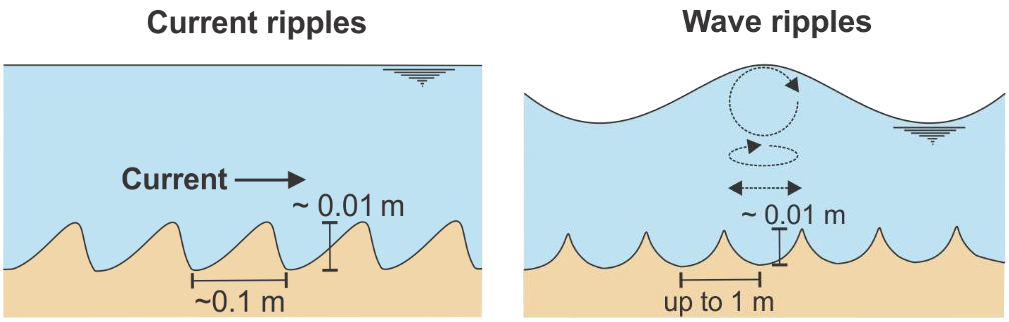

Figure 1.1. The two primary types of ripples, and the physical processes that generate them (based on Soulsby 1997).

Sand waves are meso-scale bedforms that are mostly found between 100 and 1000 meters in wavelength, and one to five meters in height (Figure 1.2; van Dijk and Kleinhans 2005; Besio et al. 2008; Borsje et al. 2014b; Cheng et al. 2020), although they can grow up to 10 meters in environments with exceptionally high currents (Liao and Yu 2005; Hanes 2012). While they are less common than the much-smaller ripples, they are very ubiquitous in certain shelf seas around the world, and are especially prevalent in certain parts of the North Sea. A distinguishing feature about sand waves, in contrast to other meso or macro-scale bedforms, is their ability to move with significant speed. This occurs largely as a result of a tidal asymmetry. The dissipation of wave or tidal energy results in seabed instability which, among other physical forces, drives sand wave growth from the trough towards the crest (e.g., net sediment transport) in the direction of the residual current (Hulscher 1996; van der Veen et al. 2006; Van Oyen and Blondeaux 2009a). This results in sand wave migration on the order of several meters or more per year (Németh et al.

2002; Besio et al. 2008; van Gerwen et al. 2018). Moreover, ripples and megaripples have often been found superimposed on certain parts of sand waves (Stride et al. 1982; Damveld et al. 2018), making the latter even more (unevenly) dynamic from a sedimentary perspective.

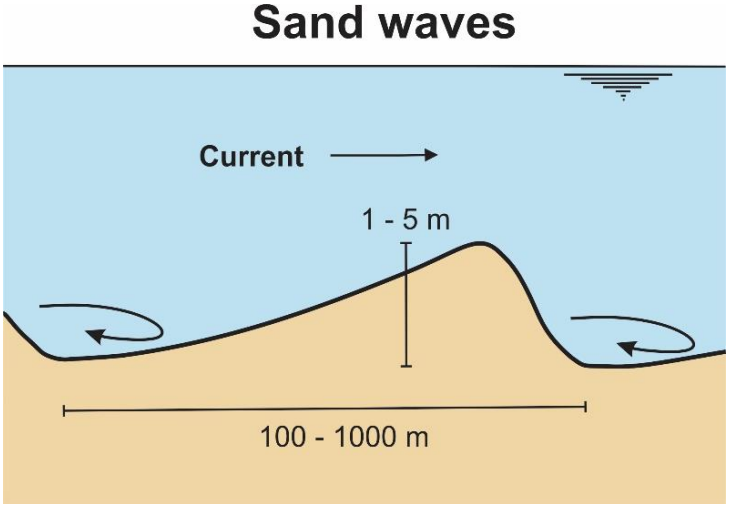

Figure 1.2. Schematic of a tidally-driven, asymmetrical sand wave (based on Soulsby 1997). In very extreme environments, sand waves can reach up to 10 m in height.

For these reasons, sand waves are not only of interest from an ecological or physical perspective, but also have socio-economic implications. On the one hand, they pose many potential challenges for coastal development and raise concerns about the integrity of offshore construction and infrastructure such as cables and pipelines (Roetert et al. 2017). On the other hand, sand waves are often located in areas of high economic activity, making them susceptible to impacts from human activities such as sand mining, offshore wind construction, fishing or other actions that physically disturb the seafloor (Bergman and Hup 1992; van Dalfsen and Essink 2001; Kaiser et al. 2002; Van Oyen et al. 2011; Jongbloed et al. 2014). This is especially concerning for coastal management, given the current projections for the ever-increasing number and intensity of offshore activities (de Jong et al. 2016; de Vrees 2019). Sand wave environments are difficult to study *in situ*, given the logistical challenges of field sampling (Best and Kostaschuk 2002; Kleinhans et al. 2009; Janssen et al. 2012). As a result, the available ones are from modeling studies since sand waves, unlike the smaller bedforms, are too large to directly study in lab flumes (Stride et al. 1982). While these have allowed for accurate predictions about sand wave movement, occurrence and development, they also tended to focus on the physical and hydrodynamic

processes and assume uniformity in bed characteristics, among other limitations (Besio et al. 2008; Borsje et al. 2009b; van Santen et al. 2011; Damveld et al. 2019). Thus, there are still many knowledge gaps concerning sand wave dynamics and the interrelations with other biogeomorphological processes, as well as the shorter- and longer-term impacts from disturbances.

1.1.2.1 Offshore zone

The offshore parts of the Dutch North Sea contain regions that are highly energetic. Here you will find common bedforms such as the meso-scale sand waves (Baptist et al. 2006; Besio et al. 2008; de Jong et al. 2015b). Because of the hydrodynamic conditions required to form them, most are predominantly located in shallow, tidally-dominated environments at water depths of 20-50 m (Figure 1.3), but well beyond the nearshore zone (Besio et al. 2008; van Santen et al. 2011). Nevertheless, they are very ubiquitous in the Dutch sector and found over a wide range of dimensions and shape (e.g., symmetries), becoming increasing asymmetric towards the coast and to the central and northern regions (Damen et al. 2018; Cheng et al. 2020).

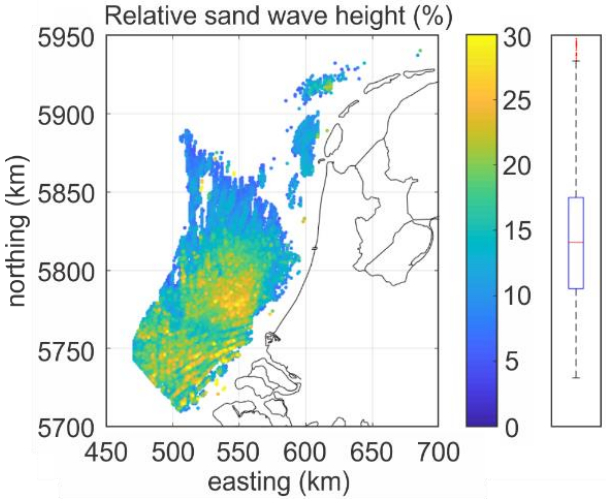

Figure 1.3. Sand wave distribution in the Dutch North Sea, with heights relative to the water depth; boxplot shows the mean (red line) and standard deviation (blue box). Data taken from Damen et al. 2018.

Similar to the ripples, the larger sand waves can also have a profound impact on the physical characteristics of the sediment. The morphology of the sand wave (level of asymmetry), together with other small-scale bottom protrusions and roughness, can influence the local

hydrodynamics in ways that result in sediment sorting (Venditti 2013; Lefebvre et al. 2016), which causes a further shift in the spatio-temporal development of various bedforms (Blondeaux 2012). While past studies have shown that the sediment composition contrasts considerably along sand waves (van Dijk and Kleinhans 2005; Baptist et al. 2006), more recent ones have demonstrated that such patterns of sediment distribution closely follow bed topography (Damveld et al. 2019; Cheng et al. 2020).

1.1.3 Benthic communities and ecological functioning

Living within these sediments are an important group of benthic-dwelling animals known as macrofauna, or macrobenthos, which are invertebrate organisms greater than 1.0 mm in size. They are responsible in driving many benthic marine ecosystem processes such as secondary production as well as geochemical conditions (Snelgrove 1998, Heip et al. 2001, Carlson et al. 1997) and can influence the surrounding landscape-forming processes. This two-way interaction between the biota and sediment dynamics is termed biogeomorphology (Viles 1988; Borsje et al. 2008; Bouma et al. 2013). Macrofauna have long been utilized in comparative studies of spatio-temporal changes in benthic ecosystems due to their low mobility, in contrast to more-mobile fauna such as demersal fish that have the ability to avoid unfavorable conditions or environmental disturbances (Rees et al. 2007). Furthermore, since many of the infauna organisms residing in the sediment are also relatively long-lived and rather sessile, they are well suited for comparative, spatio-temporal studies on benthic ecosystem and environmental changes (Pearson and Rosenberg 1977; Gray and Elliott 2009; Reiss et al. 2010).

Many efforts in the past have been undertaken to characterize large parts of the North Sea, of which the North Sea Benthos Survey (NSBS) from 1986 remains one of the most comprehensive sampling efforts to date. From this survey, the North Sea has been divided into three distinct habitat types (northern, central and southern; Heip et al. 1992). The Dutch sector falls entirely within the southern region, and can further be subdivided into two distinct habitats: the muddier, taxonomically-richer north, and the sandier, less species-rich south (Duineveld et al. 1990). Oftentimes, the specific benthic assemblages found in the North Sea are due to various environmental factors including sediment composition, silt content, water depth, current, temperature, chlorophyll *a* (chl *a*) content and latitude, etc. (Heip et al. 1992; de Jong et al. 2014b, 2015b). There is evidence that at both regional and local spatial scales, the benthic composition is

largely influenced by physical habitat characteristics such as bottom topography and substratum type (Cadée 1976; Reiss et al. 2010).

The macrofauna cover a wide variety of taxonomic and functional groups, feeding behaviors and occur at various densities and sizes. Some species of benthic organisms which are particularly important, either merely by their physical presence or through behavioral activity, both of which can alter the erosional processes in the surficial sediment layer, have been termed ecosystem engineers (Jones et al. 1997; Meysman et al. 2006). Animals that actively transform the state of their surrounding biotic and abiotic materials (e.g., the geochemical environment) are called allogenic ecosystem engineers, while those that influence their surrounding through their physical presence and/or the creation of physical structures or dense aggregations (e.g., habitat provisioning) are autogenic engineers (Jones et al. 1994, 1997; Bouma et al. 2005). One of the most significant influences on sediment mixing is bioturbation, where the benthos continuously disrupt the sediment grain distribution (Meysman et al. 2006; Jones 2012; Kristensen et al. 2012). Another related process is bioirrigation, where the benthos, through their feeding or movement, facilitate solute exchange between the pore and overlying waters, either actively or passively (Kristensen et al. 2012; De Borger et al. 2020).

Depending on how they affect the sediment distribution and local hydrodynamic flow, and thus the critical erosion threshold of soft-bottom surfaces, they can either be considered as bio-stabilizers or bio-destabilizers (Li et al. 2017, Widdows & Brinsley 2002). An example of enhanced stability is from diatoms that produce mucus compounds such as extracellular polymeric substances (EPS), which binds the particles, thereby reducing the rate of erosion (Paterson 1989; Meadows et al. 2012). Similarly, large aggregations of tube-building worms can also stabilize the surrounding conditions by reducing the flow and also the rates of sediment resuspension, often in conjunction with the microorganisms in the seabed (Krasnow and Taghon 1997; Borsje et al. 2014b). On the other hand, certain burrowing polychaetes or bivalves can destabilize the sediment surface by redistributing the sediment particles (Volkenborn and Reise 2006; Volkenborn et al. 2007b, 2012).

The majority of infaunal animals live within the upper, aerobic, unconsolidated layer of sediment where there is an availability of dissolved oxygen, which is essential to higher fauna and flora, but also for many benthic biogeochemical processes (Woulds et al. 2007; Glud 2008; Huettel et al. 2014). Examples include a myriad of tube and permanent burrow-building organisms such as the maldanid polychaetes or large decapods. Such physical structures have a tendency to stabilize the sediments. In contrast, some burrowers (e.g. scalibregmid and orbineid polychaetes,

echinoids, etc.) are actively burrowing through the sediment, and can have an opposite, destabilizing effect (Myers 1977a). In some instances, these activities could even limit or prevent the establishment of immobile suspension feeders (Rhoads and Young 1970), which are animals that remove particles or plankton from the overlying water column, improving water clarity in the process (Newell 1988; Snelgrove 1998; Whitlatch 2019).

Another common infaunal animal type includes the deposit feeders, which consists of two general feeding patterns. Some actively burrow downwards through the sediment to digest the organic material embedded within the seabed, transporting subsurface particles towards the surface in the process (upward conveyor). Others are oriented upright, with their heads at the sediment surface, to actively select and consume the particles, bringing them downwards through egestion (downward conveyor; Kristensen et al. 2012). However, the movement of sediment is not always strictly in one direction, as some upward conveyors can also drag particles into their tubes, etc. Nevertheless, both types of feeding redistribute the sediment particles, which can lead to an increase in the oxygen concentration (Rhoads 1974) or enhance the transport of solutes and organic matter (OM; Aller 1982, Blair et al. 1995, Reiss et al. 2010). They can either be selective or non-selective feeders. Ultimately, the deposit feeding activity affects the sediment stability and erodibility (Rhoads and Young 1970; Grant et al. 1982). The links between macrofaunal activity and bacterial processes are also quite strong, as oxygen availability impacts the microbial composition and processes (Thrush et al. 2006; Woulds et al. 2007; van Nugteren et al. 2009a; Volkenborn et al. 2012; Rodil et al. 2020). Simultaneously, many of these microbial organisms are also important food sources for deposit feeding macrofauna.

A more indirect consequence from the feeding activities are the effects on the immediate, surrounding environments such as through the nutrient cycling and decomposition processes (Giblin et al. 1997; Braeckman et al. 2010, 2014; Mestdagh et al. 2018). Oftentimes, many of the localized conditions are determined by the small or micro-scale processes such as advective or diffusive transport of solute and particulate matter through the sediment matrix, as well as particle interactions and biogeochemical reactions (Rusch and Huettel 2000; Winterwerp and van Kesteren 2004; Janssen et al. 2005; Huettel et al. 2014). Given their roles in facilitating these processes, the benthic macrofauna are especially important in shallow shelf seas (e.g., North Sea), and an essential link in the benthic-pelagic coupling in these regions (Reiss et al. 2010). Figure 1.4 provides an illustration of some of these common processes.

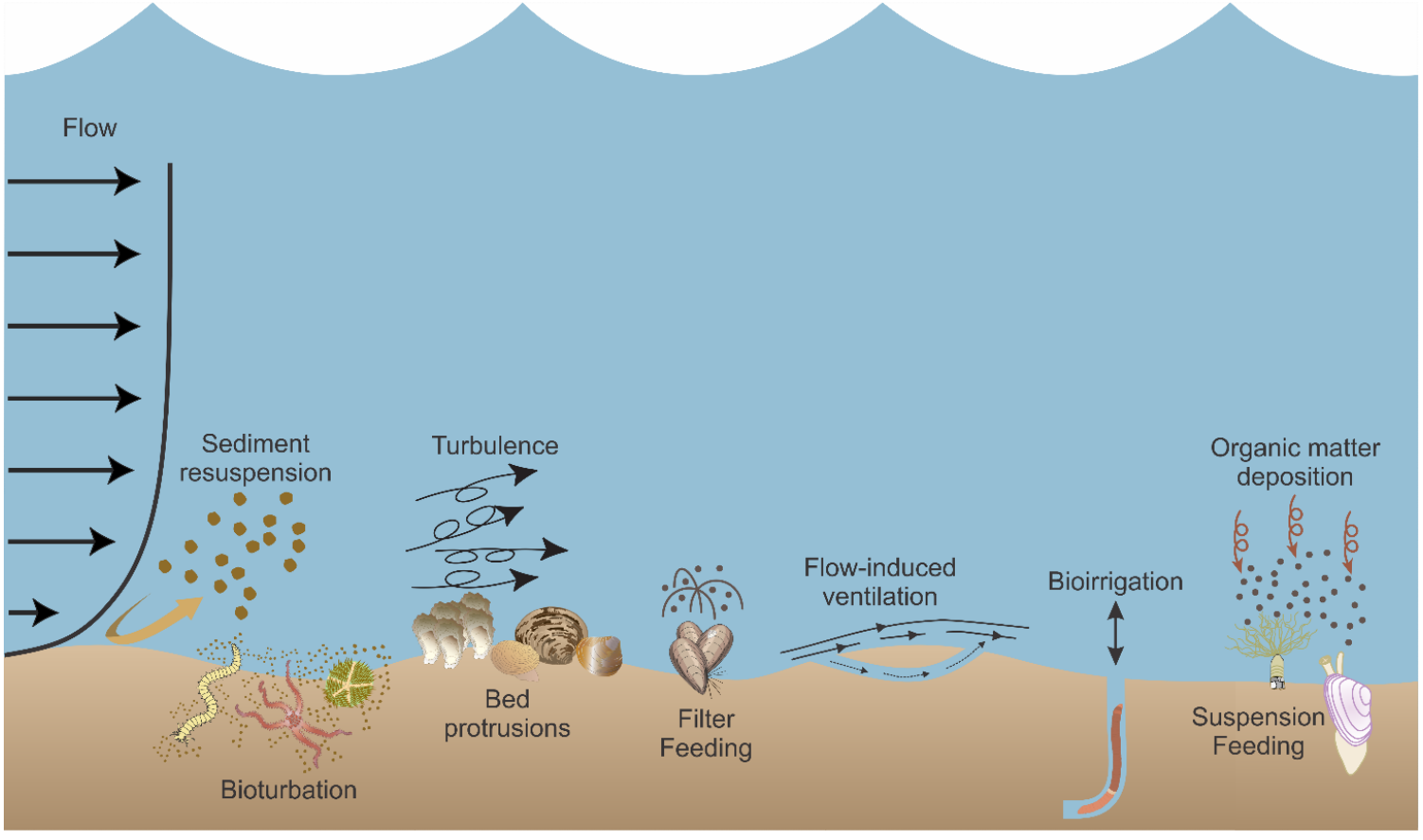

Figure 1.4. An Illustration of some of the common biogeomorphological processes occurring around the sediment bed. Schematic created by Chiu H. Cheng, in part through the use of some images from the Integration and Application Network (ian.umces.edu/media-library).

The use of functional analyses for benthic community structure has been contentious (Pearson 2001), but nonetheless widely applied to defining the key traits or functions of a given habitat based on the community composition. The grouping of organisms into units of comparable functionality provides information about the ecological community as a whole. However, these analyses have also been criticized as being superficial without a concurrent understanding about individual organism life histories and behavior, which is often not available in detail for the more esoteric or rare species (Pearson 2001). Attempts have been made to study both perspectives, and some have found the categorization of benthic groups on the basis of several functions specifically adapted to a given environmental pressure as a robust way to obtain useful ecological insights from these types of tests. For instance, the grouping of taxa by shared functional attributes (groups) or a common resource base can allow for the simplification of community structural and functional analyses (Schall and Pianka 1978; Krebs and Krebs 1985; Gee and Giller 1987; Pianka 2011). This would provide a meaningful indication about the dominant functional traits of a given habitat, as macrobenthic organisms exhibit a diverse array of behaviors that are closely linked to the environmental conditions.

At the very near-bed zone of the sediment-water interface (SWI), fluid viscosity becomes increasingly important for both microbial activities and also the transport and/or entrainment of fine particles. Depending also on the input of OM, including through biological mixing activities, this could determine the dominance by either sessile organisms or more-mobile ones (van Nugteren et al. 2009b; Van Colen et al. 2010; Kristensen et al. 2012; Woulds et al. 2016). At high input, the sessile communities tend to dominate. Thus, the use of motility is also a useful measure to determine the trophic interactions, and can be an extremely useful means to understanding the ecological relationships of different polychaete taxa, such as in the case of small suspension feeders (Myers 1977b). It has since been extended to include all other benthic taxa in studies about factors influencing benthic community structure in general (Pearson and Rosenberg 1977; Bonsdorff and Pearson 1999). At the same time, such biogenic disturbance is only one of a wide range of sedimentary disturbance mechanisms that can affect the infaunal distributions.

Disturbances, whether it be natural or anthropogenic, can negatively impact the benthic environment and subsequently, the benthic organisms inhabiting the seabed and the many associated biogeochemical processes. This is especially the case for activities such as sand mining and bottom trawl fishing, which directly remove the upper portion of the seabed, often the most active zone in the seafloor (Mayer 1993; Watling and Norse 1998; Herman et al. 1999; Watling et al. 2001; Jennings et al. 2001). Furthermore, this removal creates an open area requiring

replenishment of the sediment from natural transport processes and also the recolonization in order for the benthic community to recover (van Dalfsen and Essink 2001). The recovery potential can be quite variable and dependent on the level of impact, as well as the benthic community assemblage in the surrounding areas. Some studies have observed a recovery period of 4-6 years following shallow sand extraction (van Dalfsen et al. 2000; van Dalfsen and Essink 2001; Boyd et al. 2005). But in highly-utilized extraction locations, full recovery was not measured even after 11 years (Wan Hussin et al. 2012). Other studies have found a reduction in the abundance, biomass and number of species following repeated dredging events in the immediately impacted areas. There is still much uncertainty about longer-term consequences of routine dredging or other offshore activities, especially for the benthic communities (Wan Hussin et al. 2012; de Jong et al. 2015b). As a result, it is crucial that we have a firm understanding about the direct consequences of offshore anthropogenic activities over time, and the other implications regarding the two-way feedback between the benthic biota and seabed morphology.

As of yet, the interrelations between the physical processes, such as tides and sediment dynamics, with benthic organisms are still not very well understood. Thus far, many theoretical studies on bedforms have focused on the geomorphological conditions, while benthic organisms and their associated activities were left out. Yet the biological processes can have an important local effect on the sediment characteristics, altering roughness or transporting solutes or particulate matter. Whether or not these effects are sufficient to cause a shift (e.g., turning point) that inhibits or facilitates larger-scale bedforms over the longer term is not well known (Borsje et al. 2014a). Unfortunately, biological information is generally not available on a small-scale, but is rather conducted over regional areas (Degraer et al. 2006, Reiss et al. 2010; regular monitoring in Dutch coastal zone, etc.). Nevertheless, the alteration of habitats can affect the animal densities and/or cause behavioral changes to certain functional groups, which include key players in the sedimentary biogeochemical cycling. As a consequence, the ecosystem functions can be negatively affected (Villnäs et al. 2012; Mestdagh et al. 2018).

The amount of physical stress of a given habitat may limit the ability of an organism to inhabit the environment. Interactions, particularly positive ones, between organisms are especially important (Bertness and Callaway 1994; Bruno et al. 2003; Crain and Bertness 2006). Such positive relations often occur through engineering means, where the activity of one particular species can enhance the environmental conditions such that the other organisms in close proximity can then benefit from this (Bertness 1984; Fogel et al. 2004). Terrestrial examples have been well studied, such as in semiarid regions where the vegetation is moisture-limited. The presence of

"nurse" plants which are able to trap moisture through shading are key species in facilitating a vegetative community (Aguiar and Sala 1994). The same applies in salt marsh communities, where the existence of salt-tolerant fugitive species providing shade can mitigate evaporation levels enough for the dominant species to prosper (Shumway and Bertness 1994). Thus, ecosystem engineers can be beneficial to other organisms in environments which are physically stressful, as their activities are able to alleviate some or most of these environmental stressors and support a diverse ecosystem that otherwise likely could not exist (Bertness and Callaway 1994; Crain and Bertness 2006; Romero et al. 2014). Habitats which are lower in physical stressors can sometimes enable negative interactions that result in less favorable outcomes through interference of suitable conditions (Crain and Bertness 2005). But even here, positive effects can occur if for example, ecosystem engineers provide refuge to neighboring species from predation or competition.

1.1.4 Current knowledge gaps and problem formulation

Despite the dynamic nature of shallow, coastal seas, the nonlinear interactions between the physical, sedimentary and biological processes are not well understood. Oftentimes, they are studied exclusively under their respective sub-disciplines instead of on a comprehensive scale, such that the geomorphological perspective (Dodd et al. 2003), fine sediment dynamic perspective (Mehta et al. 1989) and ecological perspective (Urban-Malinga et al. 2008; Montserrat et al. 2008; Adam et al. 2008) are investigated separately. Benthic studies are difficult undertakings in general, given the logistical demands required for the sampling and other data collection, as well as the post-processing and identification of samples. Much of the synthesis on biodiversity and patterns have been made based on the limited number of samples available. As such, biogeographical predictions of macrofaunal groups are often lacking, with only a few exceptions such as for mollusks or sipunculids (Cutler 1994; van Bruggen et al. 1995).

On a regional level, information on polychaetes and crustaceans is more readily available, but sampling remains rather patchy (Brusca et al. 1995). The issue is further compounded by the fact that some of the previously-identified species may in fact be species complexes or different taxa altogether, which has been documented for important pollution indicator species (Grassle and Grassle 1976; McDonald and Kreitman 1991; Snelgrove 1998; Knowlton 2003). Similarly, small-scale studies on macrobenthic community composition are very limited for the same reasons, and as a result have often been done to address very specific issues

(e.g., fishing). Thus, a truly multi-disciplinary perspective on the interrelations within biogeomorphology is either completely lacking or largely underdeveloped for very specific types of environments. More-recent attempts have used theoretical studies to identify the mechanisms in sandy offshore areas in the Southern Bight of the North Sea, where there appear to be physical tipping points that determine the presence or absence of bedforms such as sand waves (Borsje et al. 2009b; a). It has been found that small changes, including from the benthic organisms, could be sufficient to having a cascading effect on such tipping points (Damveld et al. 2019, 2020b).

There is a pressing need to better-understand the community composition and associated dominant functional traits in the context of the physical and geomorphological conditions. Offshore activities, which have been shown to greatly affect sediment dynamics and the morphodynamics, especially in the nearshore, coastal waters, are ever increasing (Gonzalez-Ortiz et al. 2014; Mohr et al. 2016). There is indeed a growing interest on the effects of human activities on sediment dynamics as well as the habitat value of sediments for benthos from both an economic and ecological perspective (Reed et al. 2013, 2017), but the field information is still very limited. Another issue is the recovery of communities that have been disturbed. The current method of sand mining is focused on quick recovery and restoration of the original habitat (e.g., the created sand mining pit), rather than on optimizing the environment for a given assemblage. Perhaps a more ecosystem-based approach in offshore construction/landscaping projects could help improve the ecological value of an effected environment (de Jong et al. 2014b; a, 2015a, 2016; Rijks et al. 2014). Thus, a better understanding of the biogeomorphological interactions could also facilitate improvements in designs and implementation of offshore operations to conserve the natural environment as ideally as possible.

1.1.5 Research objectives and questions

The primary objectives of this thesis are as follows: (1) to determine to what extent the sediment characteristics are influenced by the position along asymmetrical, tidal sand waves, (2) to then identify the benthic community composition, structuring and dominant biological traits along the same sand wave gradients, (3) to measure the direct influence of biogenic shell valves on the development and migration of sand ripples and (4) to contextualize the biotic and abiotic conditions of the sand wave study site and determine the potential biogeomorphological implications of these studies for offshore sandy environments more generally.

Q1. Is the division of asymmetrical, tidal sand waves into four morphological units (e.g., crest, steep-slope, trough and gentle-slope) sufficiently sensitive to reliably identify distinct habitats?
Q2. Based on the results from the abiotic distribution along the sand waves (Q1), can the same delineation also adequately explain the benthic community compositional distribution?
Q3. To what extent does the shell content in a sandy sediment mixture affect the ripple dimensions, migration rate and the near-bed hydrodynamics?
Q4. What new information can we derive from the small-scale, high-resolution sampling combined with flume experimentation (Q1-3), and what are the implications of these findings for similar (sand wave) locations in the Dutch North Sea?

1.1.6 Field sampling and flume experimentation

In order to address this knowledge gap, we conducted field campaigns at a study site within the Dutch North Sea (Figure 1.5, left panel) with the NIOZ *RV – Pelagia* (Figure 1.5, right panel). The location of interest is a sand wave field approximately 20 km to the west of the island Texel. Situated towards the northern range of sand wave occurrence in the Dutch sector, these exhibit the average characteristics of all sand waves combined in the region. Sampling was conducted at high resolution (within tens of meters) along four different areas of the sand waves to determine the spatial differences in the sediment characteristics and benthic community composition. The first cruise was undertaken in June 2017, with a follow-up in October 2017. The sediment information is available from both campaigns, but benthos information is only available from June. A variety of samples from different sampling devices were collected (Figure 1.6). In addition, given the observation of frequent ripple occurrence and (sometimes very large) presence of shells and other biogenic debris. We also conducted a flume experiment to test the effects of shell content on ripple development and movement. The specific details can be found in Chapters 2 - 4.

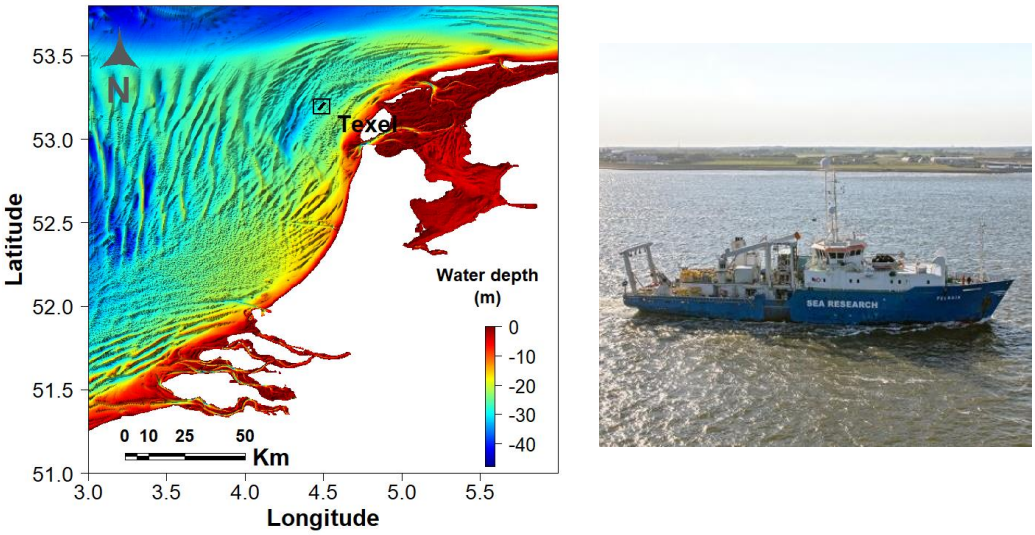

Figure 1.5. *Left panel:* Map of the Dutch North Sea showing the study location with the larger bedforms. *Right panel:* The NIOZ *RV – Pelagia* (photo by NIOZ).

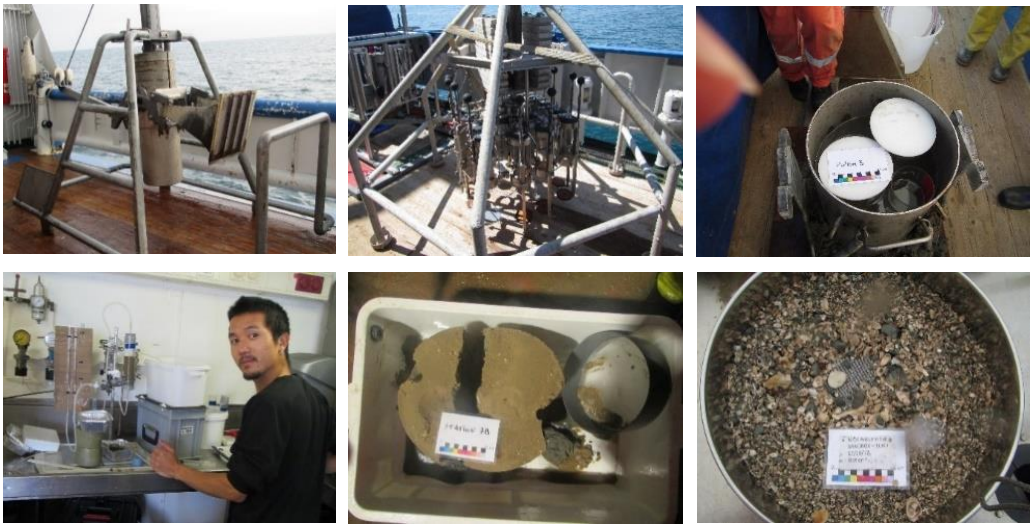

Figure 1.6. (A) NIOZ box core used to sample macrofauna, (B) the NIOZ multi corer used to collect abiotic samples, (C) the whole box core preserved for subsampling 3.5-cm diameter cores, (D) permeameter, (E) sediment collected from a box core and (F) sieved remains over a 1 mm mesh. (photos by Chiu H. Cheng and Anton Tramper).

1.1.7 Thesis structure

Chapter 2: The sediment characteristics of the Texel sand wave field are presented to show how they differ along asymmetrical sand waves. The samples were analyzed based on the categorization of the sand waves into four distinct sections: trough, gentle slope, crest and steep slope. Because the campaign was conducted in June 2017 and repeated in October 2017, the temporal effect was also considered (Q1).

Chapter 3: Continuing from the study in the previous chapter, the individual, biomass and taxon densities[1] of the benthic community were analyzed to determine any corresponding changes. Following a similar approach as with the sediment characteristics, the sand waves were again divided into four distinct sections (e.g., habitats). Multivariate analyses were conducted to show the dominant taxonomic groups and, subsequently, the dominant traits between each habitat. While sediment information could not be used for direct comparison, it was nevertheless very useful in supporting the trends observed in the benthic community (Q2).

Chapter 4: As biogenic shells are ubiquitous particles in the natural environment, we tested the influence of increasing shell percentages on the development of small sand ripples. The effects on the ripple development, migration rate and dimensions were calculated to show how the presence of shell material (e.g., roughness) not only affects the erodibility and movement of sediment, but also influences the near-bed velocities and turbulence (Q3).

Chapter 5: The information obtained from the sand wave study area and the trends observed between the different components (sediment characteristics, shell % and macrofauna) are synthesized. The main findings from these small-scale studies are evaluated to determine the potential implications for other sand wave locations and the sandy offshore environment, with a brief summary of suggestions for further research work in relevant projects (Q4).

[1] Also known as species richness.

Chapter 2

Sediment characteristics over asymmetrical tidal sand waves in the Dutch North Sea

Chiu H. Cheng[1], Karline Soetaert[1] and Bas W. Borsje[2]

[1]NIOZ Royal Netherlands Institute for Sea Research, Department of Estuarine and Delta Systems (EDS), 4401NT Yerseke, the Netherlands. [2]Water Engineering and Management, University of Twente, 7500AE Enschede, the Netherlands.

Published as

Cheng, C. H., K. Soetaert and B. W. Borsje. 2020. Sediment Characteristics over Asymmetrical Tidal Sand Waves in the Dutch North Sea. Journal of Marine Science and Engineering **8**: 1–16. https://www.mdpi.com/2077-1312/8/6/409

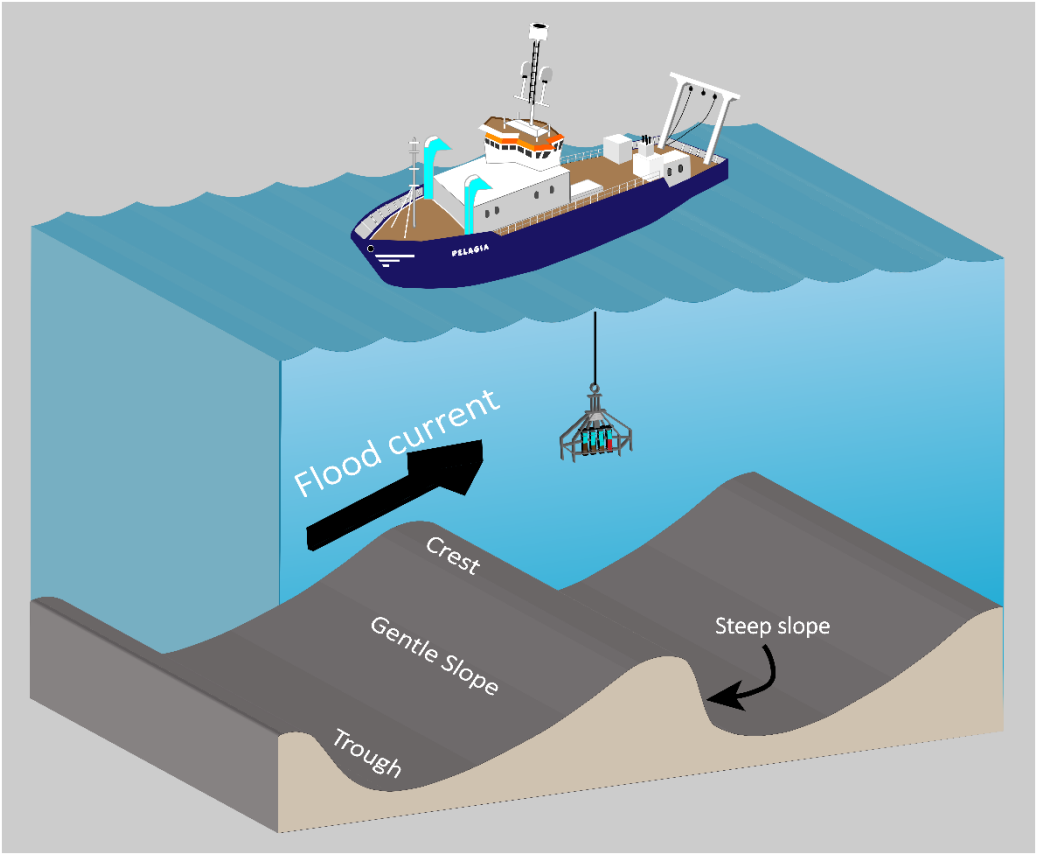

Schematic by Chiu H. Cheng

Abstract

The behavior of asymmetrical bedforms, which include many tidal sand waves, is challenging to understand. They are of particular interest since they are mostly located within areas prone to offshore engineering activities. Most experimental investigations regarding asymmetrical bedforms consider the riverine environment, are limited to a single sand wave or a few scattered ones, and focus only on differences between crest and trough. Hardly any information is available on sediment compositional changes along asymmetrical tidal sand waves, despite their abundance offshore. An asymmetrical sand wave field located off the coast of Texel Island in the North Sea was studied in June and October 2017. A total of 102 sediment samples were collected over two seasons along a single transect that covered five complete sand waves to measure the grain size composition, organic carbon concentration, chlorophyll *a* (chl *a*) concentration, and sediment permeability. We found significant variations in these sediment parameters between the sand wave trough, crest, and gentle and steep slopes, including a difference in permeability of more than 2-fold, as well as a difference in median grain size exceeding 65 µm. Based on these characteristics, a sand wave can be divided into two discrete halves: gentle slope + crest and steep slope + trough. Our results indicate a distinct sediment-sorting process along the Texel sand waves, with a significant difference between the two halves of each sand wave. These data could serve as input for process-based modeling of the link between sediment-sorting processes and seabed morphodynamics, necessary to design offshore engineering projects.

Keywords: Seabed morphology, permeability, asymmetrical sand waves, North Sea, sediment characteristics, sandy shelf seas, biogeochemistry

---

2.1 Introduction

Tidal sand waves are dynamic rhythmic bedforms, often found in tide-dominated, sandy, shallow coastal regions such as the North Sea, but also in many other environments such as straits and tidal inlets around the world (van Dijk and Kleinhans 2005; Besio et al. 2008; van Santen et al. 2011; Borsje et al. 2014a). They typically range from 100 to 1000 m in wavelength (distance from crest to crest) and have heights up to 5 m (Lobo et al. 2000; Baptist et al. 2006; Besio et al. 2008; de Jong et al. 2015b). However, giant, 10-m high sand waves have also been observed in other locations outside the North Sea (Katoh et al. 1998; Santoro et al. 2004; Liao and Yu 2005; Barnard et al. 2006; Hanes 2012). One prominent feature of sand waves is their ability to migrate

as a result of the residual current or tide asymmetry (Németh et al. 2002; Besio et al. 2004; van Gerwen et al. 2018). This movement, which involves up to tens of meters per year, can pose potential hazards to navigation and expose pipelines or buried cables (Roetert et al. 2017). Offshore engineering activities, such as sand mining, the disposal of dredged material, windfarm construction, shipping, and pipeline and cable installations, are projected to increase in the future. Thus, sand wave mobility is especially problematic for coastal management and calls for a solid understanding of the complete sand wave dynamics (van Dalfsen and Essink 2001; Van Oyen et al. 2011; Jongbloed et al. 2014; de Jong et al. 2016). A multitude of studies have utilized models to accurately predict sand wave occurrence and movement (Besio et al. 2008; Borsje et al. 2009a; c, 2014a; b; Van Oyen and Blondeaux 2009b; a; Van Oyen et al. 2010; van Santen et al. 2011; Jongbloed et al. 2014; van Gerwen et al. 2018). More recently, model studies have focused on the development of asymmetrical sand waves (Damveld et al. 2018[2]; van Gerwen et al. 2018). However, as knowledge on the sediment characteristics is limited, these state-of-the-art models do not account for spatial variability in sediment composition (e.g., grain size and roughness) yet.

Bottom roughness and topography are important factors contributing to morphological pattern development (Borsje et al. 2009a). Bedforms such as sand waves emerge because of tidal and wave energy dissipation, which causes instability in the sandy seabed. A balance is established between the steady stream transport from the bottom perturbation interacting with the oscillating tidal current, and the force of gravity dragging sediment downslope. Sand waves consequently grow from the resulting net sediment transport, which converges from troughs to the crests (Hulscher 1996; van Dijk and Kleinhans 2005; van der Veen et al. 2006; Van Oyen et al. 2010, 2013). Sediment composition is directly linked to bottom roughness and thus also affects seabed disturbance rates (Borsje et al. 2009b; Van Oyen et al. 2010, 2013; Reiss et al. 2010; Aldridge et al. 2015; Wilson et al. 2018) and sand wave emergence and growth. Furthermore, local hydrodynamic conditions often give rise to differential grain-sorting phenomena that can significantly affect the spatial and temporal development of bottom morphology (Svenson et al. 2009; Blondeaux 2012; Venditti 2013; Lefebvre et al. 2014, 2016) and result in sand waves developing either symmetrical or asymmetrical shapes. The asymmetry (A) is measured by subtracting the distance from the crest to the trough of a gentle slope or steep slope (L_1 and L_2, respectively), divided by the total length of the sand wave (L); this shows how similar or different the two halves of a given sand wave are (Figure 2.1). At present there is little information on

[2] The correct citation is Damveld et al. 2019, as cited in the introduction of Chapter 3.

asymmetrical bedforms due to the difficulties of sampling sediment at the required fine-scale level in the field (Best and Kostaschuk 2002; Kleinhans et al. 2009; Paarlberg et al. 2009; Janssen et al. 2012; Damen et al. 2018). The few field studies available on sand waves have mostly observed coarser sediments on crests compared to troughs, but did not consistently study the composition of slopes. Also, the focus has been on grain size rather than on related components such as biogeochemical compounds (Terwindt 1971; Van Lancker and Jacobs 2000; Stolk 2000; Passchier and Kleinhans 2005; van Dijk and Kleinhans 2005; Baptist et al. 2006; Roos et al. 2007; Van Oyen and Blondeaux 2009b; Venditti 2013; Koop et al. 2019).

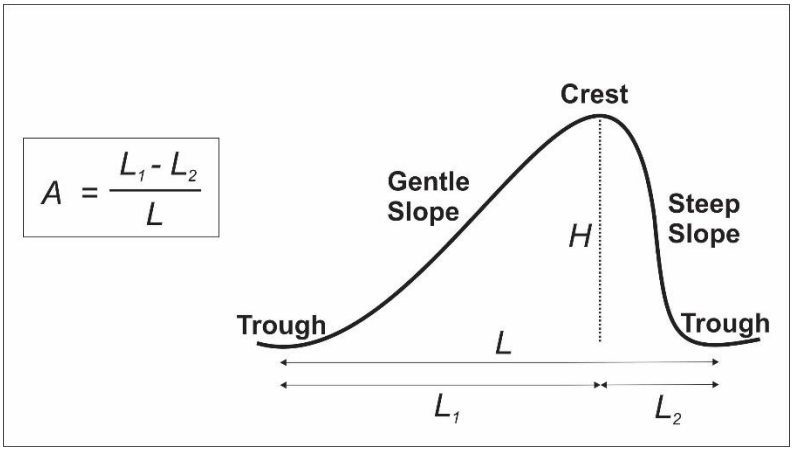

Figure 2.1. Schematic of an asymmetrical sand wave, with the equation for calculating the level of asymmetry (*A*). *H* represents the sand wave height and, similar to the length, is in units of meter. *A* is a dimensionless value.

In this study, we sampled multiple asymmetrical sand waves in one specific location over two seasons and measured the grain size composition, the organic carbon and chlorophyll *a* (chl *a*) concentration, and the sediment permeability. Organic carbon and chl *a* are important biogeochemical compounds because they support a wide range of metabolic and chemical activities within marine sediments, and are a food source for microbial and benthic organisms (van Nugteren et al. 2009c; Bauer et al. 2013). While chl *a* is a useful measure of the readily consumed (e.g., labile) fraction of organic matter (Stephens et al. 1997; Boon and Duineveld 1998; Bianchi 2011; Szymczak-Żyła 2016; Ramírez-Ortega et al. 2019), organic carbon comprises a mix of fractions, including the more refractory compounds. Sediment permeability is increasingly recognized as an important parameter driving biogeochemical and small-scale water transport

processes, especially in the upper layers of sandy sediment and around small bedforms and protrusions (Wilson et al. 2008). Particularly in sand, it is an important parameter that determines the transport of solutes and fine particles in the sediment (Jenness and Duineveld 1985; Huettel and Gust 1992; Rusch and Huettel 2000). Sediment permeability is closely related to the sediment grain size and the associated biogeochemical compounds within the finer fractions (Serpetti et al. 2016).

The aim of this study is to capture consistent, small-scale variations in sediment characteristics in a field of asymmetrical sand waves. We test whether sediment parameters differ between different sand waves, between positions within a sand wave, and between the seasons.

2.2 Materials and Methods

2.2.1 Sand wave symmetry and morphological units

Recent data have shown that sand waves are widely distributed throughout the North Sea and are asymmetrical in shape (Damen et al. 2018). A re-analysis of these data (4TU.Centre for Research Data; Damen et al. 2018) shows the mean asymmetry in the North Sea to be around 0.3, with asymmetry increasing towards the coast and northwards within the Dutch North Sea (Figure 2.2D). The level of asymmetry of sand waves is defined as the difference between the length of the gentle slope (gradual, longer side, L_1) and the length of the steep slope (steeper, shorter side, L_2), divided by the total length of the given sand wave (i.e., 0 is fully symmetrical, 1 is fully asymmetrical; Figure 2.1). We utilized the same approach for calculating the asymmetry of the Texel sand waves.

2.2.2 Study site

Two field campaigns to a sand wave field located in the Dutch North Sea, approximately 22 km offshore of Texel, were undertaken onboard the research vessel, NIOZ *RV – Pelagia*, in June and October 2017 (Figure 2.3A). The particular sampling site was chosen as the mean asymmetry of these sand waves fall within the mean asymmetry value of all sand waves found in the Dutch North Sea (Figure 2.2D). Based on the equation from Figure 2.1, our sand waves had an asymmetry value ranging from 0.29 to 0.38. In addition, as there are shipping lanes located close to the study site, the area is subject to low levels of fishing activity (Damveld et al. 2018). This greatly reduces the occurrence of activities such as trawling, which can disturb the seabed

morphology and other biogeochemical processes (Puig et al. 2012). The sand waves extend for another 1–1.5 km to the north and west of our sampling area.

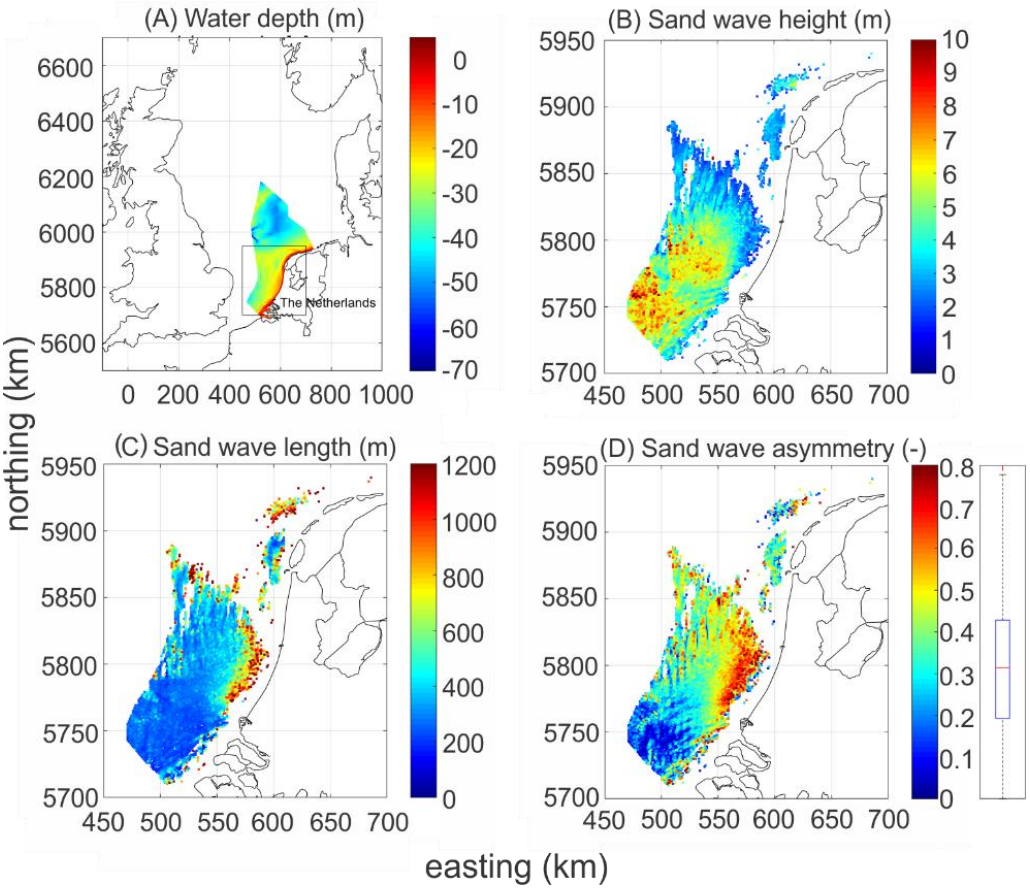

Figure 2.2. (A) Map of the North Sea, with the bathymetry information included for the Dutch region Maps showing the height (B) and the length (C) of the sand waves in the Dutch region. (D) Map showing sand wave distribution throughout the Dutch North Sea, as well as the level of sand wave asymmetry. The boxplot on the right shows the distribution of all the measured sand waves by their shape, with extreme examples ranging from 0 to almost 0.8 (outliers excluded). The most asymmetric sand waves are found near to the coast and towards the north. The data were extracted from a study on the environmental properties of sand waves, and aggregated per square kilometer (4TU.Centre for Research Data; Damen et al. 2018).

2.2.3 Multibeam data collection and selection of sampling locations

The sampling area (~1 km × 3.5 km) was mapped with a Kongsberg EM302 Swath Multibeam echo sounder (MBES) immediately prior to each sampling operation (N 53° 11.241′;

E 4° 28.628′). The data from the MBES were processed with the software Fledermaus at 1-m grid resolution, with an estimated accuracy of greater than 0.6% of the depth (values supplied by manufacturer). The data contained spikes (noise) and lines that were parallel to the navigation direction due to errors in the speed of sound or from the bottom depths not being corrected for the tidal height. The data were processed with CUBE (Combined Uncertainty Bathymetric Estimator), which estimates the most probable position of the bottom. The spikes in the data had to be manually removed. The resulting bathymetric data were converted to a raster using R 3.4.4. (R Core Team 2020), with the function *rasterFromXYZ* from the *raster* package (R. J. Hijmans, Davis, United States) (Hijmans 2017).

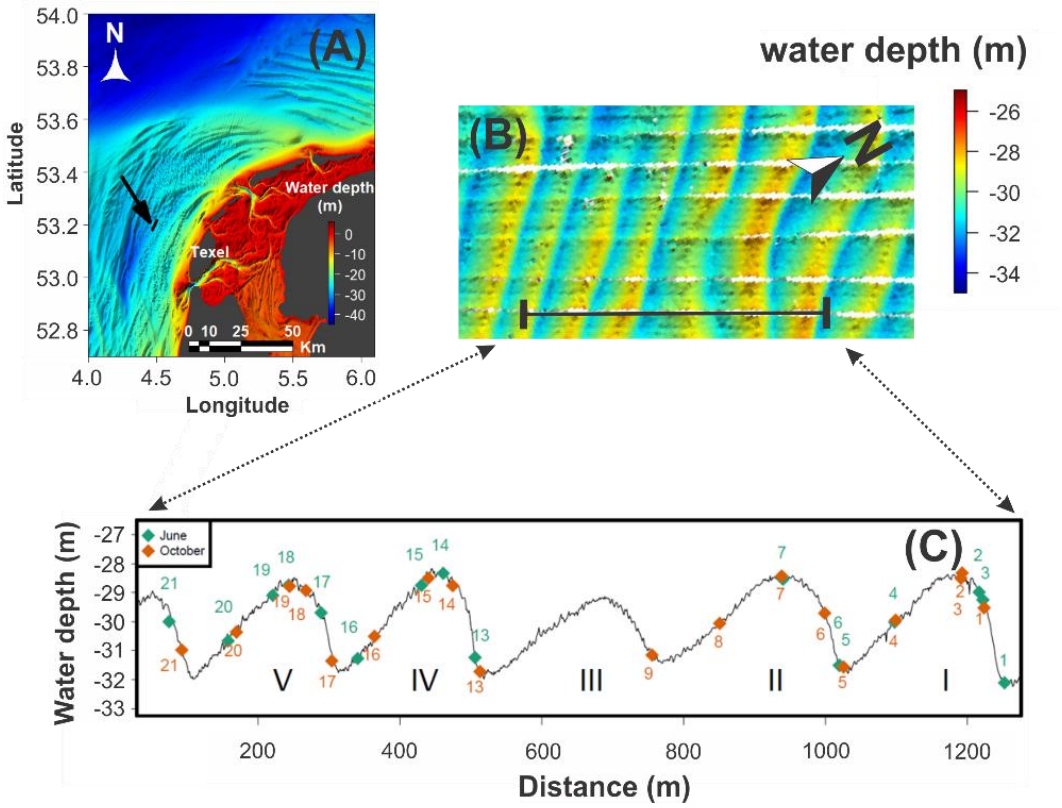

Figure 2.3. (A) Map showing the study location, offshore of Texel (IHO-IOC. 2014) (B) Subset of the mapped area. (C) The profile was created using the processed and gridded geophysical data collected with a MBES from June, and shows a cross section of our sampling transect with stations from both seasons plotted together.

During the MBES mapping in June, the sailing speed of the vessel was approximately 5 ± 1 knots. The temperature and salinity averaged 14.6 ± 0.8 °C and 35.2 ± 0.02 ppt. Wind speed averaged 1.7 ± 0.7 m s^{-1}. In October, the sailing speed was approximately 2.2 ± 1.7 knots, while the temperature and salinity averaged 15.3 ± 1.9 °C and 34.9 ± 0.02 ppt. Wind speed averaged 2.8 ± 0.9 m s^{-1}. For additional information about the weather conditions immediately preceding and during the campaigns, including for each type of sampling, please see Figure S2.1. The *RV – Pelagia* does not have a tidal correction mechanism or a DP (dynamic positioning system), but is equipped with a GNSS (Global Navigation Satellite System) positioning system.

2.2.4 Sediment sampling

All samples were collected along a single transect line (~1100 m) covering five sand waves (Figure 2.3C). Given the time limitations of the sampling, we positioned our stations only along the four highest sand waves (I, II, IV, and IV). The middle sand wave (III) was excluded from sampling because it was shorter than the adjacent sand waves, and we wanted to measure sand waves exhibiting the steepest gradients possible. The first campaign included 16 stations (1–7 on sand waves I and II and 13–21 on sand waves IV–V). Sediment was collected using the NIOZ multicorer (Oktopus model), equipped with eight 10 cm diameter cores, each 61 cm in length. The multicorer is neither a piston corer nor a vibracorer, so no additional mechanical forces are involved in the sediment sampling. From each of these cores, subsamples were taken by pushing a single 3.5 cm diameter core into the multicore sediment core, as close to the center as possible. Three subsamples were taken for grain size composition and organic carbon concentration, with another three cores subsampled for permeability. In June, the core lengths ranged from 11 to 19 cm in length. In October, the core lengths ranged from 4 to 17 cm in length[3]. From the remaining multicore, the top 1 cm of sample was collected with a 60 mL cutoff syringe for the chl *a* concentration (only one sample per station). Usually, a single deployment of the multicore was sufficient to collect all the subsamples per station. However, stations 19 and 21 were sampled with a 30-cm diameter NIOZ Box corer (K6 model) because of repeated multicorer failures due to sediment coarseness. The dimension of the box corer was approximately 32 cm in diameter and 55 cm in length. All six subsamples were taken directly from a single box core sample from the respective stations. In the second campaign, 18 stations (1–9, 13–21) were sampled along the

[3] The indicated lengths are for cores taken to measure the grain size and organic carbon. The entire cores were sliced, and all slices were measured for both parameters.

same transect (extra stations: 8 and 9 on sand wave II), using the same exact sampling protocol. However, the NIOZ multi-corer was only used for stations 1, 2, 4, and 5. The remaining stations were collected with the NIOZ Box corer. Sampling was executed in relatively calm weather, with waves at most 1 to 1.5 m in height in June and somewhat higher in October at above 2 m (Figure S2.1).

As we expected to find a difference in the sediment parameters along the sand waves, we subdivided them into the following morphological units (MUs): crest, trough, gentle slope, and steep slope. We set the boundary of the two slopes as the regions between 0.5 m above the troughs and 0.5 m below the crests (Figure 2.3C).

2.2.5 Sediment samples: Grain size distribution, organic carbon and chl a

The sediment subcores were collected and kept stable in a cool location until further processing was possible. The sediment samples were stored in plastic vials and frozen at −20 °C, weighed, freeze dried, and dry weighed; porosity was measured on 24 random samples. Samples were analyzed for grain size composition using the Malvern Mastersizer 2000 particle size analyzer (Malvern, (WM), United Kingdom) through laser diffraction (McCave et al. 1986), which measured the volume percentages of five sediment fractions: coarse sand (500–1000 µm), medium sand (250–500 µm), fine sand (125–250 µm), very fine sand (62.5–125 µm), and silt (≤63 µm). Together, these five fractions total 100% for each sample. The median grain size (D_{50}) was calculated from this information.

Additional sediment samples were analyzed for the total organic carbon concentration. Approximately 50 mg from each sample was added to silver capsules and acidified with several additions of HCl to remove the carbonate content. The samples were then measured on a Flash2000 organic elemental analyzer (Bath, (SW), United Kingdom) (Nieuwenhuize et al. 1994).

The chl *a* sediment samples were immediately stored in a −80 °C freezer upon collection, and later freeze-dried overnight back in the lab under dark conditions at −60 °C. The samples were then extracted with 90% acetone and measured on an Analytik Jena Specord 210 spectrophotometer (Jena, (TH), Germany) with a halogen lamp (Ritchie 2006).

The average length of the sediment cores was 13 cm in June and 9.5 cm in October. The results presented here are averages of the entire individual sediment cores.

2.2.6 Sediment permeability

Sediment permeability was measured using a constant head permeameter (Glud et al. 1995, 1996). The setup measures the hydraulic conductivity of sediment cores, which is used to calculate permeability as a function of the following equation:

$$k = \frac{K * \mu}{d * g}, \quad (1)$$

where k is the permeability (m^2), μ is the water viscosity (Pa*s), calculated from the temperature and salinity, d is the water density (g cm^{-3}), g is the gravitational acceleration (9.81 m s^{-2}), and K is the sediment hydraulic conductivity (cm s^{-1}), calculated as follows:

$$K = \frac{V * L}{h * A * t}, \quad (2)$$

where V is the water volume collected from the core (cm^3), L is the sediment length (cm), h is the pressure difference between the reservoir and outlet (pressure head; cm), A is the core cross-sectional area (cm^2), and t is the time to collect V (s).

2.2.7 Statistical analysis

The effects of the MU, sand waves, and seasonality on the permeability, D_{50}, the five sediment fractions, the organic carbon, and chl *a* concentrations were tested using a three-way ANOVA (Analysis of variance) test. This test looks for any interactions and effects between three independent variables and a continuous dependent variable.

To determine the cause for any statistically significant differences, a post hoc pairwise comparison (Tukey's HSD honestly significant difference test) was run. The purpose of this is to identify where the significant differences may stem from, by comparing the means of every treatment with every other treatment to identify differences between any two means that would be greater than the expected standard error. The test compared all the MUs with one another over each sediment parameter. All statistical analyses were conducted in R, with the *lsmeans* package (R. V. Lenth, Iowa City, United States) (Lenth 2016; R Core Team 2020).

2.3 Results

The Texel sand waves are largely asymmetric (Figure 2.3C), with the steep slopes oriented NNE (north-northeast), and the studied sand waves ranging from 2.8 to 3.5 m in height

and 160 to 210 m in length. Out of 16 stations in June, two were located in the gentle slope, five in the crest, five in the steep slope, and four in the trough. In October, those numbers were four, seven, two, and five, respectively.

2.3.1 A note about the MBES datasets

The cross section shown in Figures 2.3C and 2.4F was produced using the MBES data from June, as the MBES in October could not generate the bathymetry at equal resolution. The MBES mapping occurred over a three-day period at different times with respect to the tides in October, showing a considerable number of spikes at the interface.

2.3.2 Sediment Composition, organic carbon and chl a content

The percentages of fine sand, D_{50}, and sediment permeability all show a clear pattern along the sand waves, which is consistent during both seasons (Figure 2.4). The sediment composition coarsens from the gentle slope side up towards the crest and decreases again down the steep slope to the trough. The finer fractions (≤250 µm), are more abundant in the steep slope and trough locations and vice versa for the coarser fractions. A similar trend was also observed for the other sediment fractions (Table S2.1; Figure S2.2). The silt fraction was highest in the steep slope and trough stations, as was the very fine sand fraction, but the latter was also found in very small quantities (<0.5%) in the crest and gentle slope areas. The D_{50} in June averaged 288.9 ± 34.8 µm, with a range of 220–340.5 µm, while in October the average was 284.7 ± 25.8 µm, with a range of 231.1–320.5 µm. The largest difference in average D_{50} within a sand wave was 66.4 µm in June and 57.2 µm in October. The average D_{50} was higher in June except for the gentle slope (Table S2.1). The largest fraction of sediment was fine sand in the steep slope and trough, while in the crest and gentle slope it was the medium sand fraction (Figure 2.4). Higher-resolution information on the grain size distribution is available as sediment cumulative distribution plots (Figure S2.3).

The organic carbon concentration values were low overall, with the highest average falling below 0.25%. Nevertheless, the organic carbon showed variations along the sand waves, following the trend of the finer fractions of sediment (≤ 250 µm). The chl *a* content also showed a general pattern of increase up the gentle slope towards the crest, but generally had a peak in the steep slopes, followed by the troughs with almost an 8-fold difference between the steep and gentle slope averages.

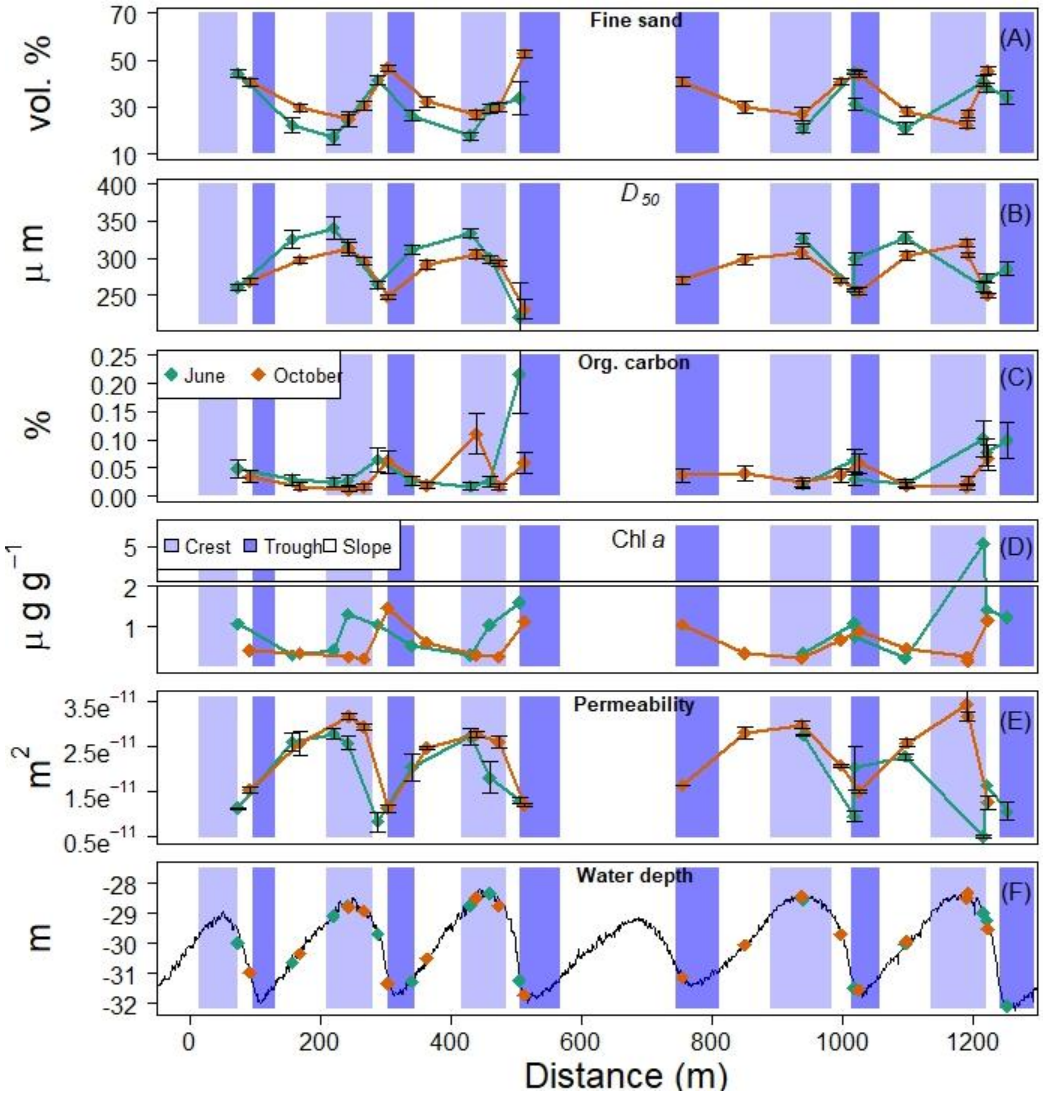

Figure 2.4. Selection of measured sediment parameters along the transect (mean and standard deviation) and for the two seasons. (A) Percent fine sand, (B) D_{50}, (C) organic carbon concentration, (D) chl *a* concentration (a break in the figure is used to "rescale" the outlier), (E) sediment permeability. (F) Transect cross section, with the sampling positions from both campaigns.

Permeability was highest on the gentle slopes in June, while in October the most permeable MU was the crests (Table S2.1). The permeability values were somewhat higher in October, with a range of 9.49×10^{-12}–4.28×10^{-11} m^2 and an average of 2.35×10^{-11} m^2. In June,

the range was 4.35×10^{-12}–3.05×10^{-11} m^2 and the average was 1.88×10^{-11} m^2. However, all the measured samples fell within the range of the threshold that is considered permeable ($\geq 10^{-12}$). Overall, the permeability in the crests was more than double that of the troughs, and was closely correlated to the D_{50}. Sediment porosity averaged 0.37 ± 0.048 in June and 0.36 ± 0.067 in October, with no significant differences between the seasons and no measurable differences along the sand wave.

2.3.3 Trends between the MUs

Averaged over the MUs, the grain size composition and level of permeability were unevenly distributed along the sand waves, with the finest fractions completely absent from the gentle slope and crest (Figure 2.5). The three-way ANOVA showed that in none of the cases did the individual sand waves themselves have a significant effect on any of the measured sediment parameters (Table S2.2). The four MUs, when compared between each sand wave, showed no statistical difference to their counterparts ($p > 0.05$). The crest from one sand wave was not significantly different from the crests from other sand waves, and similar for the other MUs. However, all four of the MUs were significantly different from one another ($p < 0.01$) for every measured parameter, while seasonality was highly significant for permeability ($p < 0.01$), the D_{50}, and the coarse and fine sand fractions. For the other parameters, the seasonality was not significant (Table S2.2). The statistical difference was larger ($p < 0.01$) when the sand waves were split into two halves (gentle slope/crest and steep slope/trough), compared to the tests that considered four individual MUs. Additional information can be found in Figure S2.4.

The post hoc pairwise comparison (Tukey′s HSD honestly significant difference test) showed that in all cases the steep slope was not as significantly different from the trough and, likewise, the crest and gentle slope MUs were less significantly different from each other. In comparison, all of the other combinations were more significantly different. In accordance with the ANOVA results, this means that the crest and gentle slope, while still statistically significantly different from each other, are much more different to the steep slope and trough. Similarly, the trough and steep slope are less significantly different from one another than they are to the crest and the gentle slope.

2.4 Discussion

Given the scarcity of field information about sediment characteristics across asymmetrical sand waves, the aim of our field campaigns was to determine the sedimentological properties of these bedforms. Therefore, we discriminated between different MUs (gentle slope, crest, steep slope, trough) and showed that this leads to measurable changes in the sediment characteristics. On the one hand, our results are consistent with previous field studies in that the sediment is mostly coarser in crests than in the troughs (Terwindt 1971; Van Lancker and Jacobs 2000; Stolk 2000; Passchier and Kleinhans 2005; Svenson et al. 2009). However, in addition to these studies (van Dijk and Kleinhans 2005; Baptist et al. 2006; Roos et al. 2007; van Dijk et al. 2012), we improved upon the sampling resolution by dividing the sand waves into smaller sections (e.g., 4 MUs). Whereas it was difficult to equally sample all MUs from every sand wave (Figure 2.3C), we successfully sampled many stations (16 in June; 18 in October) along four sand waves, and collected 102 samples in total. Bathymetric data were recorded during both campaigns, but we were not able to determine the actual migration rate of our sand waves due to the vessel's technical limitations (see Section 2.3) and also the many known sources of possible error, such as positioning, bed level noise, and depth distortions. However, previous calculations on several sand wave locations with similar orientations within the Dutch North Sea show a migration rate ranging from less than 1.0 to 8.4 m yr^{-1}, with an error of up to 2 m (Knaapen 2005), and some of these figures may even have been overestimated (van Dijk et al. 2008). Although information about the migration rate of the Texel sand waves is not presently available, it is a relevant aspect that should be taken into consideration by future studies concerning dynamic bedforms.

The difference in sediment median grain size (D_{50} in µm) between crests and troughs was up to 25% of the mean and much greater than found in sand waves of comparable size and dimensions from other studies (van Dijk and Kleinhans 2005; Baptist et al. 2006; Roos et al. 2007). Moreover, the sediment coarsened from the gentle slope towards the crest, while the three finest fractions of sediment exhibited significantly higher percentages on the steep slope and trough sections (Figure 2.5, right panels). These results suggest that sediment sorting along the asymmetrical bedforms effectively creates a distinct gradient between the crest and trough boundary, subdividing the sand waves into two halves: the gentle slope up to the crest, and the steep slope down to the trough. Our higher-resolution sampling thus clearly demonstrates that asymmetrical sand waves are highly complex bedforms with respect to sediment granulometry, permeability, and biogeochemistry.

Sediment permeability generally correlates positively with increasing grain size (Wilson et al. 2018). In line with this, permeability was about twice as high on gentle slopes compared to the troughs in the summer, while in autumn the largest difference was between the crests and troughs. Permeability is a measure for the degree to which currents and waves penetrate the sediment; this has a crucial effect on the sediment nutrient or oxygen levels and the organic carbon concentrations. It has been shown that in sediments with a permeability of $\geq 10^{-12}$ m^2, advective transport mechanisms become significant in regulating biogeochemical processes (Wilson et al. 2008; Santos et al. 2012; Serpetti et al. 2016). While all of our samples exceeded that threshold, the greater than two-fold difference means that solute transport could potentially occur at twice the rate in the coarsest areas of the sand wave. This also suggests that subtle biogeochemical differences might be found between the more permeable gentle slope and crest part of the sand waves, compared to the steep slope and trough.

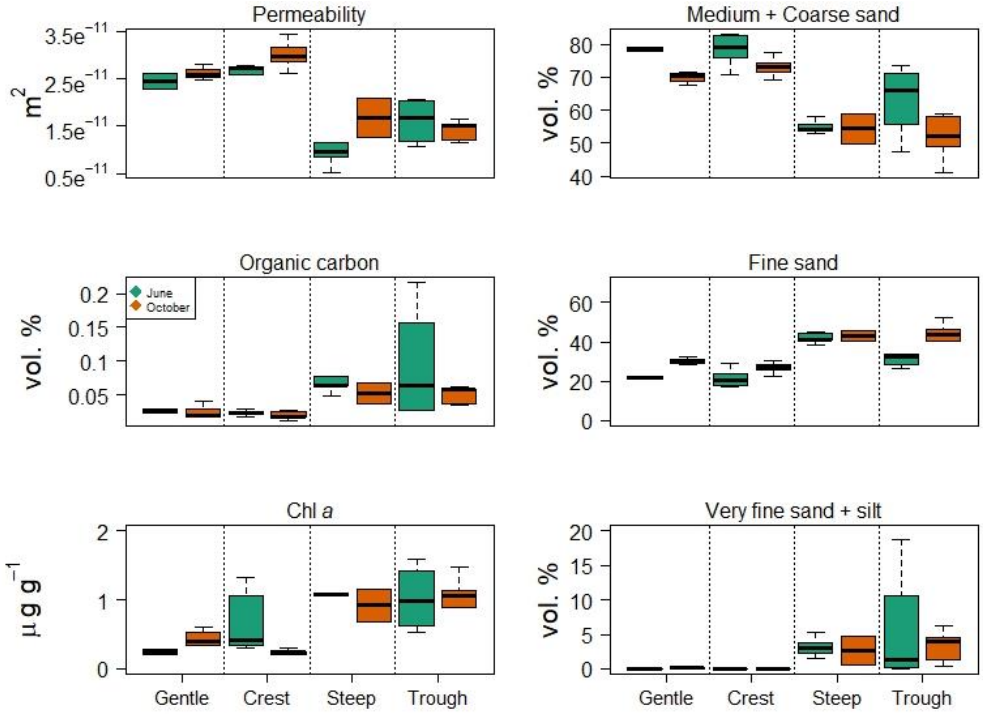

Figure 2.5. Comparison of selected sediment grain size parameters, organic carbon, chl *a* and permeability between June and October, averaged over the sand wave MUs. The coarse - medium fractions and the very fine sand – silt fractions were combined as these pairs followed the same trends over the MUs.

Organic compounds are known to accumulate more in finer sediments; in particular, their concentrations are related to the mud and silt fractions (Hedges and Keil 1995; Burdige 2007; Bianchi 2011; Serrano et al. 2016). In line with this, we found the chl *a* and organic carbon concentrations to be significantly higher on the steep slope and troughs. Chl *a* is a measure for the readily consumed (e.g., labile) fraction of organic matter, so higher concentrations can support higher overall metabolic activity in the sediment. This is consistent with the higher benthic biomass and activity found in the trough (Damveld et al. 2018). Furthermore, it is also relevant here, since benthic organisms can redistribute the upper layers of sediment, enabling the burial of fine material. A video transect study on the crest-trough comparisons showed four times more animals living on the sediment (epibenthos) and 30 times more holes (a proxy used for endobenthos) in the troughs, although the species composition could not be quantitatively determined based on this information (Damveld et al. 2018). In addition, Damveld et al. (2018) observed either highly irregular bedforms, or sometimes the complete absence of them in the troughs of the Texel sand waves. Such smaller bedforms are often superimposed on sand waves and are important as they alter the bed roughness and can slowly migrate along the gentle slope (Dalrymple 1984; van Santen et al. 2011; Hanes 2012).

Differences among MUs were clearly observed over all sand waves and during both seasons of sampling. Surprisingly, however, there were also some notable differences between June and October, although they were less pronounced than the spatial gradients. There was significant seasonal variability in some sediment fractions, sediments being coarser in June, while both the organic carbon and chl *a* content were significantly higher in June. The seasonal differences observed in sediment composition could be due to extreme weather conditions (e.g., storms), which may have winnowed the sediments preceding our June campaign, while fine particles may have accumulated in the sand between the June and October field campaigns (Baptist et al. 2006; Kröncke et al. 2013). The higher chl *a* concentration might be related to the spring phytoplankton bloom being deposited on the sediment preceding our June campaign (Boon and Duineveld 1998; Franco et al. 2010; Rumyantseva et al. 2019). Contrary to expectations, however, sediment permeability was found to be lower in June, notwithstanding the sediments being coarser. As a consequence, the relationship between permeability and D_{50} is ambiguous, showing a dependency on both the grain size and the season (Figure 2.6). This seems consistent with studies pointing to factors other than D_{50} that can also affect permeability, such as the grain shape, type of sediment, or sediment structure (Gabas et al. 1994; Kaye et al. 1997; Neumann et al. 2016)**.** It is also possible that the seasonal dependency is linked to the higher concentration of

organic carbon in June, as organic compounds in the silty fraction can alter the cohesiveness of the sediment (Hedges and Keil 1995; Burdige 2007; Mietta et al. 2009; Bianchi 2011; Serrano et al. 2016). Biogenic substances such as chl *a*, organic matter, and biofilm compounds (e.g., extracellular polymeric substances) can increase sediment flocculation or cohesion at the microscale level and have consequences on transport processes on local or even larger scales (Gerbersdorf et al. 2008; Mietta et al. 2009; Bauer et al. 2013; Decho and Gutierrez 2017). Although this was beyond the scope of our study, other properties such as sediment structure and type should also be considered in future studies, as they could have an effect on grain size determinations (Eshel et al. 2004; Blott and Pye 2006; Neumann et al. 2016).

Tidal sand waves are ubiquitous bedforms and occur over a broad range of dimensions in sandy shelf seas. Our field results demonstrate that asymmetrical sand waves exhibit significant spatio-temporal complexities in sediment sorting[4] over small spatial scales, due in part to their irregular shape. While we found consistent spatial trends over two seasons, there is also evidence that these trends are modulated by other factors, probably of biological or biogeochemical origin.

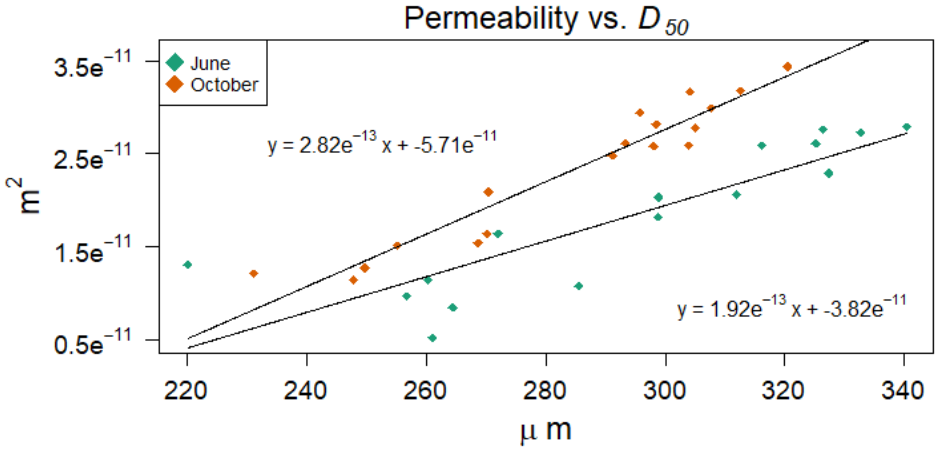

Figure 2.6. Comparison of the relationship between permeability and the D_{50} between the two seasons. The individual regressions are shown[5].

[4] For additional background about sediment sorting along sand waves, in river environments and flume studies, see Kleinhans; Powell 1998; Blom et al. 2003; Murray and Thieler 2004; van den Berg et al. 2010; Martinius and van den Berg 2011; Escobar et al. 2019 and others therein.

[5] The R^2 values are 0.75 ($p < 0.05$) for June and 0.93 ($p < 0.05$) for October.

2.5 Conclusions

The sorting of sediment along sand waves with an asymmetry value of 0.29–0.38 was studied at a sand wave field in the Dutch Continental Shelf over two seasons. By classifying the sand waves into four morphological units (gentle slope, crest, steep slope, and trough), we were able to demonstrate significant differences in the sediment grain size, organic carbon concentration, chl *a* content, and permeability. The average D_{50} differed by more than 20% (>60 µm difference in June and >50 µm in October), and permeability by more than two-fold between the crests and troughs, as well as between the crests and steep slopes. This was even more pronounced for the biogeochemical compounds of organic carbon and chl *a*, with differences from 4- to 8-fold. Moreover, all of these patterns were observed over two seasonal campaigns. This study sheds light on the small-scale processes that couple the dynamics of sand wave morphology and sediment characteristics, and contributes information previously unavailable to help improve physical or ecosystem models to better understand these environments.

Author Contributions: The listed authors in this manuscript have each contributed significantly to the collection of data, analysis and interpretation of the results, and drafting of the paper. Furthermore, each author has contributed substantial time to the editing and revising of each individual section within the manuscript. The study was initiated by the first and second authors, C.H.C. and K.S., who were also fully involved in the methodology, field campaigns, and sample collection. Data analysis was primarily conducted by C.H.C., but K.S. and B.W.B. contributed as well. Discussions of the manuscript content involved all of the co-authors (C.H.C., B.W.B., and K.S.) throughout the drafting and interpretation of the contents. Each co-author also contributed to the final stages of the writing and review. All authors have read and agreed to the published version of the manuscript.

Funding: This research was funded by the SANDBOX project, which is a part of NWO-ALW (Nederlandse Organisatie voor Wetenschappelijk Onderzoek-Aard-en Levenswetenschappen). The Royal Boskalis Westminster N.V., the Royal Netherlands Institute for Sea Research (NIOZ), and Utrecht University are acknowledged for their financial support of this project.

Acknowledgments: Many thanks to Erik Hendriks, Johan Damveld, Sarah O'Flynn, Justin Tiano, Karin van der Reijden, Leo Koop, Rob Witbaard, Pieter van Rijswijk, and Anton Tramper, who contributed to the sample collection and data contribution for this project from the cruise

campaigns. We are very grateful to Texel NMF staff for their support in making both research campaigns successful, and to Henk de Haas for his help with the MBES data and other technical details. Thanks, also, to Peter van Bruegel for the analysis of the sediment samples, Natalie Steiner for helping with the statistical analyses, Jaco de Smit for the cumulative grain distribution analyses, and the many other colleagues who offered assistance along the way. The data collected for this publication can be found in the 4TU Centre for Research Data repository at the following link: 10.4121/uuid:9f6e21c5-f35b-4bca-a468-7534e04bb240. Lastly, we want to thank the reviewers for all of their input, which aided us in further improving this manuscript.

Supplementary Materials for Chapter 2:

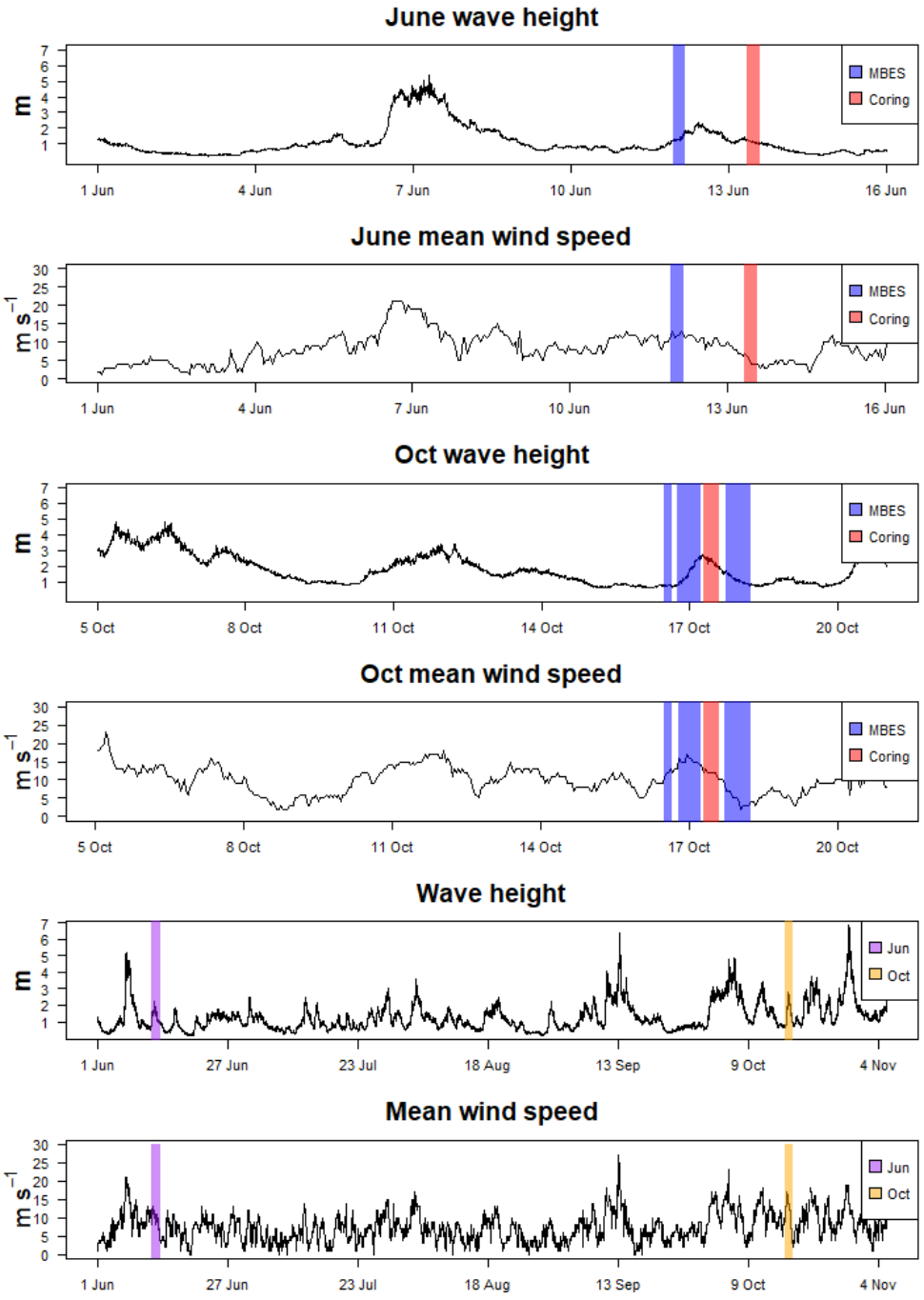

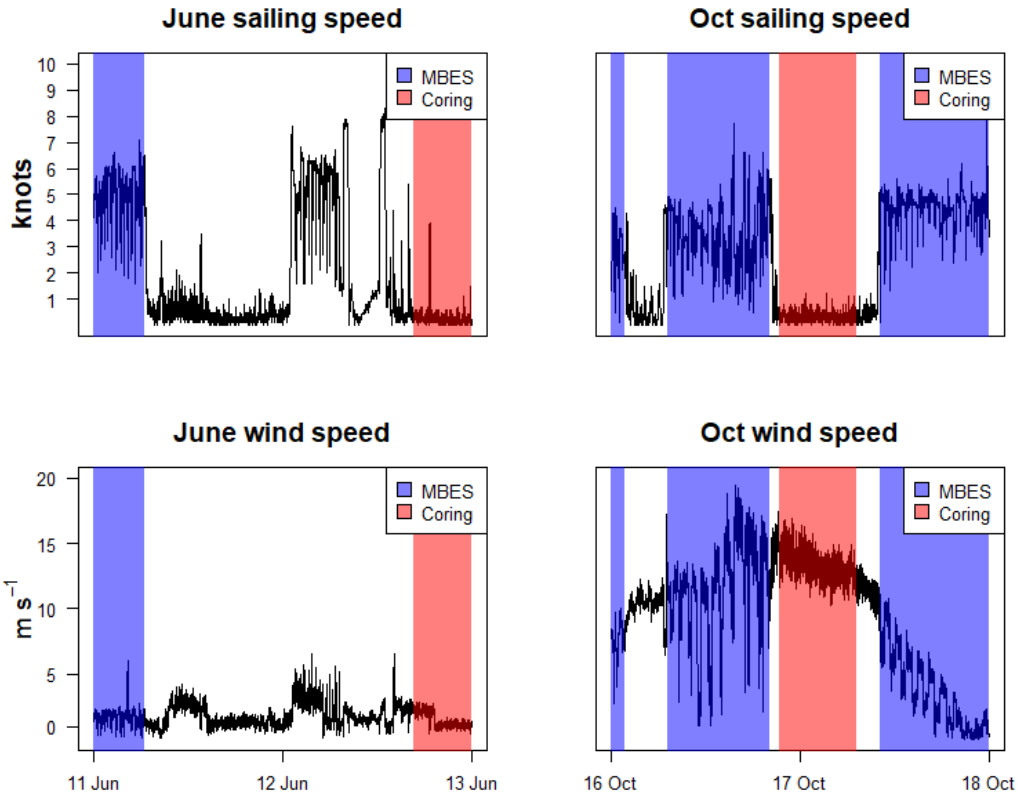

Figure S2.1. Wave height and mean wind speed during each campaign. The timing and duration of each sampling gear deployment are indicated. Panels 5 and 6 show the period from 2 weeks before the June campaign through the entire October campaign, Here, sampling intervals cover both the "MBES" and "Coring." The bottom 4 figures show the sailing speed of the *RV – Pelagia* and the wind speed during sampling. The data for June was downloaded from the Eierlandse Gat Buoy from waterinfo.rws.nl. The October data is from the Q1A Stappenbaak buoy, due to poor resolution in wave height information for October from Eierlandse Gat. Wind data was obtained from the 204-K14-FA-1C station (https://www.knmi.nl/nederland-nu/klimatologie/uurgegevens_Noordzee). The sailing speed and wind speed of the bottom four figures were obtained from the *RV – Pelagia's* logging system.

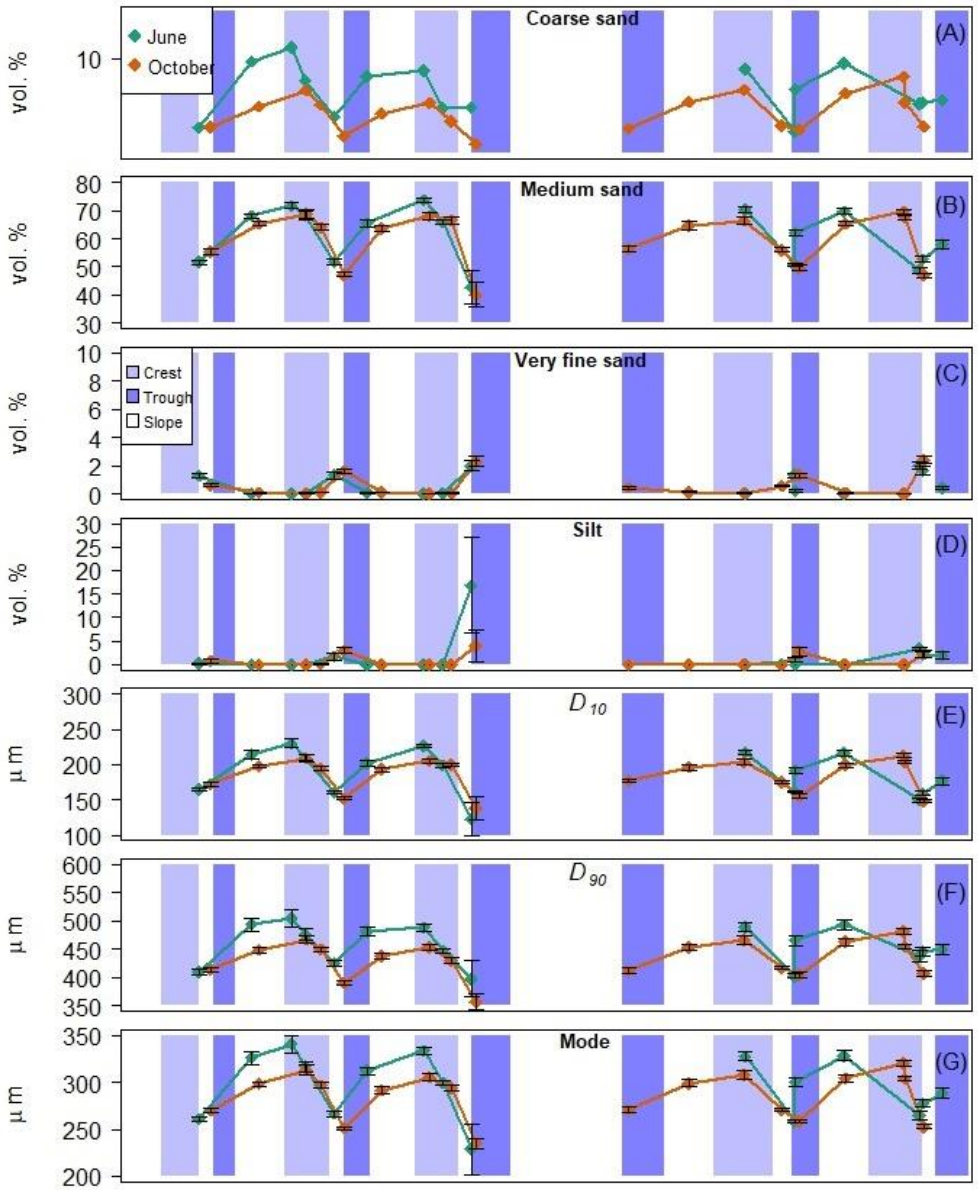

Figure S2.2. Additional grain size information**.** Panels A-D show the other four fractions of sediment by percentage. Panel E shows the D10, which is the average grain size in which 10% of the total sample falls below this value. Panel F is the D90, which means that 90% of the sample falls below this average grain size. Panel G is the mode, which is the most abundance size in the distribution.

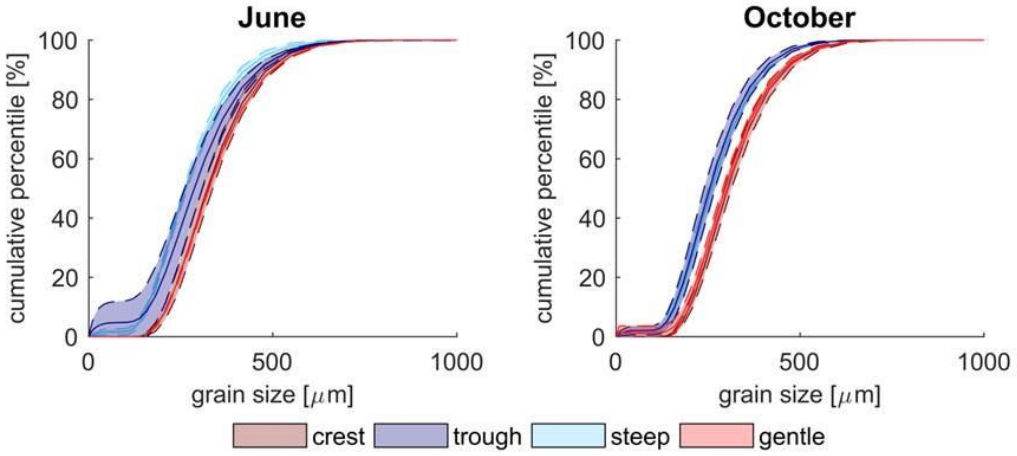

Figure S2.3. Sediment cumulative distribution plots. Samples are grouped by campaign and MUs. Dark solid lines represent average values (from all samples of each MU) and the dotted lines/lighter color shades represent the standard deviation.

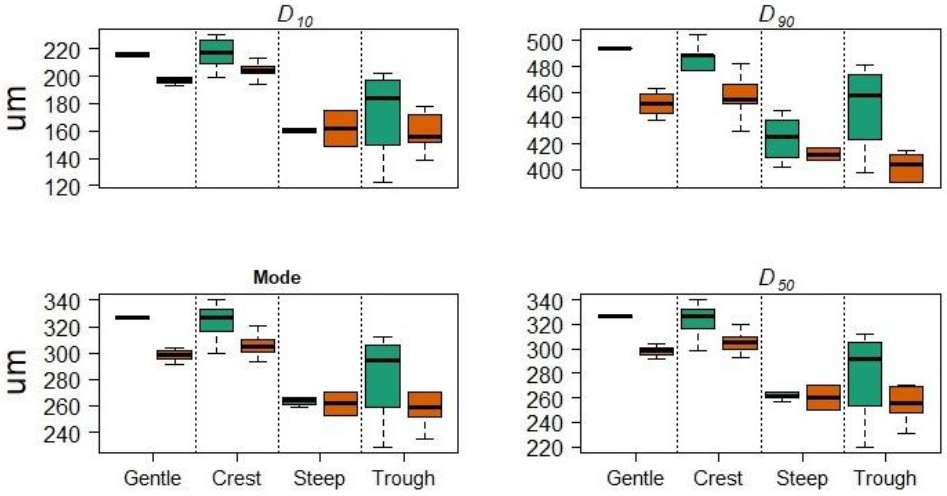

Figure S2.4. Other grain size parameters. Comparisons between June and October, averaged over the sand wave MUs.

Table S2.1: Sediment results

Averages and standard deviation (SD) of permeability and grain size per MU and season. See material and methods for a definition of these variables. For chl *a*, no SD is available.

	Crest		**Gentle slope**		**Trough**		**Steep slope**	
	June	**Oct**	**June**	**Oct**	**June**	**Oct**	**June**	**Oct**
Permeability (m^2)								
Mean (E^{-11})	2.54	3.01	2.45	2.6	1.64	1.42	0.901	1.68
SD (E^{-12})	±5.17	±3.77	±3.13	±2.91	±7.3	±2.26	±3.99	±4.88
Sediment								
D_{50} (µm)	322.92	305.44	326.52	298.07	279.37	254.76	262.92	260.15
SD	±16.27	±10.02	±3.69	±6.05	±41.1	±16.75	±5.998	±11.64
Coarse sand (vol. %)	8.2	5.75	9.6	5.22	6.28	2.1	3.83	2.82
SD	±2.46	±1.54	±0.28	±1.01	±1.65	±0.79	±1.36	±0.42
Medium sand (vol. %)	70.01	67.18	68.85	64.75	57.14	49.82	51.09	51.53
SD	±2.96	±2.14	±1.77	±1.48	±9.81	±6.89	±1.63	±4.97
Fine sand (vol. %)	21.74	27.01	21.54	29.94	31.36	44.77	41.93	43.06
SD	±4.95	±3.23	±1.67	±2.04	±4.19	±4.83	±2.67	±3.06
Very fine sand (vol. %)	0.019	0	0.0167	0.09	0.67	1.26	1.51	1.48
SD	±0.025	±0.04	±0.01	±0.05	±0.85	±0.8	±0.35	±1.04
Silt (vol. %)	0	0.0196	0	0	4.55	2.04	1.64	1.11
SD	0	±0.09	0	0	±9.06	±2.76	±1.21	±1.39
Organic C (%)	0.023	0.033	0.026	0.024	0.097	0.048	0.071	0.054
SD	±0.008	±0.18	±0.008	±0.012	±0.185	±0.027	±0.035	±0.024
Chl *a* (µg g^{-1})	0.686	0.228	0.251	0.431	1.023	0.994	1.94	0.92

Table S2.2: Statistical results

Statistical values from the ANOVA and TukeyHSD tests. Values[6] below 0.05 are considered statistically different in both tests. The letters "C," "S," "T" and "G" represent the four respective MUs, which are compared over every possible combination of pairs.

	3-way ANOVA			TukeyHSD					
	MU	**Sand wave**	**Season**	**C - S**	**C - G**	**C - T**	**S - G**	**S - T**	**G - T**
Perm.	1.14 E^{-13}	0.79	0.001	<.0001	0.87	<.0001	<.0001	0.896	<.0001
***D*$_{50}$**	2.20 E^{-16}	0.86	1.38E^{-05}	<.0001	9.94E^{-01}	<.0001	<.0001	0.18	<.0001
Coarse	4.10 E^{-12}	0.33	1.22E^{-11}	<.0001	0.88	<.0001	<.0001	0.082	<.0001
Medium	2.00 E^{-16}	0.52	0.02	<.0001	0.999	<.0001	<.0001	0.36	<.0001
Fine	2.20 E^{-16}	0.98	6.64E^{-06}	<.0001	9.98E^{-01}	<.0001	<.0001	0.063	<.0001
Very Fine	2.15 E^{-10}	0.34	0.54	<.0001	0.85	0.0001	<.0001	0.079	0.0001
Silt	0.00019	0.35	0.93	0.22	0.899	0.0008	0.12	0.62	0.0011
Org Car.	1.00 E^{-02}	0.32	0.22	0.34	0.87	0.057	0.18	0.98	0.03
Chl *a*	4.60 E^{-01}	0.27	0.1	0.991	0.82	0.91	0.75	0.99	0.53
Chl *a***	1.10 E^{-04}	0.49	0.13	0.0049	0.999	0.002	0.0114	0.99	0.0078

**the single outlier value removed.

[6] These are the p-values from the statistical analyses.

Chapter 3

Small-scale macrobenthic community structure along asymmetrical sand waves in an underwater seascape

Chiu H. Cheng[1], Bas W. Borsje[2], Olivier Beauchard[1,4], Sarah O'Flynn[1], Tom Ysebaert[1,3] and Karline Soetaert[1]

[1]NIOZ Royal Netherlands Institute for Sea Research, Department of Estuarine and Delta Systems (EDS), 4401NT Yerseke, Zeeland, the Netherlands. [2]Water Engineering and Management, University of Twente, 7500AE Enschede, Overijssel, the Netherlands. [3]Wageningen Marine Research, Wageningen University & Research, 4401NT Yerseke, Zeeland, the Netherlands. [4]Ecosystem Management Research Group, University of Antwerp, 2610 Wilrijk, Antwerp, Belgium

Published as

Cheng, C. H., Bas W. Borsje, Olivier Beauchard, Sarah O'Flynn, Tom Ysebaert and Karline Soetaert. 2021. Small-scale macrobenthic community structure along asymmetrical sand waves in an underwater seascape. Marine Ecology. **42**: 1–15. doi.org/10.1111/maec.12657

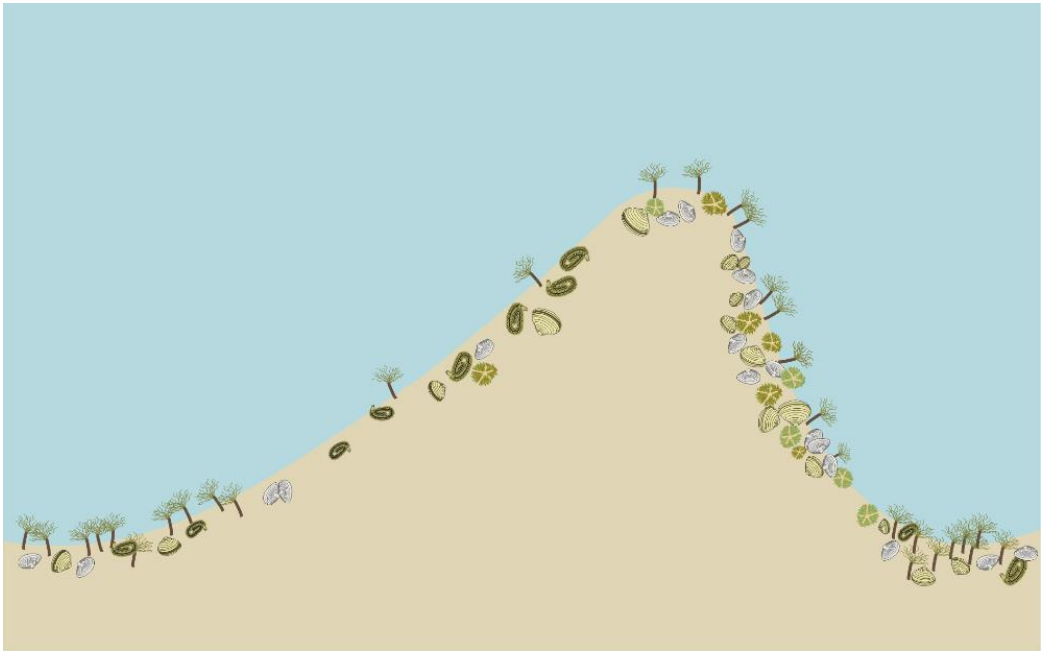

Schematic by Chiu H. Cheng

Abstract

Sand waves are dynamic and regular bedforms that are ubiquitous in sandy shelf seas. However, information about the ecological characteristics (e.g., benthic community structure) and their spatial variability within these habitats is very limited. To address this knowledge gap, we undertook a field campaign in summer 2017 to investigate the macrofaunal community composition of a sand wave area off Texel (Dutch part of the North Sea). Sand waves in this area were asymmetrical, with longer gentle slopes that were approximately double in length to the shorter steep slopes. The benthic distribution along the different parts of these sand waves was assessed by collecting a large number of box cores within a transect line (~ 1 km). We show considerable variability in the individual, biomass and taxon densities, which were all significantly higher on the steeper slopes of the sand waves. These results are consistent with the trends observed in both the abiotic parameters and video analysis that were measured in two recent studies at the same study area. Our results provide valuable insight into the small-scale patterns of variability in asymmetrical dynamic bedform environments, where gentle slopes seem to be primarily controlled by physical forces, while steep slopes are more under biotic control.

Keywords: Biogeomorphology, biological traits and functional traits, macrobenthos, sand waves

---

3.1 Introduction

In many coastal regions worldwide, the sandy seabed is seldom static or flat, but oftentimes, many types of bedforms can be found, as is the case in the Dutch sector of the North Sea (Borsje et al. 2009b). While many of these bedforms are rhythmic in nature, they can be differentiated based on their spatial dimensions. These include the largest sand banks of up to 10 km in length and 30 m in height, down to small sand ripples that are on the order of tens of cms in length and several cms in height; in between this range are several intermediaries such as megaripples (up to 10 m long, tens of cm in height) and sand waves (100-1000 m long, up to 10 m high) (Morelissen et al. 2003). Though development of these bedforms are largely driven by hydrodynamic and physical (e.g., sedimentary) processes, other factors such as benthic organisms are believed to also play an important role in shaping the sedimentary and hydrodynamic conditions of these environments (Borsje et al. 2009a; Damveld et al. 2019). This is particularly the case for the meso-scale sand waves, which are the focus of this study here.

Sand waves are found over a range of dimensions and with shapes that can be quite variable, from highly symmetrical to very asymmetrical (e.g., one side is much longer and with a gentler gradient) (Liao and Yu 2005; Baptist et al. 2006; Barnard et al. 2006; Besio et al. 2008). Similar to other rhythmic bedforms, tidally-driven sand waves are commonly found throughout shallow sea environments (e.g., North Sea), as well as some tidal inlets around the world (van Dijk and Kleinhans 2005; Besio et al. 2008; van Santen et al. 2011; Borsje et al. 2014; Wang et al. 2019). In the Dutch sector of the North Sea alone, these sinusoidal features have a wide distribution over a broad range of dimensions (Damen et al. 2018; Cheng et al. 2020). But a key defining feature is their ability to migrate at rates of several meters per year or more (Németh et al. 2002; Knaapen 2005; van Dijk et al. 2008), making them especially interesting both scientifically and economically. Abundant modeling studies on sand waves have been undertaken over the past decades in terms of the hydrodynamic and morphological processes, using different process-based models to predict their behavior (Hulscher 1996; Besio et al. 2004; Borsje et al. 2009b, 2013).

In addition to the physical aspects, sand waves are also ecologically important habitats for many benthic invertebrate organisms residing in the seabed, yet there is far less information available regarding the biological and biogeochemical aspects of these environments. All ecosystems invariably undergo natural disturbances, particularly from extreme events such as storms and anomalies in seasonality. However, anthropogenic activities, such as fishing, shipping, sand mining and oil and gas production, have increasingly been exerting additional pressures on such environments (Jennings et al. 2001; Kaiser et al. 2002; Halpern et al. 2015; de Jong et al. 2016). These activities are expected to further surge in the foreseeable future and are thus of particular relevance for sand wave environments, given their location within regions of high economic interest (Jongbloed et al. 2014). This is further exacerbated by the growing demands for alternative energy sources as well as increasing concerns due to climate change and sea level rise, necessitating ever more coastal protection. As such, many of these areas are anticipated to be impacted by activities such as sand mining or offshore windfarm construction (Deltacommissie 2008; de Jong et al. 2014b, 2016; Jongbloed et al. 2014; de Vrees 2019).

The sediment-inhabiting infauna is well-suited for comparative studies on spatio-temporal benthic ecosystem changes, due to a combination of low mobility and relatively long life spans (Reiss et al. 2010). Furthermore, greater biological diversity in an environment is generally perceived as a positive quality for having higher resiliency to environmental stresses and facilitating higher rates of biological activity such as primary and secondary production,

nutrient cycling and biogeochemistry (Hooper et al. 2005; Cardinale et al. 2012). Moreover, some species within the macrobenthos have been clearly shown to play a significant role in ecosystem functioning by acting as ecosystem engineers (Jones et al. 1994; Bouma et al. 2005; Braeckman et al. 2010; Van Colen et al. 2013). Characterizing these groups based on their functional traits in the context of environment and stressors is a useful way to gain insight about the ecology of a habitat, which is also intrinsically connected to the geomorphology (Pearson 2001; Dolan et al. 2012). In sand wave environments, organisms that change the roughness of the seabed by the creation of hard structures, by burrowing or excavating the sediment or through their pumping activity (e.g., bioturbation, bioirrigation), may be particularly influential as they alter the sediment distribution. All of these processes, facilitated largely by ecosystem engineers (Jones et al. 1997; Meysman et al. 2006; Jones 2012), can have consequences for the local geomorphology of the seabed. Moreover, these small-scale processes can even cumulatively cascade up to the sand wave environment as a whole, since ecosystem engineers often exhibit a positive effect on ecosystem functioning by facilitating greater sediment heterogeneity, resource partitioning, biogeochemical activity and overall habitat stability (Lohrer et al. 2004; Rabaut et al. 2010). Consequently, these conditions can facilitate greater biodiversity by increasing the utilization potential of the given habitat, thereby allowing organisms to make better use of the available resources (space, nutrients, food, etc.) (Bruno et al. 2003; Crain and Bertness 2006), which could then further influence the surrounding habitats (Rabaut et al. 2007).

However, the significance of the benthic community for the ecosystem functioning (e.g., biogeochemical activity, biodiversity, etc.) within the sand wave environment is still largely unclear or inconclusive. Given the logistical challenges of subtidal field sampling, relatively few campaigns have been carried out in these environments, in contrast to the ample studies from laboratory flume experiments or modeling simulations (Best and Kostaschuk 2002[7]). Thus, field information regarding the sedimentary and hydrodynamic conditions of offshore sand waves are scarce (Kleinhans et al. 2009; Paarlberg et al. 2009; Janssen et al. 2012). Although some of the available field studies have considered more than just the theoretical or physical aspect of sand wave habitats, very few (if any) have specifically focused on characterizing the benthic community composition in the context of their potential influence on the biogeochemical and sedimentological processes along the sand waves, all within the same campaign (Terwindt 1971; Van Lancker and Jacobs 2000; Stolk 2000; Passchier and Kleinhans 2005; Svenson et al. 2009).

[7] See the cited references therein for examples of past field or flume studies.

Even when available, many of these small-scale studies on benthic communities have been motivated by very specific environmental issues, such as trawling, sand mining or oil and gas work, rather than the direct influence of morphology (Kröncke and Bergfeld 2003; Baptist et al. 2006). Consequently, much of our understanding about sand waves is derived from modeling studies (Hulscher, 1996; van Dijk and Kleinhans, 2005; Van Oyen et al., 2013; Van Oyen and Blondeaux, 2009; Borsje et al. 2014).

In order to further unravel the spatial variation in both environmental parameters and benthic infauna in a sand wave environment and their effect on ecosystem functioning, a cruise campaign was undertaken on board the NIOZ *RV-Pelagia* in June 2017 to measure not only the environmental parameters, but also determine the sediment characteristics and the benthic community composition in a sand wave area off Texel. Our study complements two other studies from the same cruise. The first was a video transect study of the epibenthic community composition, the endobenthic individual abundance and ripple occurrence/regularity through visual quantification using video footage. The aim of this study was to look for differences between the crest and trough (Damveld et al. 2018). The second study addressed the sediment characteristics along four different areas of the sand waves, and showed a significant difference in the abiotic parameters based on the positioning (Cheng et al. 2020). Based on this information, we hypothesize that geomorphology of the sand wave bedform will have a significant influence on the benthic community structure.

Here we present new information about the benthic community structure and the associated biogeochemical processes along a sand wave field. We investigate (a) if there is a measurable pattern in how benthic communities are organized along the sand wave continuum, (b) and what the most revealing and extreme functional types of communities may be.

3.2 Materials and Methods

3.2.1 Study area description

All of the benthic macrofauna samples were collected onboard the NIOZ *RV – Pelagia* in the summer (June) of 2017. The study area is a sand wave field situated approximately 22 km to the west of island Texel (53°11.241' N; 4°28.628' E; Figure 3.1), and these sand waves have a northwest orientation, roughly perpendicular to the coast (Damveld et al. 2018). This area has a relatively sandy seafloor and a water depth between 20-30 meters. Prior to sampling, we mapped

the study area (~1 km x 3.5 km) with a Kongsberg EM302 Swath Multibeam echo sounder (MBES). The sampling transect and stations were chosen based on the MBES information (Figure 3.1c). For further technical details about the post-processing of the MBES data and the sampling capabilities and accuracy of the vessel, see Cheng et al. (2020). Adjacent to the sampling area are two shipping lanes that closely flank it on the east and west sides. As a result, the demersal fishing activity is very low in this area (Damveld et al. 2018). The temperature and salinity was approximately 15.2 °C and 34.6 ppt. The sand waves ranged from 2.8 to 3.5 m in height and 160 to 210 m in length.

The Texel sand waves are overall sandy in nature with an average median grain size (D_{50}) > 250 µm, and with an asymmetry level of about ~0.29-0.38 (0 is fully symmetrical, 1 is fully asymmetrical). Consequently, the sediment composition, permeability, chlorophyll *a* (chl *a*) and organic carbon largely differed between the two sides, where the gentle slope/crest were on average coarser, with a D_{50} about 40-60 µm higher, compared to the steep slope/trough (Table 3.1; Cheng et al. 2020). The silt and very fine sand fractions were almost entirely absent on the gentle side of the sand waves. Furthermore, the occurrence of sand ripples also significantly differed between the crest (abundant and regularly shaped ripples) and the trough (low abundance with highly irregularly shaped ripples) (Damveld et al. 2018). As these are important parameters for biogeochemical cycling and the transport of particulate matter and solutes, these spatial patterns could have important ramifications for the benthic community as well.

Table 3.1. Select sediment parameters between the different habitats (data from Cheng et al. 2020).

	Crest		Gentle slope		Trough		Steep slope	
	Mean	**SD**	**Mean**	**SD**	**Mean**	**SD**	**Mean**	**SD**
Permeability (m^2)	2.54 E^{-11}	±5.17 E^{-12}	2.45 E^{-11}	±3.13 E^{-12}	1.64 E^{-11}	±7.3 E^{-12}	0.901 E^{-11}	±3.99 E^{-12}
D_{50} (µm)	322.9	±16.27	326.5	±3.69	279.4	±41.1	262.9	±5.998
Org. carbon (%)	0.023	±0.008	0.026	±0.008	0.097	±0.185	0.071	±0.035
Chl *a* (µg g^{-1})	0.69	±0.47	0.25	±0.05	1.02	±0.48	1.94	±1.76
Water depth (m)	-28.53	±0.14	-30.08	±0.52	-31.75	±0.16	-29.27	±0.85

Sampling was carried out along one transect line, which measured ~1,100 m in length and covered five, full sand waves (Figures 3.1b and c). We positioned all of our sampling stations along the 4 highest sand waves to maximize the gradient between the crests and troughs (e.g., the steepness of the sand wave flanks on both sides). In total, 16 stations were positioned at the center of each part of the sand wave (gentle slope, crest, steep slope and trough). The NIOZ Box corer

(K6 model) was deployed to obtain macrofauna samples at each station. All samples fell between -32.04 and -28.25 m water depth (Figure 3.1c).

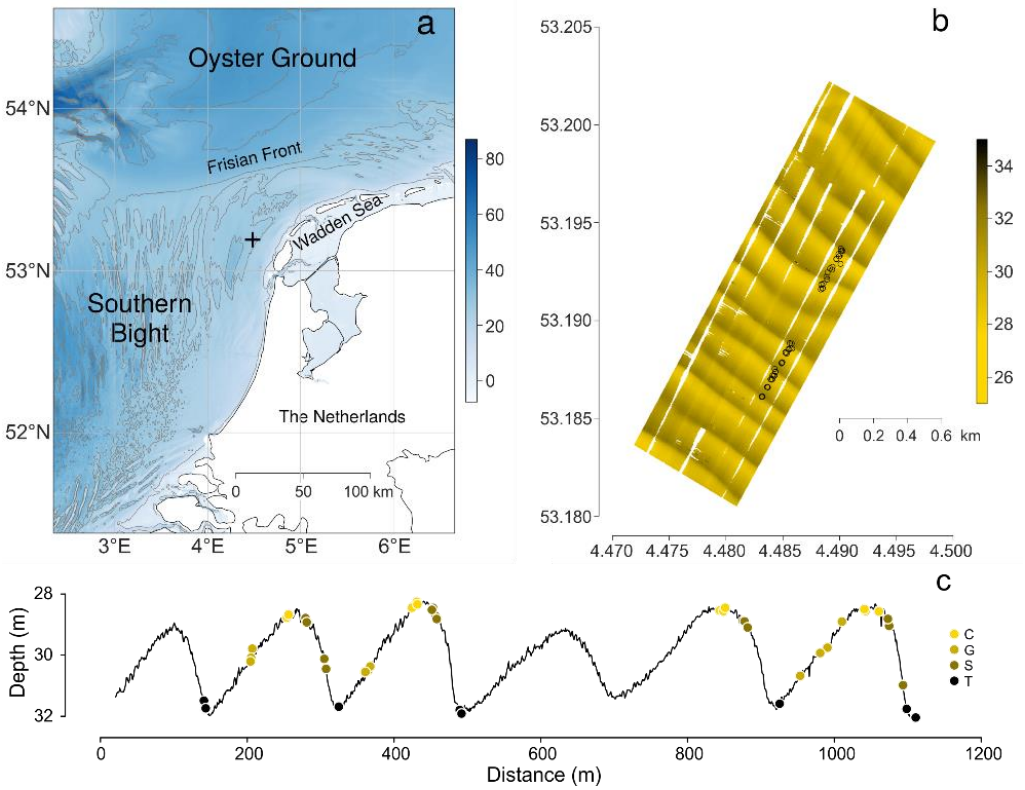

Figure 3.1. Study area[8]. a) "+" indicates the location of the studied sand wave field in the southern North Sea. b) Close up of the sand wave field (processed and gridded MBES data); dots indicate benthic sampling stations. c) Cross section of the sampled transect from south to north; dots, benthic sample locations (n = 48): "G" ,"C", "S" and "T" for gentle slope, crest, steep slope and trough habitat, respectively. Color bars in a and b indicate depth in meters.

3.2.2 Benthic macrofauna sampling

The dimension of the NIOZ box corer (K6 model) was approximately 32 cm in diameter and 55 cm in length, with the complete frame weighing about 850-900 kg. The entire frame was lowered onto the seabed, followed by the corer being pushed into the sediment by the integrated lead weights. An attached blade sealed the bottom of the box core upon retrieval of the frame. At

[8] The two axes from Figures 3.1 a and b represent the latitude (y) and longitude (x).

every station, three replicates were collected with the box corer. In total, 48 samples were collected. All of the sediment collected from each box core was sieved on a 1-mm mesh, preserved in a 4% buffered formalin solution and stored into plastic bottles or buckets, depending on the sample size.

The benthic macrofauna were analyzed by taxonomic experts located on NIOZ-Texel, to the lowest taxonomic unit possible. Each individual was first counted, then weighed[9]. In the latter case, the blotted fresh weight was obtained from each identified sample. This enabled the description of community patterns based on three densities: individual, biomass and taxon. From this, the main biological traits were also assigned to each taxa based on information from literature (Queiros et al. 2013 and others therein).

3.2.3 Habitat identification

3.2.3.1 Relative positioning of samples and habitat identification

The position of each box core sample was determined relative to its respective sand wave, because each of them were slightly different in length and height (Figure 3.1c); this way, it would be possible to compare all samples. Based on the average asymmetry of the sand waves, each one was then rescaled to a range of -1.0 to 0.53, with both ends representing the troughs and the crest situated at 0.0. The unequal scale approximates the asymmetry of the sand waves, where the gentle side is roughly double in length to that of the steep side. The macrofauna individual counts, biomasses and taxon densities were first compared on this relative scale to show the total distribution.

In addition, the box corer samples were initially categorized using a similar methodology from Cheng et al. (2020), where the sand waves were divided into four morphological units (MUs): gentle slope, crest, steep slope and trough. This was determined based on the original dimensions of each respective sand wave, and not the rescaled one. As with the previous study on the sediment characteristics, this method also yielded satisfactory results for the community composition categorization, overall. However, initial statistical analyses showed a strong dichotomy between the stations located within the gentle-slope -half of the crest vs. the stations found very near the interface between the crest and steep slope. Thus, the latter stations were grouped with the other steep slope stations instead, but no further modification was made to the

[9] The shells of the bivalves were not removed.

methodology. For the purposes of the macrofauna distribution, each of these MUs was considered as a separate "habitat" within the sand wave, and all references will use this terminology thereafter.

3.2.3.2 Benthic community analyses

Firstly, we investigated the organism density trends along the sand wave gradient; the significance of habitat effect was assessed by Kruskal-Wallis rank sum test (Kruskal and Wallis 1952) and Dunn test (Dunn 1964). The latter is a non-parametric post hoc test that is used to show where the significant differences are occurring. Since the analyses involved multiple comparisons on the same variables, a Bonferroni correction was also applied. This limits the chance for Type 1 errors by lowering the alpha value. Then, we explored the community structure across the four habitats by means of a Between-Class Analysis (BCA; Dolédec and Chessel 1987, Thioulouse et al. 2018). BCA builds axes of maximum covariances between the taxa that discriminate each habitat to the greatest extent. Prior to the BCA, we processed *ln*-transformed individual densities of organisms by centred Principal Component Analysis (PCA). The effect of the habitat on the variation of community structure was tested based on 999 random permutations of the samples × taxa matrix (Manly 1991). The BCA is equivalent to a Redundancy analysis (RDA) when performed on a unique qualitative explanatory variable (i.e. habitat partitioning, as in the case of our study). Hence, in this specific context, the use of BCA enables us to specifically emphasize on the variations in community composition solely due to habitat specificities, unlike through basic PCA or nonmetric multidimensional scaling (nMDS), both of which could encompass additional sources of variations (e.g. variations in abundances of generalist species).

We completed the investigation on community structure by using biological traits that could account for taxon distributions among the different habitats. Body mass was considered to reflect habitat production and, together alongside motility, burrowing depth and feeding type, as adaptations to sediment properties (Pearson 1978). We also considered sediment mixing types to account for potential biogeochemical properties of habitats (Queiros et al. 2013). The biological trait data was combined with field data by aggregating within-trait organism densities per sample to generate a samples × trait modalities matrix (community weighted mean; Kleyer et al. 2012). Analyses and graphical representations were done with R 3.6.3 (R Core Team 2020); BCA with the package *ade4* (Chessel et al. 2004).

3.3 Results

3.3.1 Community patterns

3.3.1.1 Trends in organism densities

In total, 63 different taxa were identified in the samples. The taxa which could not be identified to species level and, concurrently, had a similar function to other closely-related taxa were combined at the same taxonomic group (e.g., *Genus* sp.). By rescaling each sand wave, we compared all of the samples based on their relative positions (Figure 3.2a-c). High density values were mostly concentrated on the steep slope (relative distance > 0) and, to a lesser extent, in the trough, at least for taxonomic and individual densities. A clear habitat effect was detected (Kruskal-Wallis test, $p < 0.001$), with steep slope densities being systematically the highest, and trough densities being intermediate (Figure 3.2). Steep slope taxon and individual densities were ca two times higher than in the other habitats, and ten times higher for biomass.

3.3.1.2 Taxonomic composition

A prominent feature of faunal distributions among the four habitats was the taxonomic specificity of the steep slope that hosted 53 taxa, of which 13 were specific only to this habitat (Figure 3.3). Although *Corophium* sp. and *Syllis gracilis* were specific to trough, and Nassaridae, Oedicerotidae, *Scolelepis bonnieri* and *Spio martinensis* to gentle slope, these taxa were low in abundance, such that most of the communities from the gentle slope, crest and trough were actually also subsets of the steep slope community. Among the more abundant taxa, Echinoidea, *Magelona* sp., *Nephtys* sp., *Spisula* sp. and Terebellidae were the most common to the four habitats. Crustaceans such as *Bathyporeia* sp., *Gastrosaccus spinifer* and *Megaluropus agilis* were very characteristic of the gentle slope, along with Pharidae and Ophiuroidea. Phoronida, although present in all four habitats, was the least abundant on the gentle slope, where seven other taxa had a higher abundance. In contrast, Phoronids were the most dominant on the crest, but also co-occurring with the dominant taxa of the gentle slope (*Nephtys* sp. and Terebellidae). On the steep slope, Phoronids were third most abundant (second among the habitats in absolute terms) next to the dominant *Tellimya ferruginosa* and *Fabulina fabula*, followed by *Spisula* sp., Echinoidea and *Magelona* sp. In the trough habitat, Phoronids were the most dominant of all, co-occurring with the dominant taxa of *Spisula* sp. and *T. ferruginosa* from the steep slope. However, there was a

substantial drop of *F. fabula* density and the trough was instead more characterized by *Parexogone hebes* and Copepoda.

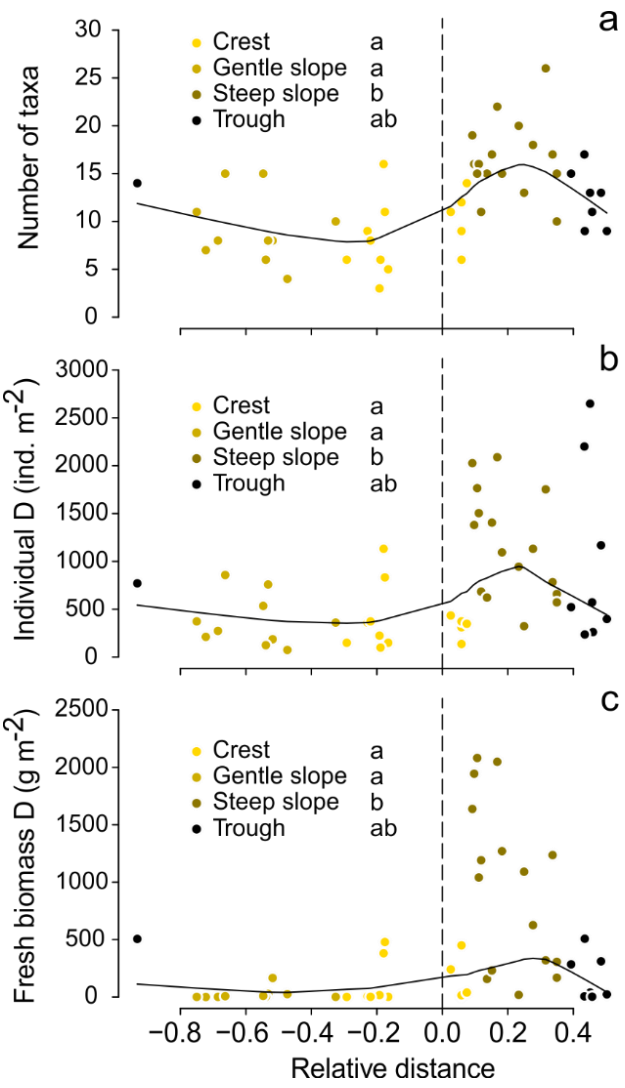

Figure 3.2. (a–c) Relative positions of organism densities along the sand wave continuum; black line, non-parametric Lowess fitting; color dots, organism densities per habitat (e.g., MU); common letters indicate no statistical difference according to multiple comparisons of Dunn test with Bonferroni correction.

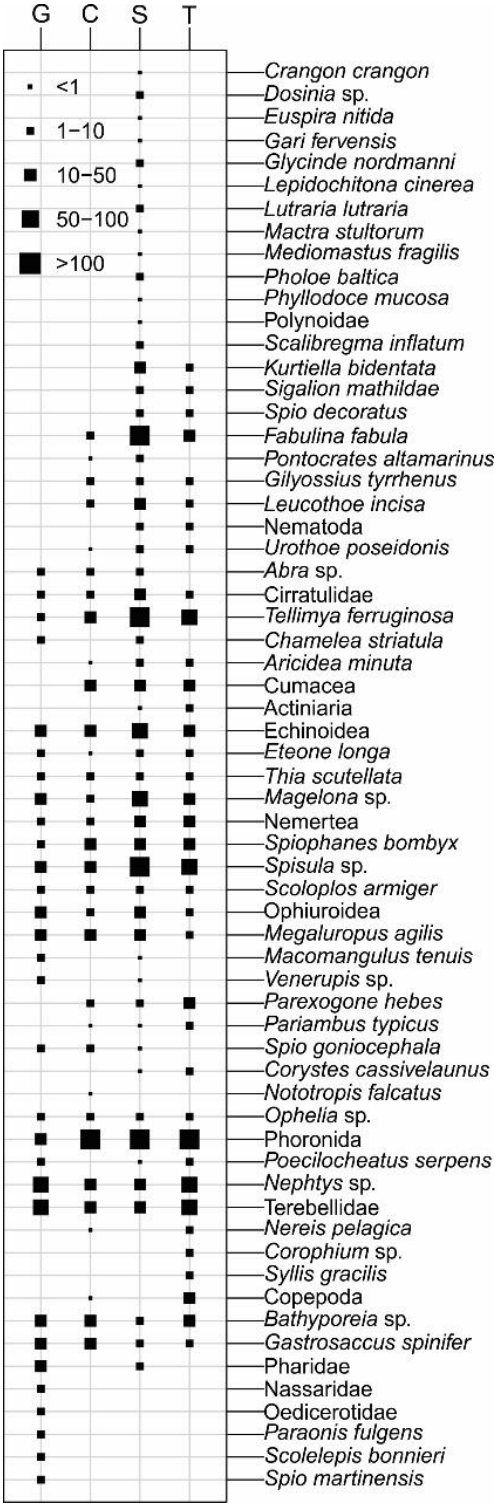

Figure 3.3. Taxon distributions along the sand wave continuum; "G" ,"C", "S" and "T" for gentle slope, crest, steep slope and trough habitat, respectively. Taxa are sorted according to niche preference (horizontal profiles). Square size expresses average individual density (ind. m^{-2}).

Although biomass exhibited the same trend as individual density along the sand wave continuum, it was much less evenly distributed among taxa. Indeed, more than 90% of the total biomass was comprised by Echinoidea (mainly represented by *Echinocardium cordatum*), of which 80% was concentrated on the steep slope. Another highly dominant taxon, *F. fabula*, also largely contributed to the total biomass of the steep slope, followed by *Gilvossius tyrrhena*, which was only absent from the gentle slope. Detailed densities of the ten most abundant and heavy taxa of each habitat are listed in the supplementary material (Table S3.1).

3.3.1.3 Community structure

BCA revealed a significant habitat structuring in terms of community composition (Figure 3.4). Habitat explained 24% of the variation ($p < 0.001$), mostly along the first axis. This gradient contrasted the highest densities encountered in the steep slope to densities from the other three habitats (Figure 3.4b). Furthermore, the BCA showed that all four habitats could be clearly distinguished by combining compositional aspects. Surprisingly, community ordination was not dominantly expressed following the geomorphological continuum, e.g., from trough to the gentle slope, crest, steep slope and again back to trough. Along the first axis (horizontal), from left to right, the trough immediately progressed to crest, and not the steep slope, the latter being positioned according to a density gradient (Figure 3.2). In addition, within-habitat variation increased along this gradient, with the gentle slope encompassing the most homogeneous community. From gentle to steep slope, the trend was driven by the most abundant or density-specific taxa such as *T. ferruginosa*, *F. fabula*, Echinoidea, *Spisula* sp. and *Magelona* sp. (Figure 3.4a). Whereas this gradient was due to a size effect overall, in which most of the taxa covaried positively together (e.g., the same direction in the ordination plot), there were specific crustaceans (*Bathyporeia* sp. and *G. spinifer*) on the gentle slope which deviated from this trend. The second axis (vertical) was predominantly expressed by Phoronida, which was highly characteristic of the trough. However, the variability of the second axis was also explained by ubiquitous taxa that represented a substantial part of the densities of the crest (Phoronida, *Spisula* sp. and *T. ferruginosa*), trough (Phoronida) and steep slope (*F. fabula* and *T. ferruginosa*); the trough and steep slope habitats were inflated in part by the dominant taxa reaching maximum densities in these two habitats. The third axis (Figures 3.4c and d, vertical), although expressing only a slight part of the total variation in community structure, interestingly exhibited the spatial contiguity between the gentle slope and trough (Terebellidae, Nemertea, *Nephtys* sp. and *Bathyporeia* sp.)

in the lower part of the factorial plane to the contiguity of the steep slope and crest in the top (*Spio goniocephala, Leucothoe incisa, Spisula* sp. *and F. fabula*). This plane reconstituted the spatial habitat succession in a circular way (Figure 3.4d), from trough (bottom right) to gentle slope (bottom left), then transitioning to crest (top left) and completing the cycle in the steep slope (top right). The top 10 highest and lowest ordination scores from each axis are shown in the supplementary material (Table S3.2).

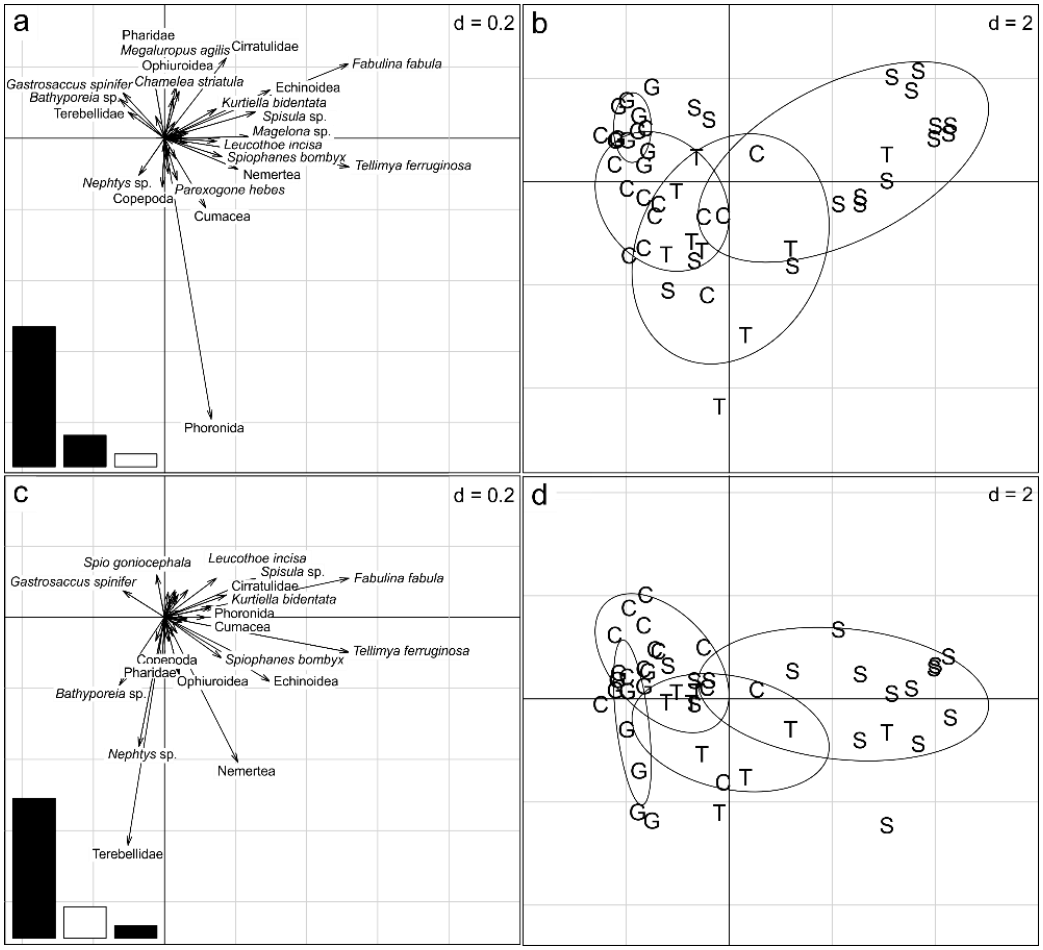

Figure 3.4. BCA; top, axes 1 and 2; bottom, axes 1 and 3. a and c) Projections of the taxa; for clarity, only taxa with substantial contributions are labelled; bar diagram, eigenvalues. b and d) Samples grouped per habitat; "Gentle slope = G", "Crest = C", "Steep slope = S" and "Trough = T". "d" indicates the grid scale.

3.3.1.4 Biological traits

In total, 63 taxa were documented for traits, encompassing 96 % of the total individual organism count. The trait modality distributions along the sand wave continuum are shown in Figure 3.5. In each of the traits distinguished, some modalities were clearly dominant in the benthic communities in certain habitats along the sand wave (Figure 3.5). Overall, the organisms were on average of small body mass, predominantly crawlers, followed by tubicolous, and mostly surficial modifiers, followed by sediment diffusors. From the gentle slope down to the trough, monotonous trends were detected for small body mass, which increased at the expense of the intermediate body mass (Figure 3.5a). In addition, the burrowing depth progressively switched from surface dwellers to deeper burrowers towards the trough from both flanks (Figure 3.5c). To a lesser extent, the swimming ability also decreased along the gradient, being the highest on the gentle slope, followed by the crest and then the lowest on both the steep slope and trough (Figure 3.5b). Also somewhat more specific on the steep slope was that the motility was predominantly represented by crawlers while exhibiting a substantial drop in tubicolous worms. In most cases, when a significant effect was detected within a given trait modality, it was induced by the extremes in the percentages of taxa that was found between the gentle and steep slopes, with negligible difference between the steep slope and trough. This was also the case for the opposing trends observed between the suspension feeders, which were highest on the steep slope, and carnivorous-scavengers, which were the lowest there (Figure 3.5d). Percentages of both surficial modifiers and deep burrowers were the highest on the steep slope especially since some from the latter group (e.g. phoronids, *Urothoe poseidonis*, and a few bivalves) can affect the sediment surface. In summary, the gentle and steep slope habitats appeared to consistently exhibit the most extreme functional types through their contrasting taxonomic oppositions (Figure 3.4).

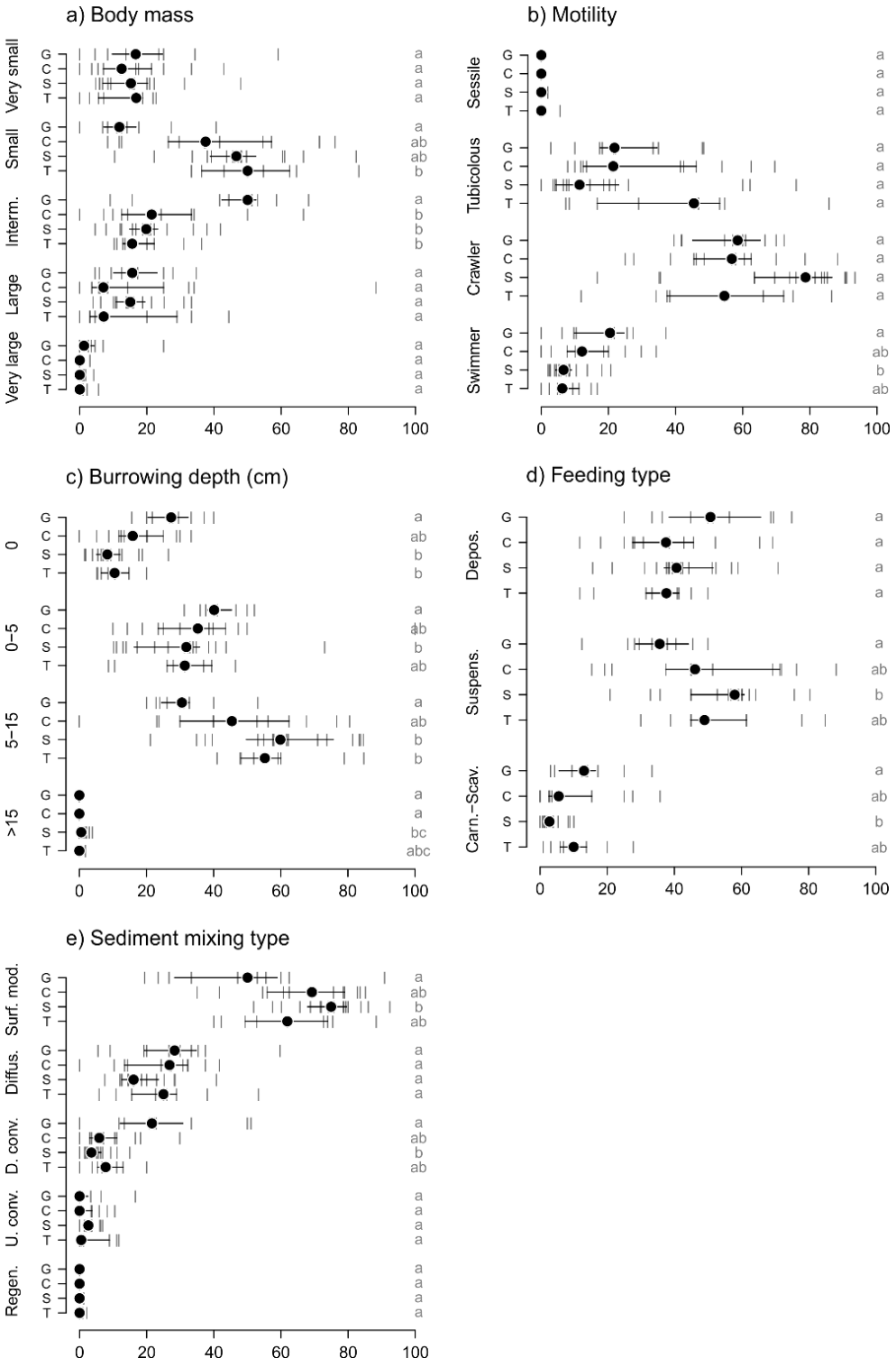
a) Body mass
Very small
Small
Interm.
Large
Very large
G
C
S
T
0
20
40
60
80
100
b) Motility
Sessile
Tubicolous
Crawler
Swimmer
c) Burrowing depth (cm)
0
0–5
5–15
>15
d) Feeding type
Depos.
Suspens.
Carn.–Scav.
e) Sediment mixing type
Surf. mod.
Diffus.
D. conv.
U. conv.
Regen.

Figure 3.5. Within-trait distributions of individual densities of the taxa. For each trait modality, densities are distributed along the sand wave continuum (habitats): “Gentle slope = G”, “Crest = C”, “Steep slope = S” and “Trough = T”. a) “Interm.”, intermediate. d) “Depos.”, deposit feeding; “Suspens.”, suspension feeding; “Carn.-Scav.”, carnivory-scavenging. e) “surf. mod.”, surficial modifier; “Diffus.”, diffusers; “D. conv.”, downward conveyor; “U. conv.”, upward conveyor; “Regen.”, regenerator. Values are expressed in percentages of total individual density for each trait within each of the four habitats; grey vertical segments are sample observations; black dots represent median values; bars extend from 25^{th} to 75^{th} percentiles. Common letters indicate no statistical difference according to multiple comparisons of Dunn test within trait modality with Bonferroni correction.

3.4 Discussion

The sand waves in Dutch waters exhibit a shift of increasing asymmetry towards the coastal regions (Cheng et al. 2020[10]). As recent studies have shown, such morphological differences (e.g., asymmetry) have resulted in significant, small-scale variability in the sediment characteristics (Table 3.1), bed roughness as well as benthic organism densities (Damen et al. 2018; Damveld et al. 2018; Cheng et al. 2020). In this study, we showed that the morphology of the asymmetrical sand waves has a profound effect on the benthic community structure, as seen in the individual, biomass and taxon densities. Yet the closer proximity to the coast also increases the likelihood for these asymmetrical sand waves to be impacted by human activity, either directly through fishing activity, such as bottom trawling, dredging or installation of hard infrastructure, or indirectly from the resulting changes in hydrodynamics and/or sediment properties (Bergman and Hup 1992; Tillin et al. 2006; Maar et al. 2009; Coates et al. 2013; Reubens et al. 2014; van Denderen et al. 2014; Eigaard et al. 2016). Thus, it is necessary to gain a thorough understanding of the different, but linked, processes in these sand waves in order to be able to predict the magnitude and type of impacts that could result. There is presently a knowledge gap regarding the interrelations in the biogeomorphology over a small spatial scale within a dynamic bedform environment, which was the main motivation for our study.

Conducted a long time ago, the North Sea Benthos Survey (NSBS) still provides a large scale reference work on macrobenthic communities (Heip et al. 1992). At the large scale, the particular benthic assemblages correspond well to factors including sediment chl *a* content, silt content, grain size, percentage of organic carbon, location (latitude) and water depth. Largely from the latter two factors, three distinct regions have been identified (northern, central and southern) (Heip et al. 1992). Künitzer et al. (1992) further subdivided the North Sea into eight regions based on depth contours, followed by sediment type. Even more assemblages were found when analyzed at a finer scale, as was done in the study by Duineveld et al. (1990), which looked specifically at the Dutch sector of the North Sea. While they categorized the region into four subareas based on topography, bathymetry and grain size, there were in actuality, two distinct regions of benthic assemblages between the north and south, the latter of which encompasses the Texel sand waves. To a certain extent, the classification of entire areas or regions into benthic assemblages is a matter of scale (Künitzer et al. 1992). The aforementioned studies all made use of data from the same campaign, but came to different conclusions largely due to a change in the scale of analyses. Our

[10] Data first made available in Damen et al. 2018.

results suggest that sampling resolution is another important aspect that must also be considered, especially for dynamic environments such as asymmetrical sand waves.

The difference in spatial scale (NSBS stations were each > 40 km apart with 5 box cores and/or van Veen grabs; our stations were tens of m apart with 3 box cores each) between Duineveld et al. (1990) and our study still presents limitations for extrapolating habitat-specific conditions or associated trends in benthic assemblages. For instance, we found some commonalities in dominant taxa between the southern Dutch North Sea habitat and our study site (e.g., *E. cordatum, Magelona sp., Bathyporeia sp., T. ferruginosa* and *F. fabula*), but the NSBS data does not contain high enough resolution to show how, where or why our taxa are spatially distributed across the sand waves. While the abiotic parameters (e.g., grain size, water depth, etc.) are largely consistent, the species richness of all four of our habitats are at or above the upper range of those measured from the southern region. The steep slope with 53 taxa, is actually within the average of the northern region. As a result, our data demonstrates that a large-scale campaign, with lower sampling resolution, could very well result in an underestimation of the actual taxon richness, even in the taxonomically-poorer Southern Bight. Furthermore, the variation in richness is also much greater (30 – 53 taxa in our samples vs. ~20 – 30 in the southern region, based on the NSBS). Again, the range observed between our four habitats overlaps more with the northern region near the muddy and more species rich Oyster Ground (~ 40 – 70 taxa). This is especially interesting, given that sandy environments as the Texel sand waves are typically believed to be less biologically diverse compared to the more muddier environments (Duineveld et al. 1990; Heip et al. 1992; Künitzer et al. 1992; Santos et al. 2012). Our results suggest that local variability could well exceed what has been observed from regional trends, including in regions that are more species rich. Over a small spatial scale of only tens of meters or less, we were able to measure significant differences in the benthic community structure at much higher levels than what has been found for the southern region of the Dutch North Sea in previous studies. Such observations could bring new insight into the biogeomorphological dynamics of rhythmic bedforms in shallow coastal seas, specifically in the benthic community structuring.

3.4.1 Geomorphological effects on community structure and associated biological traits

A minute difference in strength between the tidal residual flow (~0.05 m s^{-1}) is sufficient to provoke sand wave migration of up to several meters or more per year (Borsje et al. 2013), as

well as develop sand wave asymmetry. Although the latter process is estimated to occur on time scales of multiple decades based on modeling studies (van Gerwen et al. 2018; Damveld et al. 2019), it is not certain how and whether this would affect the biological communities. While the predominant flow is slightly stronger in the flood than ebb direction, which drives the migration of sand uphill on the gentle slope to the crest, it seems unlikely that there would be much sheltering during ebb flow. Interestingly, there is a near-absence of sessile taxa in all samples, which likely reflects the relatively mobile nature of sand waves, which are less favorable to immobile groups (Pearson 2001). This appears to be the case even in the troughs, which are largely devoid of fast-moving bedforms such as sand ripples (Damveld et al. 2018). However, the exact flow dynamics are not readily available along these sand waves, and care must be taken in interpreting these patterns. What is clear is that both the abiotic measurements along the sand wave (Cheng et al. 2020) and the ripple and epibenthic density differences between the crest and trough (Damveld et al. 2018) suggest flow conditions to be significantly different between each habitat.

Different hydrodynamic conditions along the sand wave environment may be a major explanation of benthic community structuring. Generally speaking, tidal velocities lower than 16 cm s^{-1} enable organic matter to settle (Creutzberg et al. 1984), such that the combined variations in physical and sediment properties can result in an alternative benthic community structure. What is generally observed on a larger scale, and according to the stability-time hypothesis (Sanders 1968), is that a higher physical stability enables more individual organisms to survive, thereby supporting a higher number of species overall. Benthos that inhabit the upper layers of sediment are adapted to the flow rates near the bed (Pearson 2001) and although not the only factor, hydrodynamics can select stress-resistant organisms or affect sediment deposition rate. The highly unequal distribution of macrofauna densities along the studied sand waves seems to suggest that similar ecological patterns may also be established and distinguishable at the smaller-scale. Community diversity tends to increase in environments that are more heterogeneous in sediment composition and more stable over time (Sanders 1968; Pearson and Rosenberg 1977), as appears to be the case for the steep slope and troughs. The individual abundance, biomass and taxon density all showed a pattern of distribution consistent to the abiotic variables between each of the habitats (Cheng et al. 2020).

Likewise, the physical movement of sediment can have important consequences, especially for certain feeding groups such as deposit feeders or suspension feeders. On the one hand, tube-building worms (tubicolous) and burrowing animals can increase the sediment surface

area[11] significantly enough to enhance the exchange rates with the overlying water (Forster et al. 1999; Stieglitz et al. 2000; Santos et al. 2012). However, increased deposition (e.g., elevated levels of silt and organic matter), could exclude less mobile species with a limited ability to escape burial or clogging of their feeding apparatus (Lohrer et al. 2004; Mestdagh et al. 2018). This is significant as some benthic organisms can redistribute the upper layers of sediment and enable the burial of fine material, particularly as their densities become higher (e.g., steep slope and trough) (Volkenborn et al. 2007a; Santos et al. 2012). Evidently, the steep slope contained high numbers of deposit feeders while the tube-building worms were much less frequent compared to the trough. But overall, our data demonstrated that the majority of the taxa prefer the finer, siltier steep slope and trough habitats. Concurrently, these areas consistently exhibited higher chl *a* and organic matter concentrations (Table 3.1), indicating a higher availability of food resources (van Nugteren et al. 2009b; Bauer et al. 2013; Cheng et al. 2020). Our results are consistent to previous studies that have found higher diversity in both small and large rhythmic bedform troughs, which also tended to be finer in sediment composition (Tilman 1982; Ramey-Balci et al. 2009; van Dijk et al. 2012; Van Lancker et al. 2012; Damveld et al. 2018; Mestdagh et al. 2020). In contrast, the gentle side of the sand waves, which was coarser, more permeable and lower in organic material (Cheng et al. 2020), had by far the lowest diversity and biomass, despite encompassing a larger surface area than the steep slope. The taxa on the gentle slope clearly exhibited the most homogeneity in community structure, and the few taxa which stood out in this habitat included the mobile fauna such as the swimmers (e.g., *Nephtys* sp., *Bathyporeia* sp., Ophiuroidea, *G. spinifer* and Terebellidae).

Moreover, the asymmetrical nature of these bedforms can also give rise to different levels of bed roughness, as was shown in the video transect study at the Texel sand wave area by Damveld et al. (2018). Such variability in size and the type of bed feature, particularly smaller ones, is known to be relevant for the biology (Dolan et al. 2012). The troughs contained very few, irregularly shaped sand ripples as opposed to the high regularity and number of ripples at the crests. Concomitantly, these authors measured four times the number of epibenthos and observed 30 times more holes (a proxy for endobenthos) in the troughs. The differences we found between the crest and trough, although somewhat lower (only up to 2.9 times higher abundance in the trough), is consistent with these observations. But more importantly, we found larger extremes in

[11] The creation of tubes, burrows and other features in the sediment increases the total surface area for which processes such as advective water exchange can occur.

diversity and biomass between the two types of slopes; unfortunately information about the roughness in these habitats is not available as the video study only focused on the crest and trough. The variable bed roughness could have important consequences in these permeable sands, where ripples exert pressure differences induced on the sediment surface which allows flows to penetrate through the sand grains (Jenness and Duineveld 1985; Huettel and Gust 1992; Rusch and Huettel 2000). This process, which entrains solutes and fine particles that accumulate under low to moderate flows while being carried out of the sediment at higher flow conditions, may partially explain the elevated levels of fine particles on the steep slope and trough (Cheng et al. 2020). As the physical steering via currents diminishes, the influence of bioturbation becomes increasingly important (Pearson 2001), especially when coupled with the simultaneous decrease in permeability. Thus, the drastic decrease in ripples in the troughs, coupled with the simultaneous decrease in permeability, restricts physical transport in and out of the sediment. Under these conditions, the influence of animal activity in enhancing these rates become increasingly important with animal density (Forster et al. 2003; Volkenborn et al. 2007a). These sedimentary processes could be one possible explanation for the rather abrupt transitions observed between the habitats in the BCA (Figures 3.4a and c). In this sense, the biological traits are useful in further elaborating the possible causes for some of the observed patterns.

As with the abiotic parameters and macrofauna densities, the most extreme contrasts in the associated functional traits were also found between the two different slopes of the sand waves. Additionally, the majority of the gentle-slope taxa lived superficially in the sediment (<5 cm depth), indicative of the fact that sedimentary organic matter content is significantly lower there. The dominant feeding mode was the downward conveyor (e.g., Terebellidae), which are organisms that predominantly feed at the surface and drag fecal particles into the sediment (Kristensen et al. 2012). A relatively high number of deposit feeders and carnivore-scavenging fauna were also observed on the gentle slope and crest, as was the highly mobile polychaete, *Nephtys sp.*, known for its high resiliency to environment stress (Arndt-Sullivan and Schiedek 1997; Van Lancker et al. 2012). As such, these two habitats are characterized by highly resilient, highly mobile taxa residing and feeding close to the sediment surface. However, the crest was notably different from other habitats only with its relatively high number of surficial modifying organisms; contrary to the gentle slope, the tops of the sand waves contained many more species that were in common with the steep half. This suggests that the crest is actually more of a transition zone that, although it overwhelmingly shares its sediment characteristics with the gentle slope (Table 3.1), its species composition overlaps with both slopes.

In contrast, the steep slopes were characterized by a large percentage of crawlers and contained the most surficial modifiers. In direct opposition to the more organically poor gentle slope, the steep slope also contained upward conveyors, which feed into the sediment and transport particles towards the surface (Kristensen et al. 2012), thus relying on dissolved and particulate carbon from deeper sediment layers (Clough and Lopez 1993; Pearson 2001). Despite having the largest concentration of suspension feeders, notably the bivalves *T. ferruginosa* and the suspension-deposit feeding *F. fabula*, the tubicolous worms were the lowest in proportion in this habitat. Rather, densities of tube-dwelling worms, comprised mostly of Phoronida, were highest in the trough. Despite similar sediment characteristics, the fauna between the trough and steep slope exhibited somewhat less overlap. The deepest burrowers were found in both habitats, along with higher organic matter concentrations and amounts of silty material, indicative of environments where the grain composition and particle quality (e.g., organic matter) are most important for the benthos (Graf 1992; Pearson 2001). The disproportionately high biomass and elevated organic matter concentration on the steep slope habitat is an indication of a relatively stable environment with just the right amount of food, so that oxygen depletion is not a detrimental problem (Pearson and Rosenberg 1977). The lower number of resilient groups are also indicative that the steeper side of the sand waves is somewhat less stressful than the gentle slope and crest, although the low percentage of tubicolous worms also means that this environment is slightly more stressful than the trough. The significantly higher numbers of echinoderms, some of which are active deposit feeders, on the steep slope would suggest this habitat to be more affected by the benthic community (Ziebis et al. 1996; Pearson 2001), as opposed to the gentle slope that appears to be more physically controlled: the sediment was significantly coarser and the permeability about twice as high on the gentle slope and crest vs. the other two habitats (Cheng et al. 2020). The strong physical control is also a probable explanation for the low numbers of sedentary tubicolous worms on the steep slope. Their establishment may be restricted by the destabilizing effect of continuous displacement of sediment both by motile subsurface deposit feeders (Rhoads and Young 1970; Myers 1977a; Pearson 2001) and also potential burial by the physical movement of sediment as the sand wave migrates towards the direction of the steep slope (Besio et al. 2004, 2008; Van Oyen et al. 2013; Borsje et al. 2014a). Such possible negative effects due to biotic interactions become more pronounced in environments where the physical influences are lessened (Menge and Sutherland 1987; Crain and Bertness 2005). On the other hand, the presence of key engineers has also been shown to positively facilitate ecosystem functioning and biodiversity,

through the creation of more suitable habitats, thereby increasing the overall habitat heterogeneity (Crain and Bertness 2006). Hence, the largest differences were observed between the two slopes.

3.4.2 Implications and conclusion

Our study demonstrates that significant contrasts in benthic community structure occur over a very small spatial scale (10-100 m) in soft sediment shelves, such as a sand wave environments. In this context, within-habitat conditions such as the position along a single sand wave are the most important determinants of community structure. In spite of the importance attributed to water depth, both at regional and sand wave scales (Heip et al. 1992; Künitzer et al. 1992; Baptist et al. 2006), our results show a much stronger effect from bottom geomorphology. We found the largest differences in most of the measured parameters between the two sides of the Texel sand waves, irrespective of their comparable water depths. Thus, a lower sampling resolution of only the crest and trough would likely have given a totally different observation. Water depth is not a useful indicator for asymmetrical sand wave environments, as it is unable to distinguish between the two sides of the bedforms. Instead, it appears that the specific location (habitat) along the sand wave will have the largest influence over the sedimentary conditions. Despite the fact that the Texel sand waves were overall sandy, all three studies have now demonstrated significant variability in the sediment characteristics, bed roughness and benthic community composition along the asymmetrical sand waves (Damveld et al. 2018; Cheng et al. 2020). In the case of benthic diversity (e.g., species richness), the Texel sand waves are more resembling the assemblage from the more-diverse (and somewhat more muddy) northern region within the Dutch sector.

Although sand waves are ubiquitous throughout the Dutch North Sea, they are predominantly located 20 km or more from the coast given the particular hydrodynamic and sedimentological conditions required for these bedforms to develop and persist. But as biological and environmental processes are often closely-coupled, further investigations should consider both aspects simultaneously (Snelder et al. 2007). In addition, a higher spatial resolution of sampling is required to be able to fully grasp the interrelations between sedimentology, morphology, benthic community structure and biogeochemistry of heterogeneous habitats such as dynamic sand wave environments. The use of habitat classification schemes could be a useful predictor for environments that are similar in terms of sedimentary or other physical characteristics, as these rely on the abiotic parameters that are of significance to both physical and biological patterns (Roff et al. 2003; Gregr and Bodtker 2007; Reiss et al. 2010). Furthermore, a

thorough investigation on the specific interactions between the dominant taxon groups and their influence on one another would provide valuable insight on the significance of biotic controls on community structure, relative to other factors (e.g., physical). Based on our data, we have been able to identify at least four distinct habitats (trough, gentle slope, crest and steep slope), each with a few dominant predictors within an asymmetrical sand wave. Although the transitional zones between habitats were sometimes rather abrupt, we believe that our findings will provide a basis for a full understanding on the benthic ecological functioning of sand waves.

Author contributions

Chiu H. Cheng: Conceptualization, Methodology, Investigation, Formal analysis, Visualization, Writing – Original Draft, Writing – Review & Editing, Project administration. **Bas W. Borsje**: Conceptualization, Writing – Review & Editing, Supervision. **Olivier Beauchard**: Methodology, Formal analysis, Visualization, Writing – Original Draft, Writing – Review & Editing, Software, Resources. **Sarah O'Flynn**: Methodology, Investigation, Writing – Review & Editing, Resources. **Tom Ysebaert**: Resources, Writing – Review & Editing, Funding acquisition. **Karline Soetaert**: Conceptualization, Methodology, Investigation, Formal analysis, Visualization, Writing – Review & Editing, Supervision, Project administration, Funding acquisition.

Funding information: Nederlandse Organisatie voor Wetenschappelijk Onderzoek-Aard-en Levenswetenschappen, Grant Number: 871.15.011; Royal Boskalis Westminster N.V., Grant Number: 871.15.011.

Acknowledgments: This work is part of the NWO-ALW funded SANDBOX project. The Royal Boskalis Westminster N.V., the Royal Netherlands Institute for Sea Research (NIOZ) and Utrecht University are greatly acknowledged for their financial support of this project. This work was also supported by the DISCLOSE project (https://discloseweb.webhosting.rug.nl/), funded by the Gieskes Strijbis Fonds. Many thanks to Erik Hendriks, Johan Damveld, Sarah O'Flynn, Justin Tiano, Karin van der Reijden, Leo Koop, Rob Witbaard, Pieter van Rijswijk and Anton Tramper, who contributed to the sample collection and data contribution for this project from the cruise campaigns. The benthos samples were pre-sorted by Ymke Temmerman and identified by Loran

Kleine Schaars. We are very grateful to Texel NMF staff for their support in making both research campaigns successful.

Data availability statement: The data that support the findings of this study are openly available in the 4TU Centre for Research Data repository at https://doi.org/10.4121/14152187.

Supplementary Materials for Chapter 3:

Table S3.1. The top 10 taxa based on individual density (ind. m^{-2}) and biomass (g m^{-2}) in total, as well as for the four habitats[12].

Total counts	**Total**	**SD**	**Total biomass**	**Total**	**SD**
Phoronida	7610	362	Echinoidea	17680	568
Tellimya ferruginosa	5322	210	*Fabulina fabula*	453	24
Fabulina fabula	3307	161	*Gilyossius tyrrhena*	199	10
Spisula sp.	3208	82	*Lutraria lutraria*	107	14
Echinoidea	2263	61	*Thia scutellata*	83	5
Terebellidae	2176	70	*Nephtys* sp.	46	2
Nephtys sp.	1840	44	*Gari fervensis*	39	6
Magelona sp.	1480	45.	*Mactra stultorum*	32	5
Spiophanes bombyx	933	30	*Chamelea striatula*	31	4
Cumacea	908	55	Phoronida	30	2

Gentle counts	**Total**	**SD**	**Gentle biomass**	**Total**	**SD**
Terebellidae	895	100	Echinoidea	156	49
Nephtys sp.	510	61	*Chamelea striatula*	25	8
Bathyporeia sp.	348	47	Pharidae	16	5
Echinoidea	348	76	Nemertea	10	3
Spisula sp.	298	35	*Thia scutellata*	9	3
Gastrosaccus spinifer	199	28	*Nephtys* sp.	7	1
Magelona sp.	124	23	Phoronida	4	1
Phoronida	124	21	*Magelona* sp.	3	1
Megaluropus agilis	112	12	*Scolelepis bonnieri*	3	1
Ophiuroidea	112	16	*Scoloplos armiger*	3	1

[12] "Gentle" and "Steep" refer to the respective slopes.

Crest counts	**Total**	**SD**	**Steep biomass**	**Total**	**SD**
Phoronida	1442	156	Echinoidea	1527	191
Spisula sp.	597	67	*Gilyossius tyrrhena*	44	9
Nephtys sp.	386	26	*Thia scutellata*	26	4
Terebellidae	373	71	*Nephtys* sp.	11	1
Echinoidea	323	56	*Ophelia* sp.	6	1
Tellimya ferruginosa	261	54	*Scoloplos armiger*	5	1
Cumacea	162	31	*Magelona* sp.	5	1
Gastrosaccusspinifer	162	18	Phoronida	4	1
Bathyporeia sp.	137	12	*Spisula* sp.	4	0.2
Megaluropus agilis	137	21	*Tellimya ferruginosa*	1	0.3

Steep counts	**Total**	**SD**	**Steep biomass**	**Total**	**SD**
Tellimya ferruginosa	4377	294	Echinoidea	14390	704
Fabulina fabula	3121	235	*Fabulina fabula*	450	36
Phoronida	2114	226	*Gilyossius tyrrhena*	134	14
Spisula sp.	1616	87	*Lutraria lutraria*	107	23
Echinoidea	1306	57	*Thia scutellata*	47	7
Magelona sp.	870	52	*Gari fervensis*	39	10
Spiophanes bombyx	472	33	*Mactra stultorum*	32	8
Cumacea	448	74	Terebellidae	21	3
Terebellidae	435	42	*Nephtys* sp.	18	3
Cirratulidae	423	30	*Spisula* sp.	18	2

Trough counts	**Total**	**SD**	**Trough biomass**	**Total**	**SD**
Phoronida	3929	719	Echinoidea	1607	220
Spisula sp.	696	111	*Gilyossius tyrrhena*	22	7
Tellimya ferruginosa	634	98	*Nephtys* sp.	10	2
Nephtys sp.	522	47	Phoronida	9	2
Terebellidae	473	52	Nemertea	8	2
Magelona sp.	361	62	Ophiuroidea	7	2
Cumacea	298	73	*Magelona* sp.	4	1
Echinoidea	286	30	*Fabulina fabula*	4	1
Spiophanes bombyx	236	38	*Spisula* sp.	3	1
Parexogone hebes	149	45	*Tellimya ferruginosa*	2	0.4

Table S3.2. The top 10 highest and lowest ordination scores for taxa along the three axes, derived from the BCA analyses.

Lowest ordination scores					
Taxa	**Axis 1**	**Taxa**	**Axis 2**	**Taxa**	**Axis 3**
Tellimya ferruginosa	-0.520	Cirratulidae	-0.226	Terebellidae	-0.644
Fabulina fabula	-0.519	*Fabulina fabula*	-0.212	Nemertea	-0.409
Echinoidea	-0.297	Pharidae	-0.156	*Nephtys* sp.	-0.364
Spisula sp.	-0.256	*Megaluropus agilis*	-0.147	*Bathyporeia* sp.	-0.192
Magelona sp.	-0.238	Echinoidea	-0.136	Echinoidea	-0.183
Nemertea	-0.207	*Gastrosaccus spinifer*	-0.129	Ophiuroidea	-0.157
Cirratulidae	-0.174	Ophiuroidea	-0.129	Pharidae	-0.132
Spiophanes bombyx	-0.161	*Chamelea striatula*	-0.112	*Magelona* sp.	-0.121
Leucothoe incisa	-0.146	*Bathyporeia* sp.	-0.111	Copepoda	-0.119
Kurtiella bidentata	-0.146	*Kurtiella bidentata*	-0.083	*Spiophanes bombyx*	-0.115
Highest ordination scores					
Taxa	**Axis 1**	**Taxa**	**Axis 2**	**Taxa**	**Axis 3**
Paraonis fulgens	0.010	*Scoloplos armiger*	0.057	*Thia scutellata*	0.064
Scolelepis bonnieri	0.010	*Pariambus typicus*	0.059	*Scoloplos armiger*	0.070
Spio martinensis	0.010	*Tellimya ferruginosa*	0.080	*Ophelia* sp.	0.071
Spio goniocephala	0.022	Nemertea	0.088	*Gastrosaccus spinifer*	0.074
Pharidae	0.024	*Ophelia* sp.	0.099	*Abra* sp.	0.076
Oedicerotidae	0.025	*Nephtys* sp.	0.106	*Gilyossius tyrrhena*	0.077
Nephtys sp.	0.072	*Parexogone hebes*	0.118	*Fabulina fabula*	0.107
Terebellidae	0.103	Copepoda	0.137	*Spisula* sp.	0.108
Gastrosaccus spinifer	0.118	Cumacea	0.195	*Leucothoe incisa*	0.110
Bathyporeia sp.	0.127	Phoronida	0.792	*Spio goniocephala*	0.119

Chapter 4

Sediment shell-content diminishes current-driven sand ripple development and migration

Chiu H. Cheng[1,2], Jaco C. de Smit[1,3], Greg S. Fivash[1], Suzanne J. M. H. Hulscher[4], Bas W. Borsje[4] and Karline Soetaert[1]

[1]NIOZ Royal Netherlands Institute for Sea Research, Department of Estuarine and Delta Systems (EDS), 4401NT Yerseke, The Netherlands. [2]Wageningen Marine Research, Wageningen University & Research, 4400 AB Yerseke, The Netherlands. [3]Faculty of Geosciences, Department of Physical Geography, Utrecht University, 3584 CB Utrecht, The Netherlands. [4]Water Engineering and Management, University of Twente, 7500 AE Enschede, The Netherlands.

Manuscript submitted for review to *Earth Surface Dynamics*

Photo by Jaco de Smit

Abstract

Shells and shell fragments are biogenic structures that are widespread throughout natural sandy shelf seas and whose presence can affect the bed roughness and erodibility of the seabed. An important and direct consequence is the effect on the formation and movement of small bedforms such as sand ripples. We experimentally measured ripple formation and migration of a mixture of natural sand with increasing volumes of shell material in a racetrack flume. Our experiments reveal the impacts of shells on ripple development in sandy sediment, providing information that was previously lacking. Shells expedite the onset of sediment transport while simultaneously reducing ripple dimensions and slowing down their migration rates. Moreover, increasing shell content enhances near-bed flow velocity due to the reduction of bed friction that is partly caused by a decrease in average ripple size and occurrence. This, in essence, limits the rate and magnitude of bedload transport. Given the large influence of shell content on sediment dynamics on the one hand, and the high shell concentrations found naturally in the sediments of shallow seas on the other hand, a significant control from shells on the morphodynamics of sandy marine habitats is expected.

4.1 Introduction

Ripples are the most common bedforms found in the marine environment, including in shallow, sandy environments (Langlois and Valance 2007; Bartholdy et al. 2015). They form over a broad range of sandy grain mixtures under low energy flow or wave conditions that exceed the erosion threshold (Soulsby 1997; Precht and Huettel 2003). With increasing water depth, ripples become progressively driven by currents rather than waves. Current-generated ripples are very dynamic microscale bedforms, with typical sizes of around 0.1 m in wavelength and up to 0.01 m or more in height (Ashley et al. 1990; van Rijn et al. 1993). They continuously develop and erode, typically on the order of minutes to days, and can migrate at rates exceeding 0.4 cm min^{-1} (Baas and De Koning 1995; Baas et al. 2000; Bartholdy et al. 2015; Lichtman et al. 2018). As the ripples move and change in dimension, the bed roughness is correspondingly altered, which can have cascading effects on the surrounding areas such as larger bedforms (e.g., tidal sand waves) on which they are often superimposed (Idier et al. 2004; Damveld et al. 2018, 2019; Brakenhoff et al. 2020). Additionally, ripples also generate distinct spatial variations in sediment composition and alter the distribution of particulate organic matter by their effect on hydrodynamics, some of

which can further modify the sediment properties in ways that influence erosion (Mietta et al. 2009; Kösters and Winter 2014; Ahmerkamp et al. 2015).

Shells, a biogenic material created by marine bivalves, are widely distributed in certain regions of the marine environment (Russell-Hunter 1983). These calcareous structures remain present long after the death of the organisms (Kidwell 1985; Gutiérrez et al. 2003), and they are mostly found in the form of separated single shell valves and shell fragments. In environments where shells are prevalent, they may constitute 20–70 % of the total sediment composition (by volumetric percentage), although even higher percentages have been observed in very extreme cases (Soulsby 1997; Dey 2003). Since they have a lower bulk density, their presence reduces the bulk density of the sediment by diluting the quartz fraction (Soulsby 1997). As shell material is rather plate-like, irregular and angular in shape, they also change the general composition compared to the smaller, surrounding sediment particles (Al-Dabbas and McManus 1987). Intact shells and larger fragments may inhibit sediment transport through bed armoring. Armoring occurs when the mean shear stress is below the critical erosion threshold for the coarsest fractions, but above that for the finer particles, resulting in their entrainment. This winnowing causes the surface to become coarser and coarser, essentially building up an armor layer (Vericat et al. 2006). In riverine environments, coarse material such as gravel has been shown to facilitate bed armoring, causing the upper layers of the sediment to become significantly coarser than the median grain size (D_{50}) of the sediment beneath, ultimately reducing or inhibiting sediment transport (Wilcock and Detemple 2005; Curran 2010). Shells may also be able to provide a similar armoring effect against sand erosion given that they are more difficult to erode (Ramsdell and Miedema 2010; Miedema and Ramsdell 2011).

Thus far, very few studies have investigated the direct influence of shell material on the bedload transport dynamics through the alteration of bed roughness (Nowell and Jumars 1984; Gutiérrez et al. 2003). Some studies have explored the ways in which shells could be used as tracers for sediment motion, given their widespread occurrence (Al-Dabbas and McManus 1987). The drag and incipient motion of the valves of a few bivalve species have also been investigated in the laboratory (Dey 2003). Similar studies have focused on the erosion and settling velocities of shells, based on shapes, shell positioning and associated drag, being transported through a pipeline (Ramsdell and Miedema 2010; Miedema and Ramsdell 2011). Although these studies have considered how the irregularity in shape and orientation of shell valves potentially interact with flow, the focus has been more within a hydrodynamic context rather than a sedimentary one.

To our knowledge, there have not been studies addressing the direct effects of a natural, representative mixture of shells and sandy sediment on the development and movement of ripples.

From a hydraulic point of view, biogenic materials such as shells do not exhibit the same response as compared to rock fragments of a similar size, although some shells (e.g., the mussel family, Mytilidae) have been shown to behave more similarly to the smaller sand particles (Al-Dabbas and McManus 1987). However, due to the shape and size of most shells, combined with their lower density, they are known to have a much lower settling velocity and much larger erosion velocity threshold than sand particles (Ramsdell and Miedema 2010). The mere presence of empty shells has also been shown to facilitate silt and other fine-particle entrainment in the sediment (Pilditch et al. 1997; Huettel and Rusch 2000; Witbaard et al. 2016). But despite their prevalent nature and potential to affect sediment dynamics in several ways, there is at present a knowledge gap in terms of the direct influence of shells on the geomorphology of sandy sediments.

The objective of this experiment was to determine the effect of biogenic shells on the development of ripples in medium sand, in relation to unidirectional flow and turbulence along the bed. The combination of flow velocity and turbulence intensity largely dictates the sediment dynamics, thereby affecting bedform development and sediment stability (Blanchard et al. 1997; Paterson et al. 2001; Herman et al. 2001). Bottom roughness and small-scale topography are important contributing factors to bedform pattern development (Van Oyen et al. 2010), and past studies have found a significant effect of epibenthic structures at different densities (e.g., mimics of tube worm reef patches) on flow and sediment erosion (Friedrichs et al. 2000, 2009). However, the influence of shell material on the ripple dynamics, in relation to flow and turbulence, is still not well understood. Thus, we aimed to quantify the turbulence generated by the flow along sand ripples, simulating scenarios both with and without the presence of shells. We used shells from common bivalve species found in the sandy Dutch North Sea including *Spisula* spp., *Tellimya* spp. and *Cerastoderma edule*, at increasing densities. Using empty shells, we determined the influence, via autogenic engineering, of shell material on sediment transport by testing the effects of increasing shell content on ripple formation, shape and migration rates.

Our paper is organized as follows. The experimental setup, instrumentation and analyses utilized are described in section 2. The results, including the incipient sediment motion, ripple migration and other ripple calculations are presented in section 3. The significance of our findings are discussed in section 4. In section 5, the final conclusions are presented.

4.2 Materials and Methods

4.2.1 The experimental setup

Our experiments were performed in a racetrack flume facility located at the NIOZ Royal Netherlands Institute for Sea Research, Yerseke, The Netherlands. This large, unidirectional flow channel measures approximately 17.5 m in length and 3.25 m in width and can generate depth-averaged currents up to 60 cm s^{-1} (Figure 4.1a). A test section containing a sediment basin measuring 200 x 60 x 25 cm (L x W x H) is located at the far end of one of the long, straight sections of the flume to minimize the effect of bend flows (Figure 4.1b). The drive belt equipped on the backside allows the flow to be controlled with high precision.

The basin of the 2 m test section was filled using North Sea sandy sediment (see Table S4.1 for the properties). To maintain a sediment supply throughout the duration of each individual experiment, a thin layer of sand (~3 cm) was also placed over the 3 m preceding the measurement section of the flume track. The bed was fully mixed and flattened before each experimental run. The total water depth was 40 cm and only freshwater was used.

For the shell treatments, we used a mixture that consisted of, on average, approximately 29 % intact shells valves and 71 % fragments (in absolute number of pieces). All non-shell materials (e.g., rocks and wood detritus) were removed prior to the addition. We took a random sampling of the shell stockpile to determine the average dimensional properties of the shell valves and fragments (Table S4.2; Figure S4.1).

Two separate experiments were conducted. A constant flow experiment was used to measure equilibrium ripple dimensions and migration rates. An acceleration (ACC) flow experiment was run to measure the incipient sediment motion. The flow settings used in the two experiments are shown in Figure 4.1c. Both experiments consisted of several experimental runs, which were varied by changing the volumetric percentage of shell content. The control (0 % shells) contained only sandy sediment, while each subsequent treatment was modified by the addition of shell material. The volumetric percentage of shell increased by 2.5 or 5 % intervals, up to 30 %, while the last two treatments contained 40 % and 50 % shells, respectively. The flume was filled with water overnight, and all experimental runs were always performed the very next day to maintain consistency (e.g., minimize variability due to compaction, etc.). The constant flow experiment consisted of six treatments (0, 5, 10, 15, 20, and 50 % shell), while the ACC flow

experiment included 11 treatments (0, 2.5, 7.5, 10, 12.5, 15, 20, 25, 30, 40 and 50; see Table S4.3 for a summary of the experimental settings and measurements).

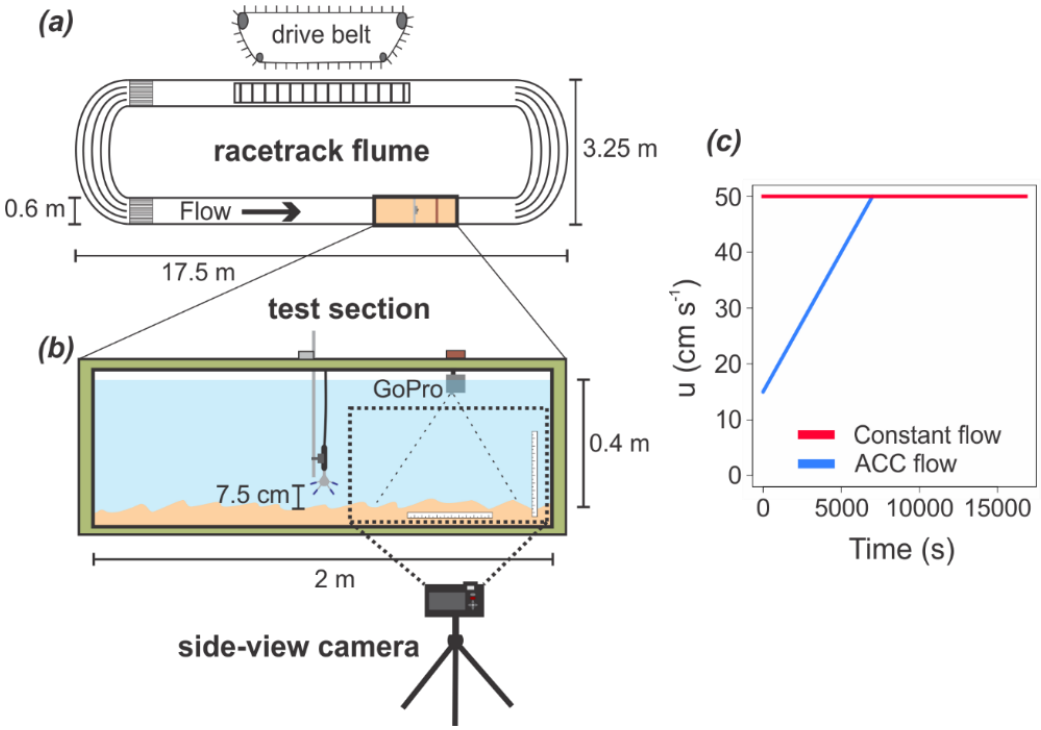

Figure 4.1. *(a)* The top view of the NIOZ racetrack flume. *(b)* A side view of the 2 m long test section showing the ADV vectrino, GoPro and side-view cameras used in each experimental run. Both cameras were positioned within the 2nd half of the viewing window of the test section. *(c)* The flume flow settings implemented in the two separate experiments. *Note*: Although ripples are shown for illustrative purposes, the indicated water depth and ADV height are based on the initial (flat bed) condition.

4.2.2 Constant flow experiment

In the constant flow experimental runs, a 50 cm s^{-1} depth-averaged flow velocity was maintained for more than 4 hours, so as to achieve equilibrium conditions (Figure 4.1c). Preliminary runs showed that morphological equilibrium was achieved well within one hour at this flow rate. A Canon EOS 1000D camera, equipped with an EX Sigma lens (DG Macro, 50 mm, 1:2.8) was positioned at the side of the flume, targeting the 2nd half of the test section to record time-lapse photos from the side at 10-second intervals. The photos recorded a section 76.5

cm in width and 51 cm in height. Two rulers were attached at the edges of the frame as dimensional guides for the image analyses (Figure 4.1b).

Concurrently, a Nortek Vectrino ADV profiler was used to record the 3-dimensional flow rates, through coherent Doppler processing, at a frequency of 30 Hz. Data was filtered for minimum correlation values of 90 %, minimum signal-to-noise ratio of 20 dB and minimum amplitude of -35 dB. The probe was placed approximately 7.5 cm above the bed, which was initially flat in each experimental run. With a blanking distance of 4 cm, it measured the bottom section of the water column from 0 to 3.5 cm above the initial flat bed, over a total of 35 cells (1 mm intervals). The ADV was held in place through the duration of the experimental run. Therefore, near-bed flow profiles were corrected for changing bed elevation during ripple migration.

4.2.3 Sediment image processing

Identification of ripples within the sediment bed was performed through image analysis of the photo time-series obtained by the camera. The vertical position of the sediment-water interface was identified using Canny edge detection of the green band with the *wvtool* R package (Sugiyama and Kobayashi 2016), which showed highest contrast. Gamma transformation of the green band further enhanced this contrast to improve the quality of the detection. The fine-grain noise in the sediment surface was filtered out using a low-pass 2nd-order Butterworth filter to produce a smooth surface from which peaks and troughs can be easily identified, using the *signal* R package (Ligges et al. 2015). Ripples were then classified from the identified sediment surface using peak analysis, which isolated peaks and troughs in the sediment surface with the *pracma* R package (Borchers 2019). This ultimately allowed us to characterize the dimensions of individual ripples and track their movement and development in time. Using 1600 unique frames from each of the six constant flow experimental runs, we quantified the following ripple parameters: (1) the ripple height, (2) length, (3) asymmetry and (4) migration rate.

Each ripple was defined as encompassing the region between two neighboring troughs, separated by a peak. The ripple height and length were defined as the maximum vertical and lateral extent of the ripple. The ripple asymmetry was defined as the difference in length between the two halves of the ripple, separated by the center of its peak, divided by its total length (trough-trough); values change from 0 (highest symmetry) to 1 (highest asymmetry). The migration rate was calculated as the total distance travelled by the peak of a unique ripple over 24 frames

(constituting an interval of four minutes). This frame interval allowed ripples to travel measurable distances while limiting the likelihood of them moving out of frame before measurements could be taken. All four of the ripple parameters were measured throughout the experimental duration using each frame. Only whole ripples were used in the analyses, as ripples that were partially in (upstream) or out (downstream) of the frame were excluded. Given that the migration rate was calculated over 24 frames, measurements were not generated from the first or last 23 frames in each run. All image analyses were conducted in R version 3.4.4 (R Core Development Team 2020).

4.2.4 Near-bed flow calculations

The near-bed turbulent kinetic energy (TKE) was derived from the near-bed flow velocity fluctuations (Pope et al. 2006). This value indicates the mean kinetic energy associated with eddies from the turbulent flow. It is a more-robust method for determining the bed shear stress than e.g., quadrant analysis or Reynold's stress, as these are highly sensitive to the orientation of the ADV profiler. The near-bed TKE was calculated from near-bed flow velocity fluctuations in the x, y and z directions as:

$$TKE = 1/2\left(\overline{u'_{b,x}}^2 + \overline{u'_{b,y}}^2 + \overline{u'_{b,z}}^2\right) \quad (1)$$

where $\overline{u'_{b,x}}$, $\overline{u'_{b,y}}$ and $\overline{u'_{b,z}}$ represent the root-mean-squares of the near-bed flow velocity fluctuations in the x, y and z directions, respectively. These values were extracted from the flow velocity signal through means of applying a 0.1 Hz high-pass 5th order Butterworth filter. This ensures removal of the background velocity during the measurement period. Another 10 Hz low-pass 5th order Butterworth filter was used to remove the higher frequencies where the signal was dominated by noise. The corresponding bottom shear stress (BSS) was calculated as (Soulsby 1983):

$$BSS = 0.19\rho TKE \quad (2)$$

Where ρ is the water density (1000 kg m^{-3} for freshwater). Subsequently, the corresponding total bed roughness, which is affected by both shells and bed forms, can be calculated from the depth-averaged velocity and the BSS. For a unidirectional flow, the BSS can be calculated from the depth-averaged velocity as (van Rijn 1993):

$$BSS = \rho g u^2 / C^2 \quad (3)$$

Where u is the depth-averaged velocity (m s^{-1}), g is the gravitational acceleration (9.81 m s^{-2}) and C is the Chézy roughness coefficient ($m^{0.5}$ s^{-1}). The Chézy roughness coefficient is a function of the water depth and bed roughness (van Rijn 1993):

$$C = 18\log(12h/ks) \quad (4)$$

Where h is the water depth (0.4 m in this flume experiment), and ks is the total bed roughness (m) by combined grain friction and form drag.

4.2.5 ACC flow experiment

This experiment was conducted to measure the onset of incipient sediment transport, as well as the corresponding boundary layer conditions. Incipient sediment transport was measured for a flat bed configuration in order to quantify the direct effect of shells on sediment stability. Sandy sediment with a D_{50} of 350 µm is not expected to exhibit sediment motion below about 30 cm s^{-1} (van Rijn 1993), and an initial test run with our setup showed that there was indeed no sediment movement occurring below 20 cm s^{-1}. Thus, the starting velocity of each run was set at 15 cm s^{-1}. The flow speed was linearly increased at a rate of 0.3 cm s^{-1} per minute from 15 to 50 cm s^{-1} (over a time frame of 116.6 minutes).

The ADV profiler was again anchored in the middle of the test section. One GoPro Hero3 camera was positioned just below the water surface, looking downward, 1.5 m along the test section to produce top-view video recordings of the sediment surface at 2 frames per second. The onset of incipient motion, which was defined as the frequent movement of particles across the entire flume area, was derived visually from the GoPro footage (van Rijn 1993). Visual observation is an accurate method to determine erosion thresholds. As bedload transport is proportional to flow velocity to the power of 3, a small change in velocity will lead to a significant and well-observable change in sediment transport. The depth-averaged velocity was determined from the flume setting at the identified time when incipient motion was observed (Figure 4.1c). The critical mean near-bed flow velocity, TKE and BSS were derived from the ADV measurements over the 5 minutes preceding and 5 minutes after the onset of incipient motion following Equations (1) and (2). The total bed roughness for flat beds with varying shell content was calculated following Equations (3) and (4), using a 10-minute window of ADV measurements at an average flow rate of 20 cm s^{-1}, before any ripples had formed.

4.3 Results

We tested a large range in the shell content in our constant flow experiment, and the results clearly demonstrate that the reduction of ripples is strongly correlated to the shell fraction of sandy sediments. Consequently, the ripple height, length and migration rate were all significantly reduced by the increasing shell content, while the ripple shape became slightly more asymmetric. In the constant flow experiments, the ripples appeared to achieve equilibrium conditions within the first hour at a flow rate of 50 cm s^{-1}. The change in ripple length and height, in particular, can clearly be seen in the concluding frames of each experimental run, particularly around 20 % shell content in the constant flow experiment (Figure 4.2a). The ripple height, length, asymmetry and migration rate were not measured in the ACC flow experiment, as we were interested in determining the incipient motion from these runs. Nevertheless, a similar observation could still be seen at around 15 % shell content, even though these ripples were less equilibrated given the lower flow rates for much of the experimental duration (Figure 4.2b). In addition, as the shell percentage increased in the experimental runs, they began to exhibit larger, denser aggregations (Figure 4.3). What appeared to be bands of shells were actually immobile surficial shells that would periodically appear or disappear as ripples migrated over them. Furthermore, the already-smaller ripples were observed from the GoPro videos to either migrate around the denser and slightly higher–positioned shells, or disappear altogether, so the shells did not incorporate themselves into the (migrating) ripples. Even in the lower shell concentrations, where larger ripples frequently migrated over the sparser quantity of shells, the vast majority of these surficial shells were not moved by either the moving ripples or flow (Figure S4.2). By performing two types of measurements, we investigated both the (theoretical) equilibrium situation at constant high flow conditions (50 cm s^{-1}), as well as the sequence of events that occur as the velocity increases (the ACC flow experiment). The latter pointed to the physical conditions under which sediment dynamics begin to change (e.g., incipient motion).

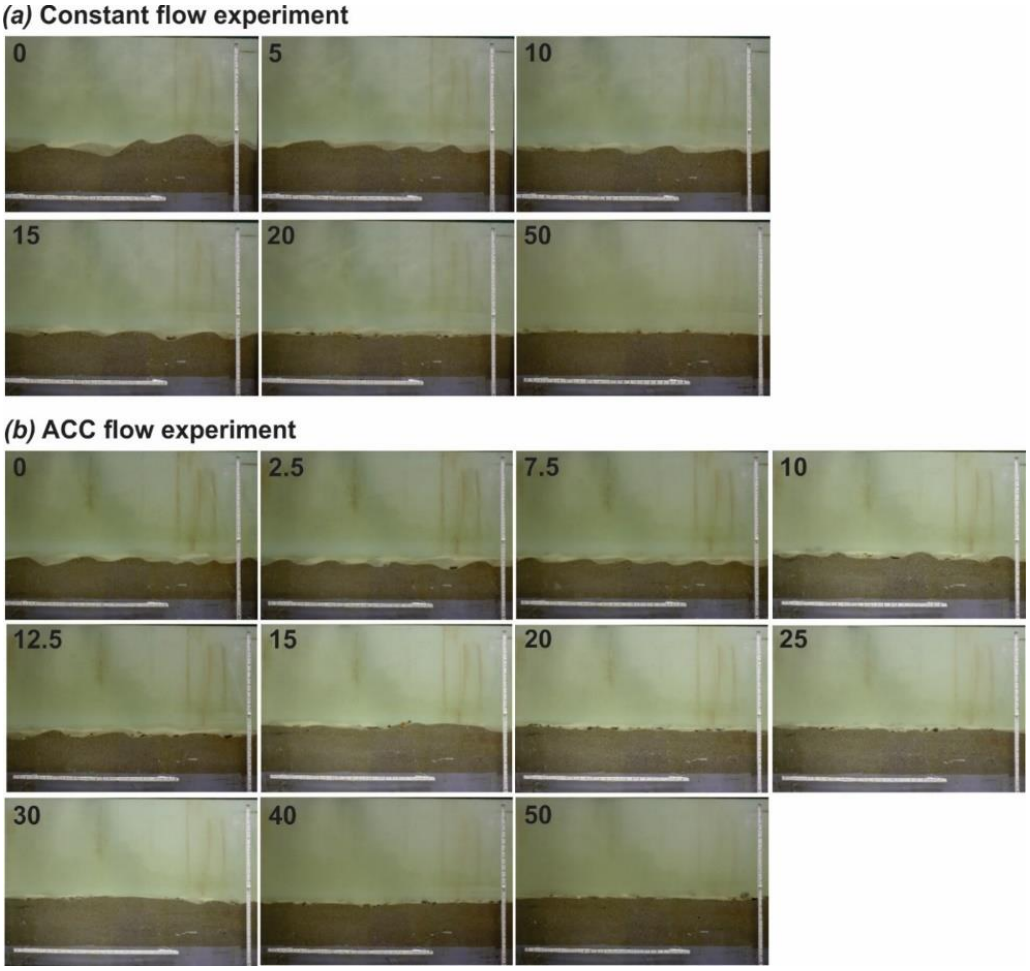

Figure 4.2. The final frame from each *(a)* Constant flow and *(b)* ACC flow experimental run. Numbers represent the shell %. The white vertical and horizontal rulers are both 50 cm in length.

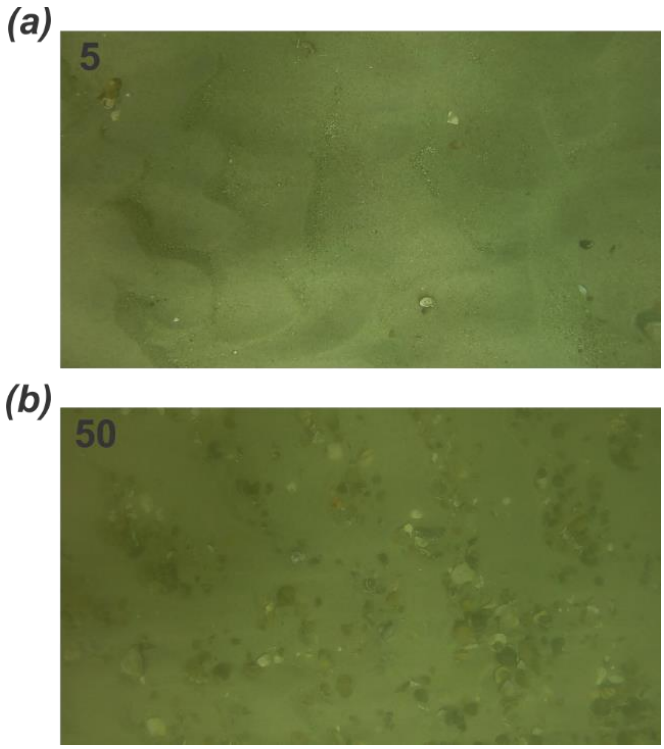

Figure 4.3. Stills taken from the GoPro videos (constant flow experiment) to show the contrast between a *(a)* low-density and *(b)* high-density treatment. Shells increasingly appear as immobile clusters at higher concentrations, as they are periodically exposed due to sand movement. The numbers represent the shell %.

4.3.1 Changes to ripple characteristics (constant flow experiments)

An increase in the shell percentage reduced the spatial dimensions of the ripples, and all of the ripple parameters, except ripple symmetry, were highly affected by the presence of shells. The ripple height, length and migration rate all decreased exponentially as a function of shell content, such that the ripples almost entirely disappeared at 50 % shell content (Figure 4.2). The ripples also became slightly more asymmetric with increasing shell content (Figure 4.4c). Overall, the lengths and heights of the ripples decreased at an average rate of -0.03 cm shell $\%^{-1}$ for the height, and -0.16 cm shell $\%^{-1}$ for the length (Figure 4.4a and b). Ripple asymmetry increased at an average rate of 0.002 shell $\%^{-1}$ (Figure 4.4c). The migration rate showed a consistent decrease with increasing shell content, slowing at an average rate of -0.016 cm min^{-1} shell $\%^{-1}$ (Figure 4.4c and d). Approximately 18, 20, 14, 13, 13, and 12 ripples were included in the calculations for each experimental run (from 0 to 50 % shell content; Figure S4.3).

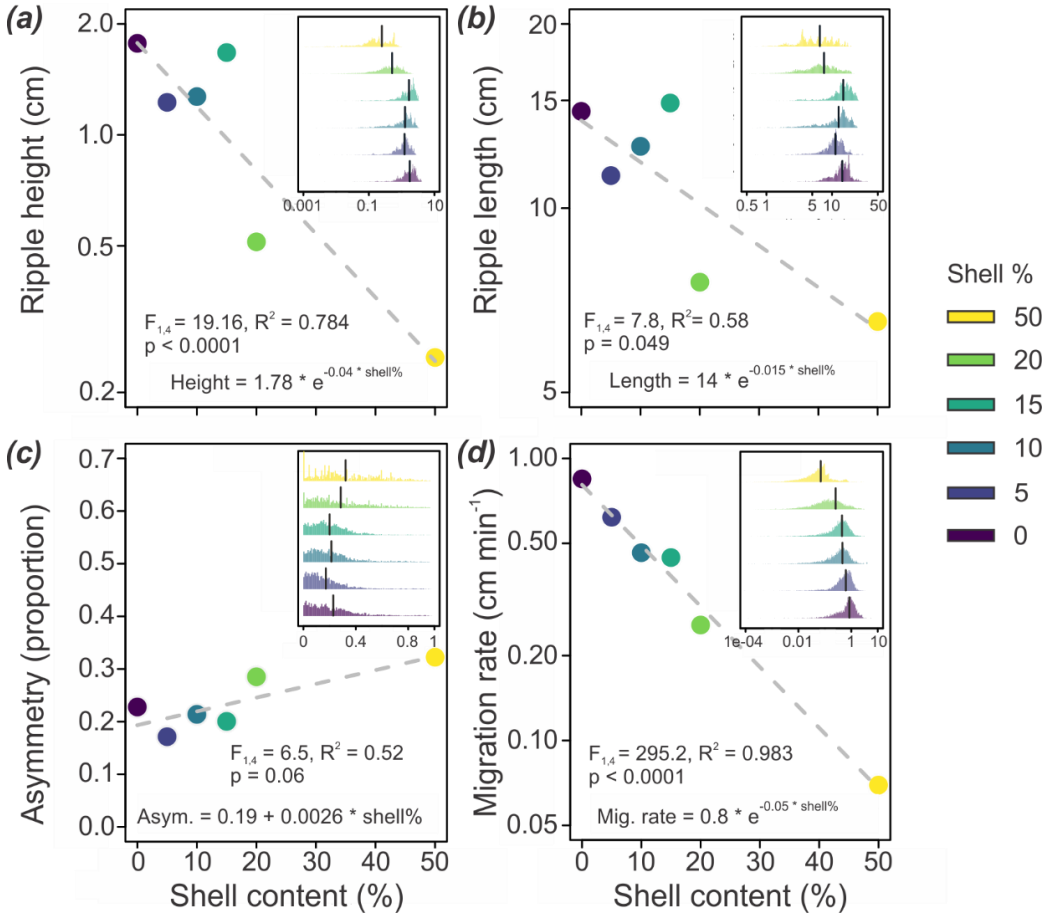

Figure 4.4. *(a)* Ripple height, *(b)* Ripple length, *(c)* Asymmetry and *(d)* Migration rate, plotted against the shell content from the constant flow experimental runs (n = 6). The y-axis of the ripple height, length and migration are plotted under a log scale. *Inset panels:* The corresponding histograms for each ripple parameter, with the x-axis values representing the y-axis values of the respective regression plots. Vertical lines represent mean values.

4.3.2 Changes to near-bed hydrodynamics and critical BSS

In the constant flow experiment, the presence of shells (at all percentages) enhanced the near-bed flow in the streamwise direction (Figure 4.5a), as ripple sizes become diminished (Figure 4.4). Near-bed vertical flow was on average directed downwards, and reduced towards increasing shell content (Figure 4.5b). Interestingly, while the increasing near-bed flow velocity with increasing shell percentages indicates a reduction in overall bed friction (Figure 4.5a), the highest

TKE is observed at 50 % shell content. Overall, there is also a consistent pattern in the turbulent structure maintained between each run (Figure S4.4).

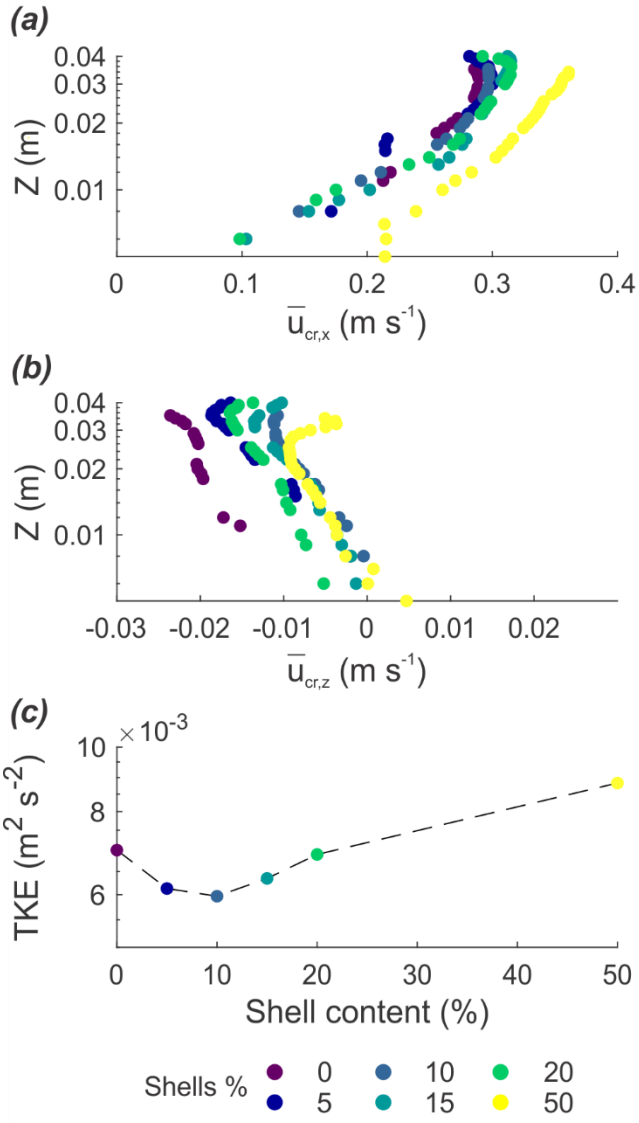

Figure 4.5. Time-averaged near-bed velocity profiles showing the *(a)* x and *(b)* z direction of the constant flow experimental runs, as well as the *(c)* peak TKE values plotted against shell content. *Note*: The profiles are time-averaged, as indicated by the overbars, over the entire duration of each experimental run.

The critical near-bed velocity profiles from the ACC flow experimental runs showed a large reduction in critical near-bed velocity between 0 and 15 % shell content, followed by a minor reduction towards the 50 % shell content (Figure 4.6a). No differences were observed between

the vertical velocity profiles (Figure 4.6b), which averaged 0 as the ripples were absent. Shells had a strong influence on the critical TKE and BSS (Figure 4.6c and 4.7a). The most immediate and drastic changes in the critical BSS occurred when the smallest quantity of shell was mixed into the sediment (2.5 %), where the addition of shell material initially increased the critical BSS from approximately 0.2 N m^{-2} at 0 % shell content to approximately 0.75 N m^{-2} at 2.5 % shell content (Figure 4.7a). Subsequently, the critical BSS dropped towards 0.25 N m^{-2} at 15 % shell content (R^2 = 0.91, Figure 4.7a). At shell concentrations above 20 %, the critical BSS slowly increased again to approximately 0.5 N m^{-2} at 50 % shell content (R^2 = 0.50, Figure 4.7a). In contrast to the critical BSS, the critical depth-averaged velocity for incipient motion consistently reduced towards 15 % shell content (R^2 = 0.99, Figure 4.7b), after which it stayed constant (R^2 = 0.29, Figure 4.7b). The quadrant analysis plots show that the turbulence-induced flow is predominantly directed forwards and downwards (Figure S4.5).

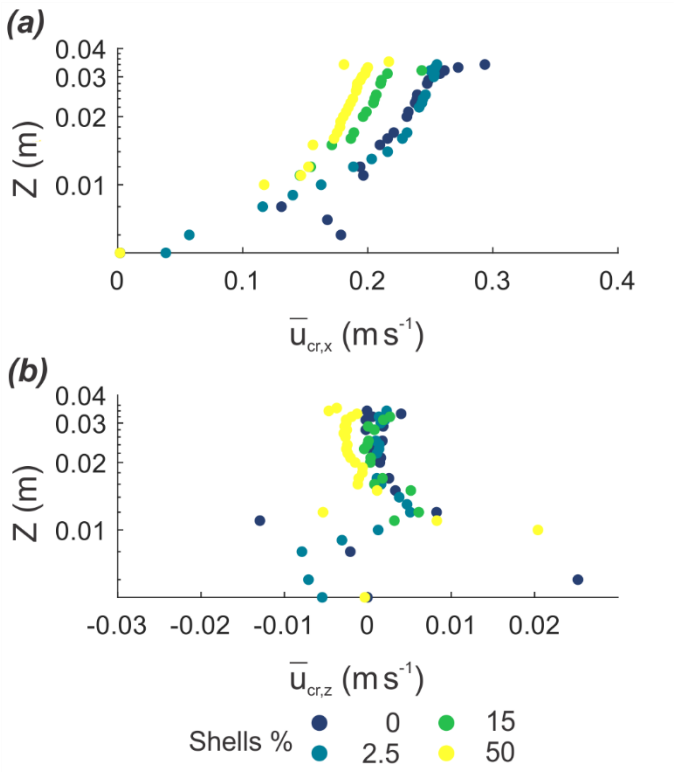

Figure 4.6. *(a)* Near-bed streamwise flow and *(b)* vertical flow at the onset of sediment transport for flat beds (ACC flow experiment). *Note*: The overbars denote that the x-axes are time-averaged, over a 10-minute period, which encompasses the 5 minutes prior to and following the incipient motion, for the four selected experimental runs.

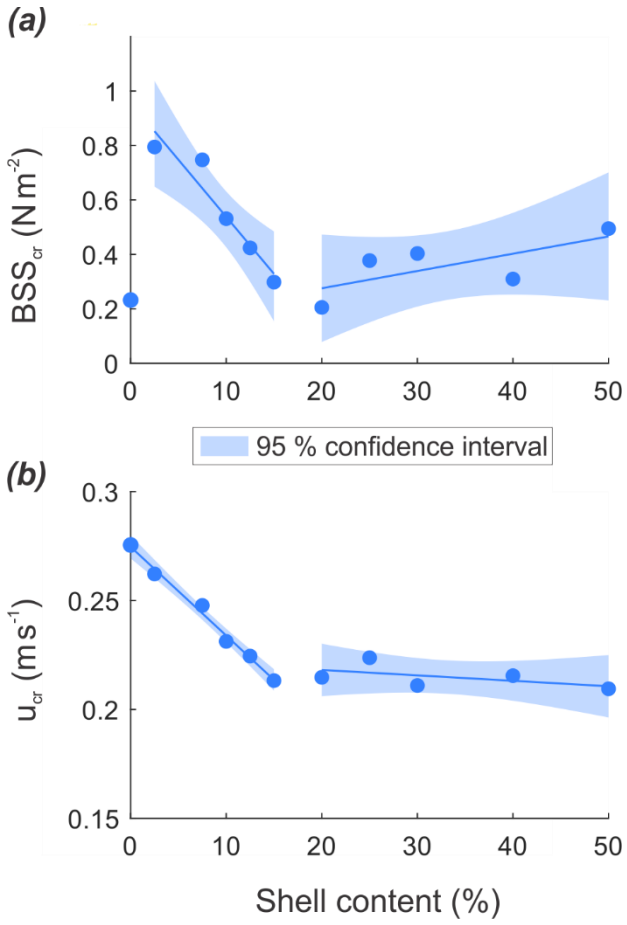

Figure 4.7. *(a):* The critical BSS for incipient motion and the *(b)* corresponding depth-averaged velocity for the ACC flow experiment. The shaded regions represent the 95th percentile confidence intervals.

The influence of shells on the total bed roughness showed contrasting behavior between flat (e.g., ACC flow experiment) and equilibrium (e.g., constant flow experiment) beds (Figure 4.8). Under the absence of bed forms, the total bed roughness showed a similar trend as the critical BSS; a large increase from 1.2×10^{-4} m to 0.042 m between 0 and 7.5 % shell content, followed by a decrease to 0.007 m at 15 % shell content, after which it stabilized at 0.005 ± 0.004 m towards 50 % shell content. When ripples were present (equilibrium bed), the total bed roughness decreased from 0.02 to 0.013 m from 0 to 10 % shell content. Beyond 10 % shell content, the total bed roughness increased to 0.036 m.

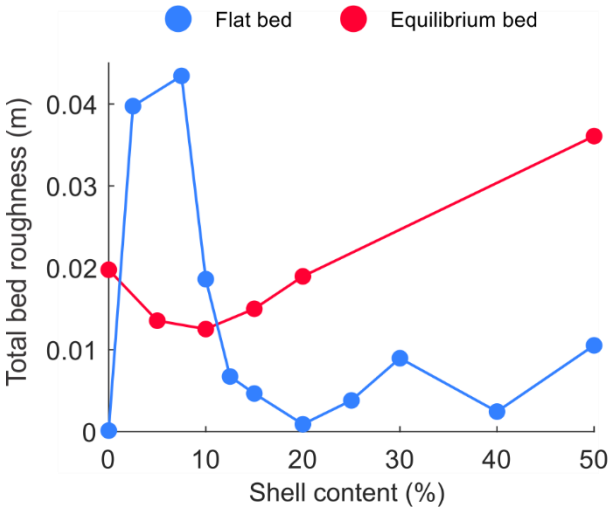

Figure 4.8. Total bed roughness against shell content for the flat beds (ACC flow experimental runs) and equilibrium beds (constant flow experimental runs).

4.4 Discussion

4.4.1 Significance of shell - ripple interactions

In gravel bed rivers, it is known that the incorporation of topography into the sediment surface creates microclusters that increase both the bed roughness as well as bed stability (Curran 2010). The anchoring of shells, even through partial burial, in sandy sediment greatly raises their critical erosion threshold compared to individual shells situated on a flat surface, irrespective of the orientation. Whereas loose shells on top of a flat sandy surface can erode at velocities well below 40–50 cm s^{-1} (Dey 2003), shells that are fixed in the sediment, especially in clusters, are much less susceptible to erosion. In our experiments, the shells were almost completely immobile over the entire duration of the experimental runs, with visually no noticeable change as evidenced by both the time series photos and video footage (Figure S4.2). What would appear as clusters or bands of shell is an artefact caused by the localized changes and movement of the sand, rather than a change to the shells. Despite flow velocities reaching these thresholds in our experiments, the shells were mostly immobile, even as ripples migrated over them. In rare cases, the smaller valves and fragments sometimes shifted a few centimeters due to ripple movement. But in the higher shell treatments, the shells were practically fixed structures (Figures 4.3 and S4.2).

Therefore, a sandy sediment bed with sufficient quantity of shells under a unidirectional flow will produce an armoring effect somewhat similar to riverine environments, where gravel

beds produce clustered structures that mediate the bed-flow interactions through a combination of bed stabilization, altered roughness and regulation of the amount of sediment available for transport (Wilcock and Detemple 2005; Tuijnder et al. 2009; Curran 2010). In addition, our experiments show that shell content has another indirect bed-mediating effect. Due to the dampening of the size of the ripples, and consequently a reduction of the bottom roughness, there was a progressive enhancement of the mean near-bed flow (Figure 4.6) as a function of increased shell content, while at the same time, a slowing down of the ripple migration rate (Figure 4.4d), due to both a decrease in overall sediment supply (from shell displacement) and immobile shells, even at the very low percentages.

The opposing behavior in terms of critical BSS and depth-averaged velocity indicates that shells may modify sediment-flow interactions in two ways: 1) by stabilizing the sediment, and 2) by increasing the total bed roughness and near-bed TKE. Following this, the large increase of critical BSS for low shell concentration is probably a consequence of a large increase in sediment stability or by a large increase in bed roughness, given that the reduction in critical depth-averaged velocity remains minimal. In the case of low shell density, shells may disrupt flow in the boundary layer and thereby increase the TKE. For higher shell densities, flow may be deflected over the shells, which progressively reduces the disturbance of the boundary layer and thus, the TKE. Similar density-dependent alterations in flow pattern from flume studies using either live animals or mimics have also been observed (Friedrichs et al. 2000, 2009). In these studies, the erosion fluxes and deposition of suspended material were substantially enhanced when densities were such that less than 4 % of the sediment area was covered, while above this coverage, both factors saw a drastic reduction.

As the flat bed transitions towards a rippled one, the initial flow and (de)stabilization effects begin to shift. As the shell content increases, the sand available for migration decreases while the immobile shells hamper ripple formation. Consequently, the attainable ripple size negatively correlates to shell content. Both the presence of ripples and shells increase the bottom roughness, and the pattern of the calculated total bed roughness, which is minimal at intermediate shell content, shows both impacts. Bed roughness was actually the largest where the shell content was also highest (Figure 4.8), despite the ripple size having diminished substantially. This contrasting pattern shows that, in the absence of ripples, small shell concentrations generate a high total bed roughness, but this effect is suppressed by the large ripples that are formed under these conditions at equilibrium. At high shell concentrations however, the direct effect of shells on total

bed roughness is smaller, but when reinforced by the presence of small ripples, results in a higher combined net roughness (Figure 4.8).

4.4.2 Potential implications of shells for larger-scale sediment dynamics

Natural sediments rarely consist of pure, clean sand, and often include other debris, fragments and particles (Gornitz 2008; Seibold and Berger 2017; Earle 2020). But sediment characteristics are important for bedform development, roughness and larger-scale implications, and even minute changes can immediately impact smaller bedforms such as sand ripples. Similar dampening effects have been shown for other biogenic substances and fine particles (van Ledden et al. 2004; Friend et al. 2008; Malarkey et al. 2015). Biogenic shells, given their size, density and dimensional aspects, behave very differently from sand grains (Soulsby 1997), and, as shown here, a composition of 2.5 % shell can already drastically enhance critical BSS and total bed roughness. As the rippled bed matures, which is likely the realistic scenario in many sandy seabeds, the effects of increasing shell content becomes more evident, through patterns of bed stabilization (e.g., armoring). Our quantities of shell material are well within the range observed in sandy coastal environments. At a sandy (sand wave) location within the Dutch North Sea (Damveld et al. 2018; Cheng et al. 2020), the shell content of the sediment samples was also determined. We measured shell percentages ranging from < 1.0 to 41 % (mean = 8 %, mode = 7 %). Given the observed complexity in the near-bed flow conditions at these shell percentages, this signifies that many such sandy environments are likely to be subjected to similar sand-shell-ripple interactions.

The primary mechanisms driving current-generated ripple dynamics are rather well established, but good indicators are still lacking for ripple size, which is dependent on the grain size, viscosity, density and flow strength (Lapôtre et al. 2017). Most model predictions typically omit other particle types or represent the sediment by a single value (e.g., D_{50}). However, given the fact that these shell valves and fragments differ in size, shape and density from sand grains and are largely immobile in our experiments, they cannot be accurately approximated by equations developed for average sand grains. Nevertheless, the addition and subsequent coarsening due to shell valves and fragments dampened the ripples up to 7-fold with height, more than 2-fold in length and with an order of magnitude reduction in migration rate (bare sand vs. 50 % shells; Figures 4.4a, b and d). The effect of shells on ripple symmetry is inconclusive. There was a very

slight increase in asymmetry, but this may be due more to the noise from the variability than being an actual trend (Figure 4.4c).

We have shown how shell percentages around 10–15 % already reduced ripple size significantly, and above 20 %, ripples are almost entirely absent. We also observed largely-immobile clusters or bands of shells, essentially stabilizing the sediment through an armoring effect. This is perhaps most comparable with the riverine gravel-bed armoring phenomenon, where due to the coarser sediment particles and flow conditions, coarser grains are partitioned to the top. Consequently, the surface becomes a relatively immobile layer inhibiting sediment transport, among other hydrodynamic interactions (Shen and Lu 1983; Dietrich et al. 1989; Tuijnder et al. 2009; Curran 2010). Storm events are often necessary to cause significant flushing of the lower layers or even break an armored layer (Vericat et al. 2006). It would be interesting to investigate how a large quantity of immobile shells would behave under such extreme conditions. Some evidence suggests that gravel bed armoring can persist through floods, but the level of mobility and partial replacement or renewal of grains in the surface layer is inconclusive (Wilcock and Detemple 2005).

Care must be taken in drawing comparisons as these are dissimilar environments with entirely different causes for the armoring. As mentioned above, the shells were already immobile from the start to finish in our experimental runs, and the long-term formation/evolution processes of sand-shell beds remains inconclusive. Moreover, unlike the riverine gravel, which is closer to a spherical shape, shells are an entirely separate class of materials with biological origins. Under typical unidirectional flow conditions, a higher shell % can be expected to dampen ripple development, migration and, consequently, the bedload transport. How shells might affect the hydrodynamics and bed morphology under more-complex systems and flow conditions, particularly in shallower, wave-dominated environments, remains to be investigated (e.g., under sheet or oscillatory flow conditions; Nelson et al., 2013; Precht & Huettel, 2003; Soulsby, 1997).

Nevertheless, we foresee many relevant implications of shell research in geomorphologic investigations as well as coastal engineering applications. Shells clearly have the ability to regulate ripple growth and migration, and consequently the bedload transport. A good estimation on the sediment-shell composition would allow us to assess the sediment dynamics for a given sandy environment and provide better insight on bed stability to produce more-accurate calculations on bedload transport. Concurrently, given the close-coupling between sediment transport and larger-scale adaptations in seabed morphology, this information could aid in developing or utilizing better methods with regards to offshore seabed patterns, shoreline

preservation, longshore sediment transport and coastal management. Our study has provided new insight on how shell material directly, and measurably, influences ripple evolution and migration in medium sand.

4.5 Conclusions

A series of sand-shell-ripple experiments were conducted to directly measure the impact of shell material on the development of current-driven ripples in sandy sediment (D_{50} = 352 µm). Our results demonstrate that the shell content has a dynamic effect on the near-bed hydrodynamics that changes over several stages. This mainly occurs as the BSS to flow velocity balance is altered, initially showing a more significant sheltering effect at low shell content (≤ 15 %) since higher shell quantities will disproportionately enhance the turbulence under a flat bed setting. However, when a sufficient flow velocity is achieved to generate ripples, the shell-induced turbulence will quickly be overcome by the developing bedforms and offset the initial trend. The armoring effect grows stronger with increasing shell content in the form of immobile shells.

In terms of sedimentary transport, shell compositions above 15–20 % exhibit a drastic change in the ability of ripples to develop and migrate. The threshold is somewhat higher in the constant flow than in the ACC flow experiment (20 % vs. 15 % shells), given the much longer exposure to higher velocity and equilibrium conditions. A sandy mixture with 2.5–50 % shell content increasingly dampens the ripples, thereby reducing the ripple migration by up to one order of magnitude. Moreover, these percentages are representative of certain areas within the natural environment. Thus, the presence of shells needs to be taken into account to better understand and predict the sedimentary processes, as compared to the more simplistic conditions that could be expected from purely siliciclastic sediment. Our experiments shed some light on the direct influences of shells on ripple dynamics in sandy sediment under unidirectional current-flow conditions. This work would greatly benefit from further studies utilizing other grain sizes combined with shells, as well as an investigation on the other particles of different origin, size, shape and density, but which are nevertheless also commonly found throughout the marine environment.

CRediT authorship contribution statement

Chiu H. Cheng: Conceptualization, Methodology, Investigation, Formal analysis, Data Curation, Visualization, Writing – Original Draft, Writing – Review & Editing, Project administration.

Jaco. C. de Smit: Conceptualization, Methodology, Investigation, Formal analysis, Software, Visualization, Writing – Original Draft, Writing – Review & Editing. **Greg. S. Fivash**: Methodology, Formal analysis, Software, Visualization, Writing – Original Draft, Writing – Review & Editing. **Suzanne J. M. H. Hulscher:** Writing – Review & Editing, Funding acquisition**. Bas W. Borsje:** Conceptualization, Writing – Review & Editing, Supervision. **Karline Soetaert:** Conceptualization, Writing – Review & Editing, Supervision, Resources, Funding acquisition.

Financial support: This work was supported by the NWO-ALW [SANDBOX project, grant number 871.15.011]; The Royal Boskalis Westminster N.V.; the Royal Netherlands Institute for Sea Research (NIOZ) and Utrecht University are also greatly acknowledged for their financial support of this project.

Acknowledgments: We would like to thank Tjeerd Bouma in the planning and conceptualization of the experiment. Many thanks also to Lennart van IJzerloo, Bert Sinke and Arne den Toonder for their assistance with the setting up of the flume.

Data availability: The data collected and used for this publication will be uploaded to the 4TU.ResearchData repository at the following link: (10.4121/12852113), hosted by TU Delft, The Netherlands.

Supplementary Materials for Chapter 4:

Table S4.1. Grain size characteristics of the sandy sediment fraction used in the experiments.

Sediment fraction	Grain size (μm)	SD
D_{10}	239	3.9
D_{50}	352	1.3
D_{90}	520	10.7

Table S4.2. Representative measurements of the shell valves and fragments used in the experiments.

Shell type	# samples	Length	Width	Height	Weight
Valves	200	27.5 (± 4.5)	23.6 (± 3.9)	9.5 (± 2.3)	2.3 (± 1.4)
Fragments	455	18.2 (± 7.8)	13 (± 6)	4.5 (± 2.6)	0.74 (± 0.9)

Length, width and height are in units of mm, while weight is in g. Height represents the thickness of the shell, from the umbra to the center hinge.

Table S4.3. Experimental settings and measurements undertaken in both experiments.

Experiment	D_{50}†	Flow (cm s^{-1})	Shell %	Duration	Measurements
ACC	352 μm	15 to 50 (increase of 0.3 min^{-1})	0, 2.5, 7.5, 10, 12.5, 15, 20, 25, 30, 40, 50	~4 hr. 26 min.	ADV†† GoPro Time-lapse‡
CF	352 μm	50	0, 5, 10, 15, 20, 50	~4 hr. 26 min.	ADV††† GoPro‡ Time-lapse

†Bare sandy sediment (control)

††Average over the 5 minutes before and after incipient motion

†††Average over the entire experiment

‡Data available but not used

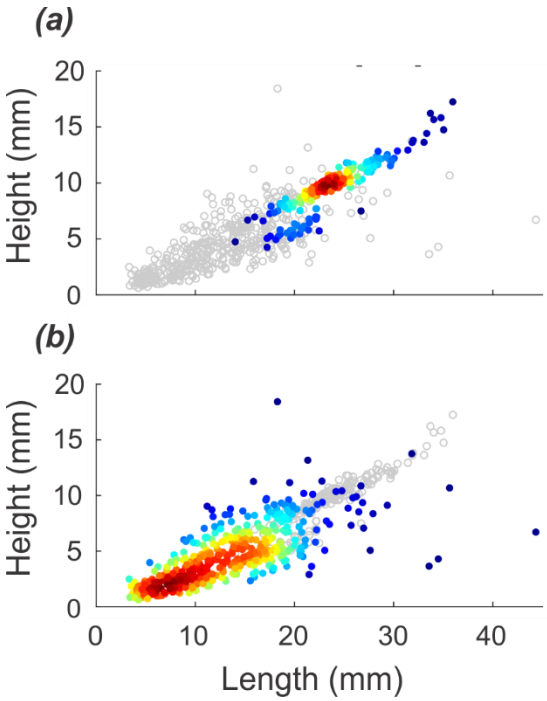

Figure S4.1. Measured shell Height (thickness) vs. Length for (a) whole shell valves and (b) shell fragments. Both panels contain all of the measurements, but the dataset of interest is indicated by the bright colors, while the points from the other dataset are plotted in grayscale. Colors indicate point density (e.g., how often a specific length – height ratio occurs with respect to the whole dataset) based on a kernel density estimate.

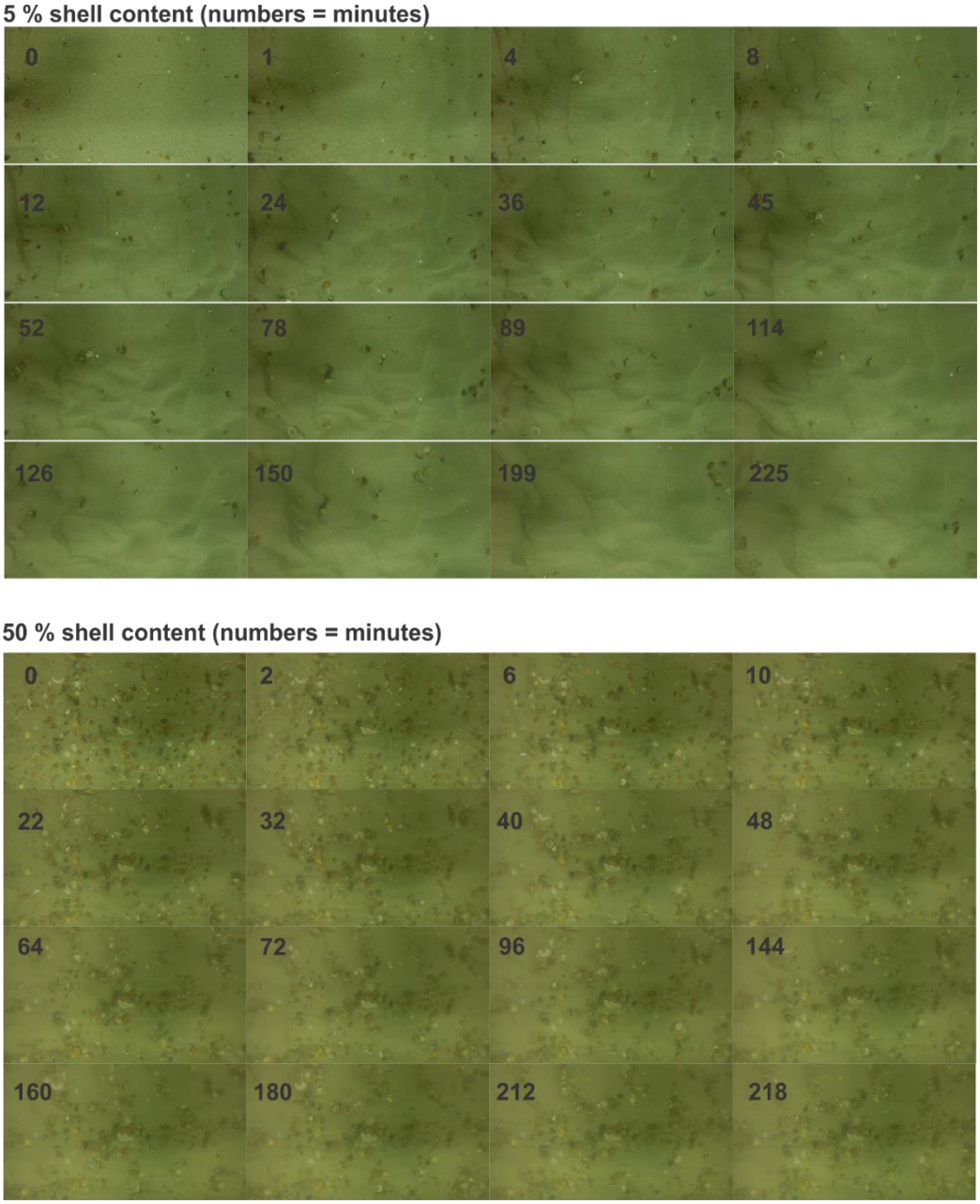

Figure S4.2. Snapshots extracted from the GoPro footage of the constant flow experiment to show that the majority of the shells remain in place throughout the duration of the experimental run at both the low and high shell treatments.

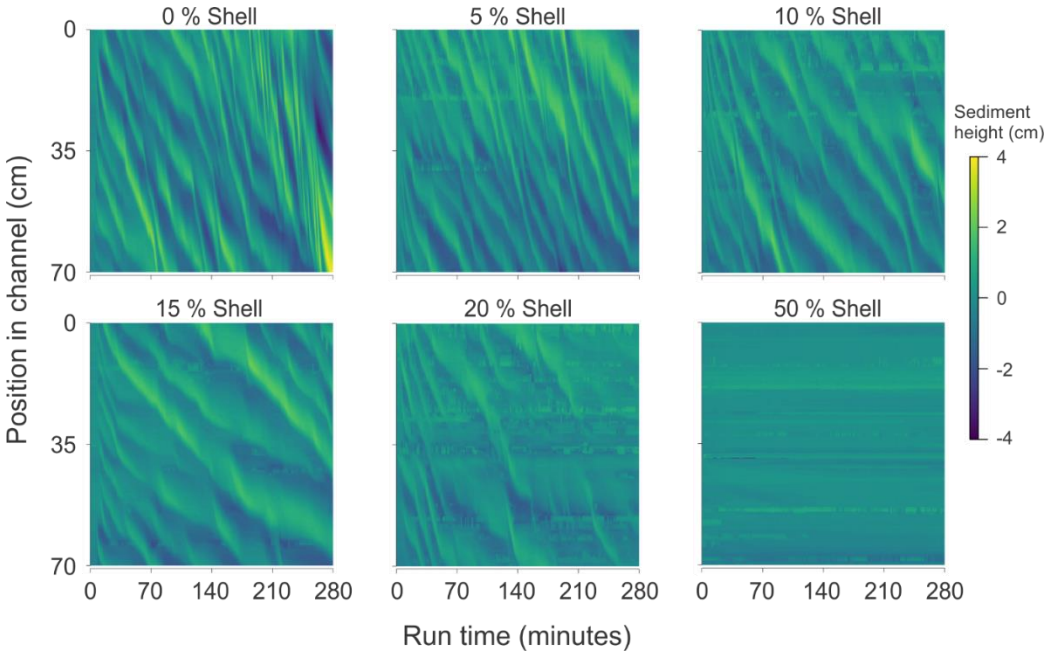

Figure S4.3. Raster plots of the sediment height of each constant flow experimental run to show the distance (y-axis) each ripple traveled along the flume channel over time (x-axis). These plots also show the approximate number of ripples that was present and used in the calculation of ripple height, length, asymmetry and migration rate for each run.

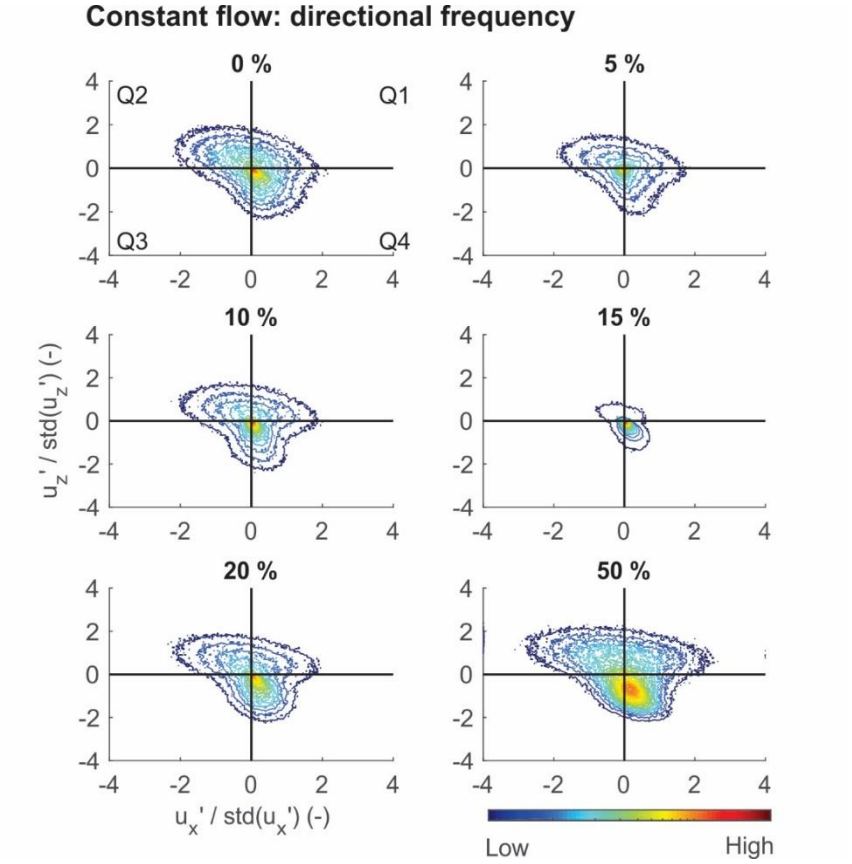

Figure S4.4. The quadrants of each constant flow experimental run, showing the presence of turbulent coherent structures, plotted along the streamwise and vertical planes. The contours represent the point density. Quadrant 2 (top left) represents the burst, or ejection (away from the bed) and quadrant 4 signifies the sweep events in the flow (towards the bed). Exact values are not indicated in the color scale bar as the relative turbulence frequency differs somewhat between each treatment.

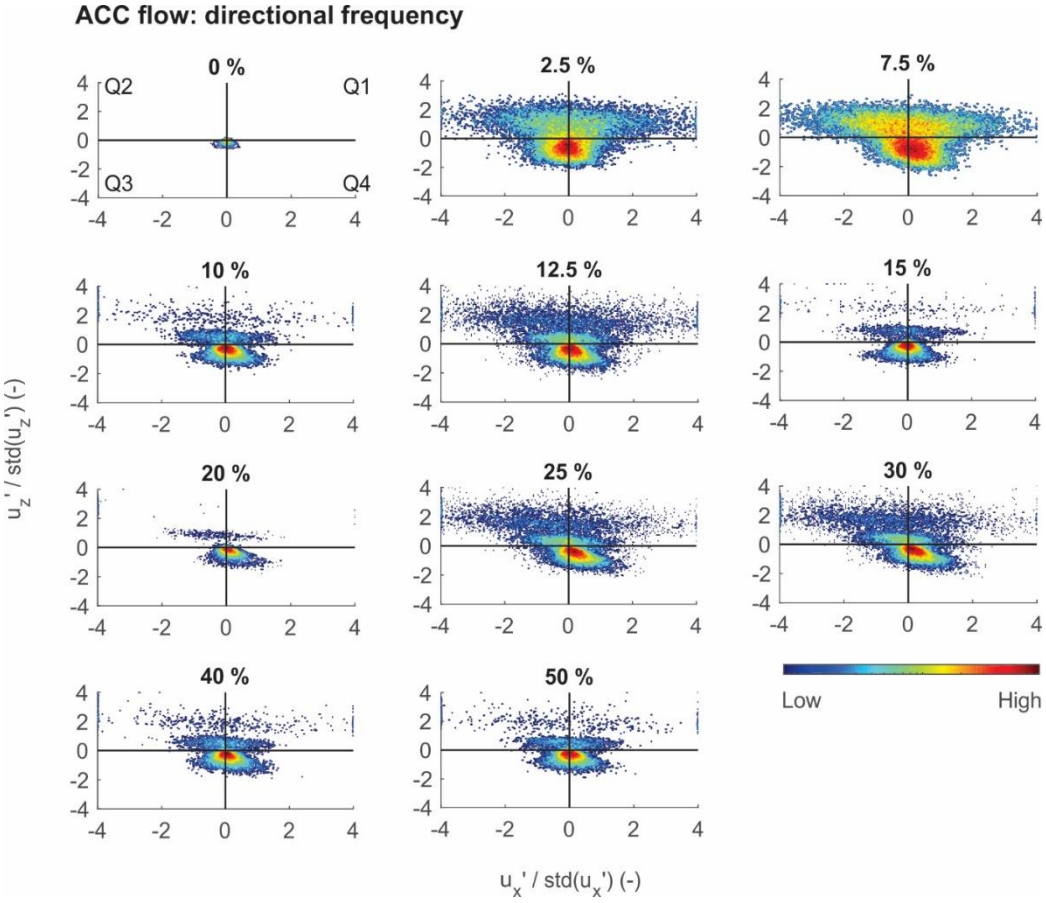

Figure S4.5. The quadrants of each acceleration flow experimental run, showing the presence of turbulent coherent structures, plotted along the streamwise and vertical planes. The contours represent the point density. The burst is represented by Quadrant 2 (top left) and the sweep by Quadrant 4 (bottom right). Exact values are not indicated in the color scale bar as the relative turbulence frequency differs somewhat between each treatment.

Chapter 5 General Discussion

Photo by Chiu H. Cheng

5.1 An outlook of the Dutch North Sea over different spatial scales

The goal of this PhD research project was to facilitate a better understanding about the biogeomorphological interactions within shallow, sandy environments. Specifically, we aimed to investigate the sedimentary bed patterns and benthic community structure at an asymmetrical sand wave field. One of the primary objectives was to determine the dominant patterns in the sedimentary and biogeomorphological characteristics over a small spatial scale. While both of these characteristics are very important in ecosystem functioning of coastal marine environments, there is still a general lack of scientific knowledge about the functional aspects at work (as opposed to the physical, structural integrity of the habitat). The North Sea has long been heavily utilized, but the intensity of human activity has increased rapidly in recent years (Deltacommissie 2008; Stolk and Dijkshoorn 2009; de Jong et al. 2016; de Vrees 2019). This is projected to further grow in order to address the mounting concerns related to climate change and sea level rise, for both ecological and also socio-economic needs (Kannen and Burkhard 2009; Provoost et al. 2010). These activities put ever-increasing pressure on our marine environments, often in the form of physical changes such as “ocean sprawl” due to the construction of rigid structures (De Mesel

et al. 2015), but also a coarsening or fining of sediment from sand extraction or other secondary effects of windfarm monopiles or other offshore infrastructure (Coates et al. 2013). In particular, there has been a recent trend of shifting renewable energy harvesting to the sea (e.g., wind; Halpern et al. 2015). Already an important activity within the Dutch sector alone, the total coverage of wind turbines is estimated to reach up to 22 percent by 2050 (de Vrees 2019). Given the large footprint required by these OWFs and the potential environmental and socio-economic implications (e.g., initial construction, followed by the exclusion of other activities such as shipping, fishing and sand mining), this only adds further complexity for the coastal marine system (Ybema et al. 2009; Gee and Burkhard 2010).

There has been much discussion about the creation of marine protected areas or other exclusion zones, in part to serve as sanctuary ecosystems for vulnerable species (Gee and Burkhard 2010; Jongbloed et al. 2014; Lindeboom et al. 2015). Whether or not these de-facto "no-take" zones and artificial reef ecosystems will yield a net benefit to the ecological community is still under discussion (Smyth et al. 2015; Lindeboom et al. 2015; Elliott et al. 2018). For example, more than 300 oil and gas facilities are expected to be decommissioned by 2025 across the North Sea. Many of these are located in, or linked to, marine protected areas. Thus, the potential impacts from the entire removal process on the ecological community is a huge cause of concern, with efforts underway to study the potential disruption to the benthic equilibrium conditions and also develop frameworks to help guide the decision-making process, such as on how and what to remove from the decommissioned infrastructure (Chandler et al. 2017; Burdon et al. 2018; Rouse et al. 2018). Other potential secondary effects that result from changes to the seabed include modifications in the biogeochemical cycling and food web structure. The removal of macrobenthos and subsequent alteration in the benthic community composition, which often plays an active role in microbial-mediated, sedimentary biogeochemical processes, could also pose significant ramifications (Stief 2013). Comprehensive studies are still largely lacking in dynamic environments such as tidal sand waves. Therefore, it is important to first establish a clear understanding of these processes for the specific habitats of interest. This could then serve as a baseline condition for regions of high economic interest, which are likely to be directly (or indirectly) impacted in the near future. But sampling at the proper spatial scale and at a sufficiently high resolution is necessary in order to capture some of the site-specific qualities.

Large monitoring campaigns such as the NSBS and the follow-up study in 2000 were able to provide a broad assessment of the ecological conditions over the entire North Sea (Duineveld et al. 1990; Heip and Craeymeersch 1995; Rees et al. 2007). However, results from

our study show that these large-scale investigations, although comprehensive, carry the disadvantage of potentially losing the minute details of the highly localized information that are only possible to obtain from smaller-scale, higher-resolution sampling, as indicated by the benthic assemblage and species richness, particularly for dynamic bedforms (Chapter 3).

This especially motivated our interest in studying sand waves, as their location, spatio-temporal scale and highly-dynamic nature places them directly at the interface between biogeomorphology and the many potentially impactful offshore activities (Damen et al. 2018; Damveld et al. 2019). We conducted a thorough study of an asymmetrical sand wave field offshore of the island of Texel, which is a sandy and dynamic location that appears to be very directly influenced and structured by the hydrodynamic forces (Chapters 2 and 3). Due to the frequent collection of samples containing high shell content, we also carried out laboratory experiments in the NIOZ racetrack flume (Chapter 4). Using shells as a proxy for living bivalves, we then investigated how these biogenic particles could affect the dynamics of sand ripples. Our detailed benthic sampling and characterization of the community composition provides a glimpse about a distinct sandy, subtidal environment, located in the southern North Sea. At the very local scale of an asymmetrical sand wave environment, the bathymetric features appear to play the most important role for both the sediment characteristics as well as the benthic community composition (Damveld et al. 2018; Cheng et al. 2020, 2021).

5.2 Biogeomorphological structuring of asymmetrical sand waves

As discussed in the first three chapters, sand waves are dynamic bedforms that are largely shaped by the hydrodynamic conditions, typically occurring in shallow environments with a relatively strong tidal current (Fredsøe and Deigaard 1992; Huntley et al. 1993). Although sediments tend to be well sorted in sandy bedforms over both small and large spatial scales (van Dijk et al. 2012; Koop et al. 2019), sand waves nevertheless exhibit distinct sediment sorting patterns (Terwindt 1971; Van Lancker and Jacobs 2000; Cheng et al. 2020), thus adding complexity to sandy environments (Damveld et al. 2019). When the tidal forcing is slightly uneven, there is a residual current. From model predictions, we know that its influence on the growth rates of sand waves and biomass is rather negligible, especially on the short term (Damveld et al. 2019). However, on longer time scales of years or decades, it produces asymmetrically-shaped sand waves (van Gerwen et al. 2018).

As shown in modeling simulations (Damveld et al. 2019, 2020a), and now also confirmed in our field studies (Chapters 2 and 3; Damveld et al. 2018; Cheng et al. 2020, 2021), asymmetrical sand wave environments exhibit a strong relationship between the positioning along the wave and the sediment characteristics of the ensuing bed morphology. Video observations clearly illustrated a contrast in the occurrence and regularity in the shape of sand ripples between the crests and troughs (Damveld et al. 2018). In addition, the measured changes in the biogeomorphological conditions were quite drastic and abrupt, occurring on the order of meters to tens of meters. By further dividing the sand waves into four morphological units (MU), we could quantify significant differences in sediment grain size, permeability, organic carbon (OC) and chlorophyll *a* (chl *a*) concentrations (Chapter 2). The four MUs are effectively distinct environments, but with some overlaps between the gentle-slope and crest (coarser, more permeable) and the steep-slope and trough (finer, less permeable and richer in organic material). Moreover, the two opposing slopes, rather than the crest and trough, were the most contrasting environments, which is a significant finding since these sections have often been neglected in field studies.

Sediment composition is known to play an important role in the benthic community composition (Künitzer et al. 1992; Heip and Craeymeersch 1995; van Nugteren et al. 2009c; Reiss et al. 2010) and the physical features (e.g., bedforms) of the seabed can also influence the spatial distribution of certain species of benthos (Markert et al. 2015; van der Wal et al. 2017). Despite limited field information (Baptist et al. 2006), large spatial variability in the physical conditions of sand waves have been shown through repeated modeling studies both with and without benthic organisms (van Gerwen et al. 2018; Damveld et al. 2019, 2020a). Modeling simulations suggest a close-coupling between sand wave formation and the sediment and benthic community composition. They are also advantageous for testing different scenarios over the full timescale, from which a flat sediment bed matures into an equilibrium sand wave (decadal or more; van Gerwen et al. 2018; Damveld et al. 2019, 2020). Such spatio-temporal scales would not realistically be possible even with thorough monitoring campaigns. However, the assumptions and simplification of the sedimentary conditions and benthic assemblages (often as single species with a homogeneous spatial distribution; Borsje et al. 2009) call into question the reliability of the model to accurately predict the actual benthic community assemblage. Therefore, field data collected to a sufficiently-high resolution could aid in the improvement of models and model inputs through a two-way coupling or, at the very least, as validation of the output. This is similar to what some riverine studies have attempted (Crouzy et al. 2015; Bärenbold et al. 2016), or

simulations of the feedback between biomass and *Lanice* patches with small-scale hydrodynamic processes in sand waves (Damveld et al. 2019, 2020b). To that end, our field study at Texel reflects both the expected abiotic and biotic variability within asymmetrical sand waves (Chapters 2 and 3).

In addition, the taxonomic and functional biodiversity are extremely important for benthic ecosystem functioning (Emmerson and Raffaelli 2000; Gerino et al. 2003; Ieno et al. 2006; Cardinale et al. 2012; Braeckman et al. 2014). Laboratory studies such as from single-core incubations provide useful information on how specific individuals or small assemblages of species can enhance the biogeochemical cycling potential, especially since eco-functioning is often a combination of different processes (Martin and Banta 1992; Kristensen 2000; Gerino et al. 2003; Fang et al. 2019). The active sediment reworking by the benthos can generate distinct micro-habitats that facilitate biogeochemical processes and gradients, which can enhance the exchange of nutrients or other metabolic constituents (Van Colen et al. 2012; Fang et al. 2019). Lab incubations of certain benthic species have demonstrated their active engagement in sediment diagenesis, through activities such as aerobic respiration and metabolic excretion (Vanni 2002; Fang et al. 2019), while minimizing the often-complex and co-varying environmental factors found in nature (Benton et al. 2007; Braeckman et al. 2014). Removal of these ecosystem engineers is likely to cause significant changes to the habitat and sedimentary structure, with deleterious, cascading effects on the overall local biodiversity and important ecosystem functioning such as organic matter (OM) mineralization (Coleman and Williams 2002; Rossi et al. 2008; Olsgard et al. 2008; Braeckman et al. 2014). Therefore, it is important to have a clear understanding on the role of species diversity and density (Marinelli and Williams 2003), as species assemblage, density, biomass and species-specific biological traits all play an important role in biogeochemical cycling, sediment mixing and bioirrigation (Matisoff 1982; Sandnes et al. 2000; Aller 2001; Nizzoli et al. 2002; Gerino et al. 2003; Solan et al. 2004).

The use of proxies for functional biodiversity could be one way to gain a better understanding of the ecosystem functioning (Braeckman et al. 2014). For example, indices such as the Bioturbation Potential or Irrigation Potential could predict the level of particle reworking and burrow ventilation activity (Toussaint et al. 2021). In the same study, permeability was found to be one of the most significant factors in explaining the variability of both the carbon and nitrogen mineralization. Although it is not often measured for marine sediments, permeability is an indicator of advective transport and its importance for biogeochemical processes is well established, especially in permeable sediments (Wilson et al. 2008; Santos et al. 2012; Huettel et

al. 2014). Therefore, it should be routinely determined where possible to better characterize the sedimentological properties of marine sands. But the lab experimental studies and model-based proxies should not preclude *in situ* or field investigations, as they inherently over-simplify the actual conditions and assemblages found in the real world, among other common limitations, thereby greatly limiting the upscaling potential (Braeckman et al. 2014). At present, quantitative information is often lacking regarding the benthic communities of coastal regions, owing to their difficulty to sample given the shallow water depths, seabed topography and the often-complex hydrodynamic conditions (Ellis et al. 2011). Thus, there is a knowledge gap about the spatio-temporal variability in the natural environment (Fang et al. 2019).

Our field campaigns were not able to yield definitive information about the biogeochemical potential of the sand waves, but we have nevertheless quantified the community compositional patterns, identifying four distinct habitats (Chapter 3) along the sand waves, though with a small modification to the MU classification. In contrast to the sediment characteristics, the benthic community showed greater complexity, where the steep slope-half of the crests shared more similarities with the steep slope assemblage. Presumably due to the finer, organically-richer sediment along the steep slope and trough, these habitats contained the highest benthic densities (taxonomic, individual and biomass). While most of the taxa were spread across the entire sand wave, the distribution was highly uneven, with more than 80% of *Echinocardium cordatum* and *Tellimya ferruginosa*, more than 90% of *Fabulina fabula* and more than half of *Spisula* sp. located on the steep-slope. The top three species overall included: *Phoronis* sp., *T. ferruginosa* and *F. fabula*, all of which were very characteristic of the steep slope habitat of the sand wave. In contrast, the coarser side of the sand wave was characterized by *Nephtys* sp., Terebellidae and *Bathyporeia sp.*, which were the top three taxa of the gentle slope (Table S3.1). Overall, the macrofauna wet weight was (394 g m^{-2}) and much higher on the steep slope, as the heart urchin *E. cordatum* was by far the heaviest organism (>93%). Interestingly, *Lanice conchilega* was sampled in very low numbers, even though the video transect study of Damveld et al. 2018 occasionally revealed large patches of these tube worms. However, we did collect a high abundance of other tubicolous worms (e.g., Phoronids).

In terms of trait modalities, the Texel sand waves exhibited a clear distinction between the four habitats which, alongside the sediment characteristics and morphology, suggests the gentle slope and crest, despite the lower richness, to be more dynamic as indicated by the higher number of swimmers. The steep slope was more characterized by crawlers and deeper burrowers, the latter of which was also dominant in the trough, alongside the tube-building worms. The

observations from both the sediment characteristics and the benthic assemblage suggest the steep-slope and trough habitats to be somewhat more sheltered from the hydrodynamic forces. Moreover, it was the steep slope, and not the trough, that contained the richest assemblage, with 13 taxa unique only to this habitat, almost all of which were crawlers, diffusors and/or downward conveyors in terms of sediment mixing, and consisted of a mix of different feeding modes (suspension, deposit and carnivore/scavenger). Therefore, due to the morphology of these asymmetrical sand waves, there are not only measureable differences in sediment characteristics, but also local hotspots (e.g., steep slope) in terms of species richness, biomass and functional traits such as motility, burrowing depth, sediment mixing and feeding types.

5.3 Implications of shells on sediment and hydrodynamics

Shells and their fragments, which are the leftover remains from different mollusk species that persist long after the death of the organism, are commonly found in the natural environment. When conditions for mechanical breakage or chemical dissolution are minimal, they can endure over geological time (Kidwell 1985; Powell and Staff 1989; Gutiérrez et al. 2003). The composition of natural sediment and actual shell content is spatially highly variable, but shell production by mollusks is believed to be ubiquitous in all marine habitats where they are found (Russell-Hunter 1983; Dillon 2000). This was certainly observed at the Texel sand waves (from < 1 to > 41% by volume; Figure 5.1). Many species of mollusks are known to function as ecosystem engineers by actively creating, modifying and/or maintaining their surrounding habitat conditions for themselves and other organisms, thereby mediating the availability of important biotic and abiotic resources (Jones et al. 1997; Gutiérrez et al. 2003). However, compared to documentation about the activity and influence of living mollusks for certain species, the potential role of the remaining dead shells has not been nearly as thoroughly investigated, even though the quantity that has accumulated over time often exceeds that of the living counterparts.

Nevertheless, new shell production and the presence of dead shell materials have both been attributed as an ecosystem engineering process (Gutiérrez et al. 2003). Shell valves differ in density, shape and size, and thus behave very differently from siliciclastic sediment grains (Al-Dabbas and McManus 1987; Soulsby 1997). The mere presence of dead shells, such as that of *Ensis leei* and the sea scallop, *Placopecten magellanicus*, within sandy sediment has been documented to trap fine sediment and increase the deposition of diatoms (Pilditch et al. 1997; Huettel and Rusch 2000; Witbaard et al. 2016). They also serve as attachment substrate or as

refuge from predation to a variety of organisms, depending on the type, size and condition of the valve (Wilber 1990; Brown 1992; Osorno et al. 1998). Moreover, shell presence has other potential indirect implications due to changes in the sediment and benthic structure. Protrusions by shells, as with other physical objects, have a modulating effect on the nearby water flow, such as increased shear stress and subsequent erosion in the immediate surrounding (Nowell and Jumars 1984; Gutiérrez et al. 2003). This is a well-documented observation in flume studies using mimics of different structure-forming animals (Friedrichs et al. 2000, 2009). At least in the case of single shell valves, the size, shape and orientation all appeared to positively influence the rate of erosion and deposition, for both particulate matter as well as solutes (Grant et al. 1993; Olivera and Wood 1997; Denny and Blanchette 2000).

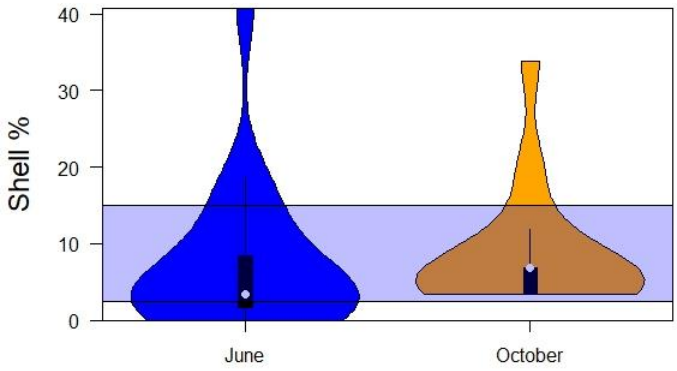

Figure 5.1. Averaged shell % (SD ± 35%) from Texel, estimated from all box core samples from June and October 2017 (n = 72). The shaded region represents the range in which the shell percentage shows a visibly-significant difference in bed development from the ACC experiment (Chapter 4, Figure 4.2).

However, the influence of shell material on the sediment and, specifically, sand ripple dynamics has not previously been closely investigated. As of yet, only a handful of studies have experimented with them, mostly utilizing individual shell valve shape and shell orientation to measure the influence on hydrodynamic flow and settling velocities within the water column (Al-Dabbas and McManus 1987; Ramsdell and Miedema 2010; Miedema and Ramsdell 2011). But these highly controlled conditions (perfectly smooth, flat surface) are not so realistic in the natural environment. To build upon these studies, we therefore conducted many experimental runs in the racetrack flume using increasing percentages of a mixture of different shell types. As both the sand and shells were extracted from the North Sea, the mixture is representative for this system.

We have shown how increasing shell content in a fine sand mixture (D_{50} 350 µm) drastically affects ripple development (Chapter 4), ultimately reducing the bedload transport. Larger quantities (15-20% in volumetric composition, or more) exhibited greater overall stability, in part through the presence of increasingly-immobile shells, as well as from a reduction in available sediment to form the ripples, which is known to occur in sand-gravel mixtures, for example (McCarron et al. 2016). Small quantities of shell (between 2.5 – 15%), however, already demonstrated rather complex, small-scale alterations to the near-bed flow. The extent to which the flow was altered depended on both the shell content, as well as the level of bed roughness (e.g., ripples of a given size) of the seabed. When the quantity was low under flat bed conditions, turbulence was enhanced, similar to how the larger individual valves tend to cause more scouring than smaller ones (Gutiérrez et al. 2003). However, at higher quantities under flat bed conditions, this effect was no longer observed, presumably due to a sufficiently large density of shells. Under equilibrium (rippled) bed conditions, the near-bed turbulence was increasingly reduced as the ripples were progressively dampened by the growing percentage of shells (Figure 5.2).

Sediment composition is an important contributing factor to the bottom roughness (Hatfield et al. 2010; Borsje et al. 2014a; Aldridge et al. 2015). Much of the marine seafloor is characterized by mixtures of sediment grains with varying particle sizes. However, shells and other types of particles are not usually considered in model predictions. Like shells, current-driven ripples are ubiquitous features of sandy coastal environments. The hydro-morphodynamic conditions driving these bedforms are well established (see van Rijn 1984, Yalin 1985, Baas 1994, Lapôtre et al. 2017). Sediment characteristics also play an important role in determining ripple size, but there are no good indicators for this as of yet. Coarser sediment grains are known to enhance ripple migration more than fine grains at a given shields value (Baas et al. 2000), but this is not the case for biogenic particles. Given the high prevalence of shell material, especially in coastal environments, we could expect there to be an alteration in ripple development, with a dampening in both their dimensions and migration rates, provided that the surficial shells do not become buried over time.

As our racetrack experiment has shown, shell concentrations at or below 15% already sufficiently influence flow and ripple dynamics, and the bulk of our box core samples contained dead shell material ≤ 20% (n = 123), ≤ 15% (n = 110), and very few were without any shells (n = 3, Figure 5.1). Unfortunately, information on the spatial distribution of dead shells over a wider scale, such as the North Sea, is not presently available. In principle, this information would be easy to retrieve from various types of benthic surveys (Sas et al. 2019). However, by interpolating

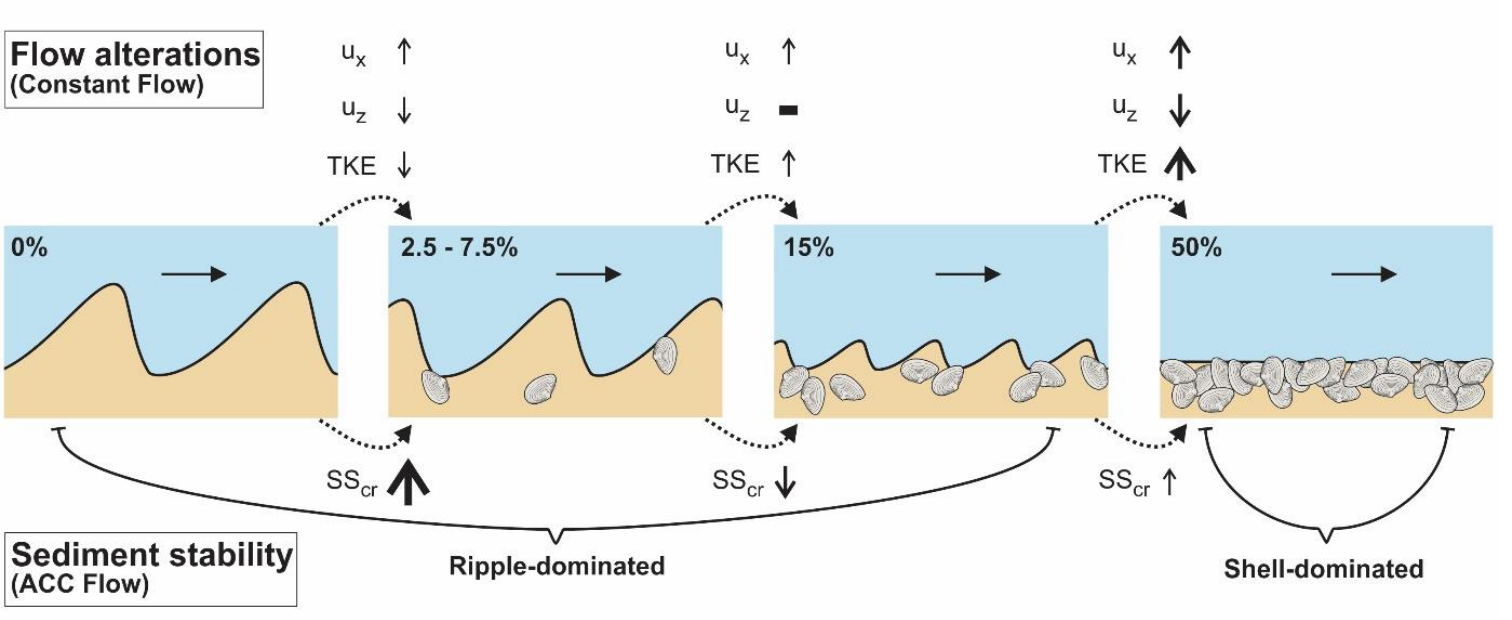

Figure 5.2. Conceptual figure showing the shell-induced changes to the flow under flat bed (Flow alterations) and rippled bed (Sediment stability) conditions. A density-driven effect from shells on near-bed flow attenuation can be observed. As the shells become increasingly dense and immobile, a dampening behavior is exhibited that is similar to reef patches. TKE = turbulent kinetic energy; u_x = depth-averaged horizontal velocity; u_z = depth-averaged vertical velocity; SS_{cr} = critical shear stress. (for in-depth details, see Chapter 4). Schematic by Chiu H. Cheng.

available information from various benthos surveys, we can map the general distribution of living mollusks. The 18-year Dutch Continental Economical Zone of the North Sea survey (MWTL) covers a relatively high spatial and temporal resolution over the entire Dutch North Sea and thus, provides a good regional estimation on this distribution.

Of course, living and dead shell assemblages may not necessarily be useful indicators for one another (Powell et al. 2017). The dead assemblage is subjected to various environmental conditions over time and transport by physical forcing (Miller 1988; Zenetos 1990; Callender et al. 1992), while living species often exhibit spatio-temporal variability and patchiness in growth (Levinton 1970; Powell et al. 1986). Thus, caution should be taken in the interpretation of this potential relationship. Nevertheless, this attempt is a first step towards mapping the distribution of these shells, whether living or dead. The more information we can accumulate on the distribution of shells, the more accurate of a "shell budget" we will be able to create. The Texel samples were averaged by MU and plotted onto the interpolated map using the MWTL dataset (Figure 5.3).

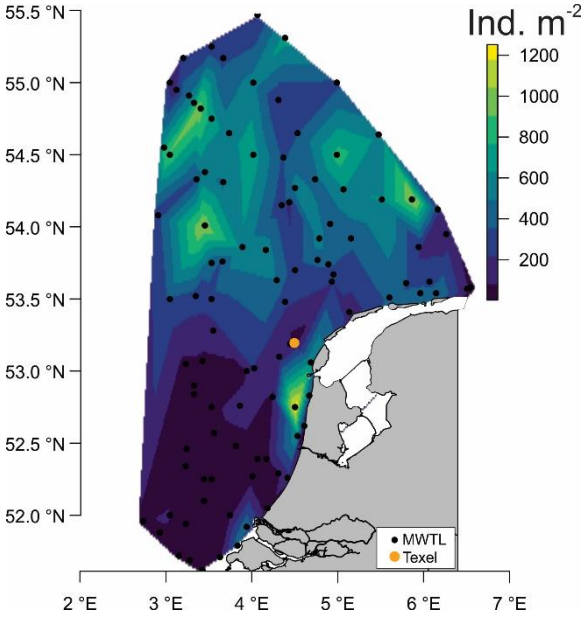

Figure 5.3. Interpolated spatial distribution of the number of living mollusks (individuals m^{-2}) across the Dutch North Sea based on the MWTL and Texel sand wave datasets. Stations are included for reference. Texel values range from 0 – 1604 individuals m^{-2}, with a mean of 267 ± 394 individuals m^{-2}.

Given the ubiquitous nature of shells, we believe that further studies on how these biogenic compounds will alter the hydrodynamic and sedimentary conditions, particularly in the longer term, should be conducted where possible. Field campaigns are difficult undertakings and an *in situ* study on sand-shell dynamics is perhaps not realistically possible. At a minimum, however, the shell content from sediment sampling should be quantified and recorded so that in the future, a regional or large-scale estimation of shell content can be compiled, similar to efforts for grain size distribution or other particles over the North Sea (Bockelmann et al. 2017; Wilson et al. 2018; Sas et al. 2019). Moreover, when the dead shells can also be taxonomically identified, they could additionally provide useful information about temporal changes in the mollusk species inhabiting a given area in the past as long as the methodology of the collection area or volume is standardized (Kidwell 2013).

5.4 Potential implications and future research

Environments that recover following natural or anthropogenic impacts may not necessarily match those prior to the impacts (Bolam et al. 2011, 2014; Wan Hussin et al. 2012). Therefore, it is necessary to have a good understanding about not only how species may be affected by the changes, but also how the larger ecosystem functioning operates and the associated, potentially-interacting, pressures (Bolam et al. 2014), in order to properly safeguard against biodiversity loss. Shallow, coastal environments, given their disproportionately-high biodiversity and productivity, have a large likelihood to be impacted by human and natural activity, making them extremely susceptible to negative impacts such as habitat loss, changes in physical conditions, pollution and eutrophication, etc. (Gray 1997; Hinrichsen 2010; Bolam et al. 2014). Field sampling is an expensive and labor-intensive endeavor that may not always be possible over a large scale. In this sense, data from campaigns with similar environmental conditions could provide a useful alternative. An advantage of using biological traits as a proxy for ecosystem functioning and productivity is that it does not generally have a geographic range, in contrast to certain species assemblages, making it more suitable for upscaling and broader application (Bolam et al. 2014).

The Texel sand wave field is located near the NAP-20 m depth contour, an area that is frequently exploited for offshore sand mining. Thus, this study location is potentially at risk from anthropogenic processes, which are placing increasing pressure on the whole system (Piet et al. 2015, 2017; Burdon et al. 2018; Borgwardt et al. 2019). The nearshore zone is directly vulnerable from both terrestrial and marine activities. Sand wave environments pose concerns to the offshore

activities and the integrity of the vast network of infrastructure, while being located in regions of economic interest for further offshore development. The potential negative consequences are thus high in both cases for socioeconomic and ecological reasons. If not carefully managed, this could lead to a loss in ecosystem functions that will invariably impact the other relevant interests (e.g., fishing, natural coastal defense, etc.). Similarly, if the current natural supply of sand to impacted areas differ from the material extracted from a given environment, then the natural processes may not be able to counterbalance the effects from high-intensity and/or frequent dredging (Bellec et al. 2010). Thus, a fine balance between economic activities and ecological integrity must be taken into consideration (Degraer et al. 2019). However, this requires us to have a thorough understanding of the complete dynamics of such environments, particularly the sediment and benthic community composition.

In addition to providing ecosystem services and resources, including for anthropogenic uses, marine environments and sediments are also important in global biogeochemical cycles and serve as shelter and important substrates for benthic organisms. But the close proximity to the coast increases its vulnerability to local influences such as the release of excess nutrients from terrestrial runoff, which contributes to coastal-zone eutrophication and hypoxia, or from the emission of greenhouse gases and pollution (Regnier et al. 2013). These local factors are superimposed upon global effects, such as climate change, in which the resulting consequences of increased CO_2 concentrations and ocean acidification are shown to occur much faster in the North Sea than that predicted for the open ocean (Provoost et al. 2010).

The human activities on the North Sea threaten the environmental health of the ecosystems (Halpern et al. 2015) as well as the ecosystem services (Breine et al. 2018). For example, there are ample cases where OWFs interfere with the natural ecosystem functions, as the artificial hard substrates are rapidly colonized by large quantities of fouling fauna (De Mesel et al. 2015), which attract fish and large crustaceans, affect water-column communities and change local sediment properties and the inhabiting fauna (Maar et al. 2009; Coates et al. 2013; Reubens et al. 2014). This can cause shifts in the local food web, from sediment to water column carbon processing. Sediment ecosystems in the coastal zone play an important role in the mediation of nutrient cycles and the biogeochemical benthic-pelagic coupling in shallow seas, with an estimated 25% of nutrients being recycled in the sediments of the North Sea (Lancelot et al. 2005). Sediments are responsible for the loss of both reactive nitrogen (Soetaert and Middelburg 2009) and phosphorus (Slomp et al. 1996), and the removal rates depend on a delicate balance between OM deposition, sediment granulometry and benthic activity. Sediments also have an important

capacity to store fine sediments (Hendriks et al. 2020), thus mediating the timing and magnitude of suspended particle concentrations in the water column, the water clarity and primary production. As the preservation of ecosystem health and the integration of best sustainable practices into offshore projects is increasingly required, it is important that we closely monitor how these vulnerable environments are affected.

Presently, we have a good statistical description for the sediment ecosystem of an asymmetrical sand wave environment, and how the different ecosystem components and sediment properties relate to certain physical and biological variables (Damveld et al. 2018; Cheng et al. 2020, 2021). In these sediments, the overlying water flowing through the upper sediment layers tightly couples the shelf water column and sedimentary biogeochemical processes (Huettel et al. 1996). Therefore, any fining that results from elevated OM concentrations, such as in areas adjacent to OWFs (Coates et al. 2013), could prevent waves and currents from entering the sediment, decoupling the water and sediment processes and consequently changing the biogeochemical cycling (Huettel et al. 2014). Changes in the geomorphology will also affect advective flows through the sediment, as these are driven by pressure gradients on the sediment surface. Coarsening due to scouring on the other hand, will enhance benthic-pelagic exchanges.

We have demonstrated that morphology (e.g., position along a sand wave) has a significant effect on the benthic conditions. However, it remains to be seen whether the actual gradients along the sand wave are abrupt under our sampling and classification scheme, or much more gradual. Future campaigns would yield valuable information to build upon the data collected in this research work, namely for the longer-term (e.g., spatio-temporal) consequences for the benthic community composition. An even higher resolution sampling along sand waves of multiple locations would potentially provide this information on both the small (individual sand wave) and regional scale (different sand wave fields). For example, taking benthos and sediment samples at 5-m intervals. Furthermore, information at this resolution would be excellent for validating the ongoing modeling studies that simulate sand wave development and sediment sorting at the different parts of the bedform over time.

In addition, given the limited number of replicates and measurements of nutrient and oxygen flux, as well as bioturbation and bioirrigation rates from incubation studies, a quantitative assessment of the biogeochemistry of the Texel sand waves was beyond the scope of this PhD work. Nevertheless, these processes are often closely linked to the benthic community, sediment composition and hydrodynamic conditions. Therefore, such information would greatly enhance our understanding about the ecological potential of sand waves. Incubation cores should be

sampled to a sufficient quantity (minimum of 4-5 cores per MU/habitat) to allow for statistical analyses. If these, like the sediment subcores, are taken directly from the box cores, then the data can then be directly compared. For a single cruise campaign, around 24 – 30 incubation cores is certainly achievable, as long as there is sufficient working space and availability of the required quantity of instruments and sensors.

Moreover, to further enhance the spatial coverage of the study, video and/or sediment profiling cameras should also be deployed, over the entire sand wave to obtain a full view of the bed morphology and the epifauna distribution, and compare that with the physical samples collected. If the sand waves are also located next to areas where they abruptly disappear, as was the case for the Texel sand waves, it would also be very interesting to compare the benthic and hydrodynamic conditions between the two adjacent areas. In available, landers should be positioned on each MU/habitat to determine the exact near-bed flow conditions, among other environmental parameters that could be measured simultaneously.

Lastly, given that most of the (Dutch) sand waves are located in regions of high economic interest, it would also be insightful to study them in the context of anthropogenic disturbances where possible. Sand extraction is an activity that would directly impact the seabed, but OWFs are increasingly growing in prevalence, sometimes near sand wave fields. Several recent projects are investigating the ecological and biogeochemical effects of these wind farms on the immediate and nearby environments. For example, three recent projects were funded by the NWA Programme (Ecology & North Sea) to study the links between ecology and the physical presence of wind parks. One of the projects, Footprint, is specifically focused on how OWFs might alter the sediment functioning for the adjacent sand wave environments. The combination of the research aims and the areas of interest for the fieldwork make these excellent opportunities to build upon the research work presented in this thesis.

The safeguarding of the sustainable management of the North Sea marine resources depends on our ability to understand and predict the changes induced by human interventions. The research work conducted as part of the SANDBOX project provides both actual and theoretical knowledge about sand waves and nearshore environments, which, together, will hopefully be relevant for other similar systems as well.

General Conclusion

Q1. Is the division of asymmetrical, tidal sand waves into four morphological units (e.g., crest, steep-slope, trough and gentle-slope) sufficiently sensitive to reliably identify distinct habitats?

From the results in Chapter 2, it is clear that the morphology (position along the wave) is very closely associated to the small-scale variability in the sediment characteristics, which occurs on the order of meters to tens of meters. The division of asymmetrical sand waves into four morphological units allowed us to successfully characterize them into distinct environments, providing a good overview of the sediment grain size, permeability, organic carbon and chlorophyll *a* content that can be expected at the different parts along such sand waves. The gentle slope and crest of the sand waves are characterized by coarser sediment and higher permeability, while the steep slope and trough are finer, less permeable and richer in organic matter. Not only are these parameters important components that largely make up the geomorphological conditions of the sediment, but they are also essential to the ecological community and associated processes within it.

Q2. Based on the results from the abiotic distribution along the sand waves (Q1), can the same delineation also adequately explain the benthic community compositional distribution?

Similar to the contrasts that were observed in the sediment conditions along the sand waves, Chapter 3 also showed a significant difference in the benthic community composition that was measured between essentially four different habitats. Overall, the steep slope exhibited the highest species richness and biomass, while the individual density was about equally high with the trough. While each habitat is clearly unique, the overlapping commonalities shared between the gentle slope-crest and the steep slope-trough were also reflected in some of the functional traits of the benthos, as would be expected based on the sediment characteristics. The coarser half of the sand wave (e.g., less sheltered) contained a higher number of highly-mobile fauna, while the steeper half was characterized by more suspension feeders, tube-building worms and less-mobile species overall, but also a relatively high number of deposit feeders, indicative of the higher food content there.

Q3. To what extent does the shell content in a sandy sediment mixture affect the ripple dimensions, migration rate and the near-bed hydrodynamics?

Our racetrack study from Chapter 4 provides new information on the potential influence of sediment composition on the biogeomorphological dynamics, through the direct impact of shell content on the development of ripples in fine sand. As the percentage of shells increases in a sandy medium, both the dimensions and migration rate of ripples are progressively dampened. In essence, these empty shells exhibit a form of ecosystem engineering. But their importance is not only limited to the physical or sedimentary conditions, which at a minimum pose indirect implications for certain benthic species. They can also function more directly as substrate or shelter. Furthermore, as shells have the ability to affect ripple development and given that both of these have been found at varying quantities, depending on the location along the sand waves, this can have potential consequences for the sand wave development over the longer term, which will have an impact on the overall biogeomorphology. Moreover, as shells, whether living or empty, are ubiquitous biogenic material in many natural habitats and not difficult to quantify, it would be worthwhile to account for the shell content wherever possible. We believe that this information would help us to more-accurately assess the bed evolution dynamics, at least in sandy sediment.

Q4. What new information can we derive from the small-scale, high-resolution sampling combined with flume experimentation (Q1-3), and what are the implications of these findings for similar (sand wave) locations in the Dutch North Sea?

In studying and finding consistent trends in both the sediment characteristics and benthic community composition over several consecutive asymmetrical sand waves, we show that they can be characterized into either two or four distinct environments for a quick assessment of the expected biogeomorphological conditions. Especially for a dynamic environmental as the Texel sand wave field, such differences can only be determined with an appropriate sampling scale and resolution (Chapter 5). Moreover, we have estimated the shell content in the field, as well as measured the potential impacts that it could have on the development and movement of small ripples. Many of these biogeomorphological processes are linked, and should be simultaneously studied to the extent possible, to obtain a comprehensive overview of such dynamic environments. Our results provide a basis on which future studies could easily build upon to further improve our understanding about the different aspects of tidal sand waves. Additional studies would also reveal

whether the trends observed at our study location could be found at other sand wave environments in the Dutch North Sea.

Tidal sand waves are very abundant in the Dutch North Sea, and many of them are located in areas of high economic activity, particularly from sand mining and, increasingly, offshore wind farms. While this presents growing challenges in terms of the ecological preservation of these large, dynamic bedforms, it also offers new opportunities to study sand waves in a different, but related, context. By continuing to improve our understanding about these environments, how they shape, and are affected by, their surrounding processes and activities, we will hopefully be better equipped to develop effective strategies for marine conservation and management.

The interplay between the benthic biological community and geomorphology is complex. Our study sheds additional light on the significance of the dynamic sand wave morphology for the sediment conditions and benthic community composition within an asymmetrical sand wave environment. Moreover, we show the magnitude to which shell content can affect ripple development and migration rates. It is our hope that the results from this study will contribute valuable knowledge towards a better understanding of the sedimentary, ecological and biogeomorphological conditions of asymmetrical sand wave fields, at least within the Dutch North Sea spatial context, but hopefully beyond as well.

Bibliography

Adam, S., A. Backer, S. Degraer, J. Monbaliu, E. Toorman, and M. Vincx. 2008. Chapter 9 sediment characterization of intertidal mudflats using remote sensing. Proc. Mar. Sci. **9**. doi:10.1016/S1568-2692(08)80011-3

Aguiar, M. R., and O. E. Sala. 1994. Competition, Facilitation, Seed Distribution and the Origin of Patches in a Patagonian Steppe. Oikos **70**: 26–34. doi:10.2307/3545695

Ahmerkamp, S., C. Winter, F. Janssen, M. M. M. Kuypers, and M. Holtappels. 2015. The impact of bedform migration on benthic oxygen fluxes. J. Geophys. Res. Biogeosciences **120**: 2229–2242. doi:10.1002/2015JG003106

Al-Dabbas, M. A. M., and J. McManus. 1987. Shell fragments as indicators of bed sediment transport in the Tay Estuary. Proc. R. Soc. Edinburgh. Sect. B. Biol. Sci. **92**: 335–344. doi:10.1017/S0269727000004759

Aldridge, J. N., E. R. Parker, L. M. Bricheno, S. L. Green, and J. van der Molen. 2015. Assessment of the physical disturbance of the northern European Continental shelf seabed by waves and currents. Cont. Shelf Res. **108**: 121–140. doi:/10.1016/j.csr.2015.03.004

Aller, R. C. 1982. The Effects of Macrobenthos on Chemical Properties of Marine Sediment and Overlying Water BT - Animal-Sediment Relations: The Biogenic Alteration of Sediments, p. 53–102. *In* P.L. McCall and M.J.S. Tevesz [eds.], Animal-Sediment Relations: The Biogenic Alteration of Sediments. Springer US.

Aller, R. C. 2001. Transport and reactions in the bioirrigated zone. Benthic Bound. Layer - Transp. Process. Biochem.

Arndt-Sullivan, C., and D. Schiedek. 1997. Nephtys hombergii a free-living predator in marine sediments: Energy production under environmental stress. Mar. Biol. **129**: 643–650. doi:10.1007/s002270050207

Ashley, G., J. C. Boothroyd, J. S. Bridge, and others. 1990. Classification of large-scale subaqueous bedforms: a new look at an old problem. J. Sediment. Petrol. **60**: 160–172. doi:10.2110/jsr.60.160

Baas, J. H. 1994. A flume study on the development and equilibrium morphology of current ripples in very fine sand. Sedimentology **41**: 185–209. doi:10.1111/j.1365-3091.1994.tb01400.x

Baas, J. H., and H. De Koning. 1995. Washed-out ripples; their equilibrium dimensions, migration rate, and relation to suspended-sediment concentration in very fine sand. J.

Sediment. Res. **65**: 431–435. doi:10.1306/D42680E5-2B26-11D7-8648000102C1865D

Baas, J. H., R. L. van Dam, and J. E. A. Storms. 2000. Duration of deposition from decelerating high-density turbidity currents. Sediment. Geol. **136**: 71–88. doi:10.1016/S0037-0738(00)00088-9

Baptist, M. J., J. van Dalfsen, A. Weber, S. Passchier, and S. van Heteren. 2006. The distribution of macrozoobenthos in the southern North Sea in relation to meso-scale bedforms. Estuar. Coast. Shelf Sci. **68**: 538–546. doi:10.1016/j.ecss.2006.02.023

Bärenbold, F., B. Crouzy, and P. Perona. 2016. Stability analysis of ecomorphodynamic equations. Water Resour. Res. **52**: 1070–1088. doi:10.1002/2015WR017492

Barnard, P. L., D. M. Hanes, D. M. Rubin, and R. G. Kvitek. 2006. Giant sand waves at the mouth of San Francisco Bay. Eos, Trans. Am. Geophys. Union **87**: 285–289. doi:10.1029/2006EO290003

Bartholdy, J., V. B. Ernstsen, B. W. Flemming, C. Winter, A. Bartholomä, and A. Kroon. 2015. On the formation of current ripples. Sci. Rep. **5**: 11390. doi:10.1038/srep11390

Bauer, J. E., W.-J. Cai, P. A. Raymond, T. S. Bianchi, C. S. Hopkinson, and P. A. G. Regnier. 2013. The changing carbon cycle of the coastal ocean. Nature **504**: 61–70. doi:10.1038/nature12857

Bellec, V., V. Van Lancker, K. Degrendele, M. Roche, and S. Le Bot. 2010. Geo-environmental Characterization of the Kwinte Bank. J. Coast. Res. **51**. doi:10.2307/40928819

Benton, T., M. Solan, J. Travis, and S. Sait. 2007. Microcosm experiments can inform global ecological problems. Trends Ecol. Evol. **22**: 516–521. doi:10.1016/j.tree.2007.08.003

Bergman, M. J. N., and M. Hup. 1992. Direct effects of beamtrawling on macrofauna in a sandy sediment in the southern North Sea. ICES J. Mar. Sci. **49**: 5–11. doi:10.1093/icesjms/49.1.5

Bergman, M., and J. Santbrink. 2000. Mortality in megafaunal benthic populations caused by trawl fisheries on the Dutch continental shelf in the North Sea in 1994. Ices J. Mar. Sci. - ICES J MAR SCI **57**: 1321–1331. doi:10.1006/jmsc.2000.0917

Bertness, M. D. 1984. Habitat and Community Modification by An Introduced Herbivorous Snail. Ecology **65**: 370–381. doi:10.2307/1941400

Bertness, M. D., and R. Callaway. 1994. Positive interactions in communities. Trends Ecol. Evol. **9**: 191–193. doi:10.1016/0169-5347(94)90088-4

Besio, G., P. Blondeaux, M. Brocchini, and G. Vittori. 2004. On the modeling of sand wave migration. J. Geophys. Res. Ocean. **109**: 1–13. doi:10.1029/2002JC001622

Besio, G., P. Blondeaux, M. Brocchini, and others. 2008. The morphodynamics of tidal sand waves: A model overview. Coast. Eng. **55**: 657–670. doi:/10.1016/j.coastaleng.2007.11.004

Best, J., and R. Kostaschuk. 2002. An experimental study of turbulent flow over a low-angle dune. J. Geophys. Res. Ocean. **107**: 18–19. doi:10.1029/2000JC000294

Betat, A., C. A. Kruelle, V. Frette, and I. Rehberg. 2002. Long-time behavior of sand ripples induced by water shear flow. Eur. Phys. J. E **8**: 465–476. doi:10.1140/epje/i2001-10110-y

Bianchi, T. S. 2011. The role of terrestrially derived organic carbon in the coastal ocean: a changing paradigm and the priming effect. Proc. Natl. Acad. Sci. U. S. A. **108**: 19473–19481. doi:10.1073/pnas.1017982108

Blair, G., R. D. B. Lefroy, and L. Lisle. 1995. Soil Carbon Fractions Based on Their Degree of Oxidation, and the Development of a Carbon Management Index for Agricultural Systems. Aust. J. Agric. Res. **46**. doi:10.1071/AR9951459

Blanchard, G. F., J.-M. Guarini, P. Gros, and P. Richard. 1997. Seasonal effect on the relationship between the photosynthetic capacity of intertidal microphytobenthos and temperature. J. Phycol. **33**: 723–728. doi:10.1111/j.0022-3646.1997.00723.x

Blom, A., J. S. Ribberink, and H. J. de Vriend. 2003. Vertical sorting in bed forms: Flume experiments with a natural and a trimodal sediment mixture. Water Resour. Res. **39**. doi:10.1029/2001WR001088

Blondeaux, P. 2012. Sediment mixtures, coastal bedforms and grain sorting phenomena: An overview of the theoretical analyses. Adv. Water Resour. **48**: 113–124. doi:10.1016/j.advwatres.2012.02.004

Blott, S. J., and K. Pye. 2006. Particle size distribution analysis of sand-sized particles by laser diffraction: an experimental investigation of instrument sensitivity and the effects of particle shape. Sedimentology **53**: 671–685. doi:10.1111/j.1365-3091.2006.00786.x

Bockelmann, F.-D., W. Puls, U. Kleeberg, D. Müller, and K. Emeis. 2017. Mapping mud content and median grain-size of North Sea sediments – A geostatistical approach. Mar. Geol. **397**. doi:10.1016/j.margeo.2017.11.003

Bolam, S. G., J. Barry, T. Bolam, C. Mason, H. S. Rumney, J. E. Thain, and R. J. Law. 2011. Impacts of maintenance dredged material disposal on macrobenthic structure and secondary productivity. Mar. Pollut. Bull. **62**: 2230–2245. doi:10.1016/j.marpolbul.2011.04.012

Bolam, S. G., R. C. Coggan, J. Eggleton, M. Diesing, and D. Stephens. 2014. Sensitivity of

macrobenthic secondary production to trawling in the English sector of the Greater North Sea: A biological trait approach. J. Sea Res. **85**: 162–177. doi:10.1016/j.seares.2013.05.003

Bonsdorff, E., and T. Pearson. 1999. Variation in the sublittoral macrozoobenthos of the Baltic Sea along environmental gradients: A functional-group approach. Aust. J. Ecol. **24**: 312–326. doi:10.1046/j.1442-9993.1999.00986.x

Boon, A., and G. Duineveld. 1998. Chlorophyll a as a marker for bioturbation and carbon flux in southern and central North Sea sediments. Mar. Ecol. Prog. Ser. **162**: 33–43. doi:10.3354/meps162033

Borchers, H. W. 2019. pracma: Practical Numerical Math Functions.

Borgwardt, F., L. Robinson, D. Trauner, and others. 2019. Exploring variability in environmental impact risk from human activities across aquatic ecosystems. Sci. Total Environ. **652**: 1396–1408. doi:10.1016/j.scitotenv.2018.10.339

Borsje, B. W., M. B. de Vries, S. J. M. H. Hulscher, and G. J. de Boer. 2008. Modeling large-scale cohesive sediment transport affected by small-scale biological activity. Estuar. Coast. Shelf Sci. **78**: 468–480. doi:10.1016/j.ecss.2008.01.009

Borsje, B. W., S. J. M. H. Hulscher, P. M. J. Herman, and M. B. De Vries. 2009a. On the parameterization of biological influences on offshore sand wave dynamics. Ocean Dyn. **59**: 659–670. doi:10.1007/s10236-009-0199-0

Borsje, B. W., M. B. de Vries, T. J. Bouma, G. Besio, S. J. M. H. Hulscher, and P. M. J. Herman. 2009b. Modeling bio-geomorphological influences for offshore sandwaves. Cont. Shelf Res. **29**: 1289–1301. doi:10.1016/j.csr.2009.02.008

Borsje, B. W., P. C. Roos, W. M. Kranenburg, and S. J. M. H. Hulscher. 2013. Modeling tidal sand wave formation in a numerical shallow water model: The role of turbulence formulation. Cont. Shelf Res. **60**: 17–27. doi:10.1016/j.csr.2013.04.023

Borsje, B. W., T. J. Bouma, M. Rabaut, P. M. J. Herman, and S. J. M. H. Hulscher. 2014a. Formation and erosion of biogeomorphological structures: A model study on the tube-building polychaete Lanice conchilega. Limnol. Oceanogr. **59**: 1297–1309. doi:10.4319/lo.2014.59.4.1297

Borsje, B. W., W. M. Kranenburg, P. C. Roos, J. Matthieu, and S. J. M. H. Hulscher. 2014b. The role of suspended load transport in the occurrence of tidal sand waves. J. Geophys. Res. Earth Surf. **119**: 701–716. doi:10.1002/2013JF002828

Bouma, T. J., M. B. De Vries, E. Low, G. Peralta, I. C. Tánczos, J. Van De Koppel, and P. M. J.

Herman. 2005. Trade-offs related to ecosystem engineering: A case study on stiffness of emerging macrophytes. Ecology **86**: 2187–2199. doi:10.1890/04-1588

Bouma, T. J., S. Temmerman, L. A. van Duren, and others. 2013. Organism traits determine the strength of scale-dependent bio-geomorphic feedbacks: A flume study on three intertidal plant species. Geomorphology **180**–**181**: 57–65. doi:10.1016/j.geomorph.2012.09.005

Boyd, S. E., D. S. Limpenny, H. L. Rees, and K. M. Cooper. 2005. The effects of marine sand and gravel extraction on the macrobenthos at a commercial dredging site (results 6 years post-dredging). ICES J. Mar. Sci. J. du Cons. **62**: 145–162. doi:10.1016/j.icesjms.2004.11.014

Braeckman, U., P. Provoost, B. Gribsholt, D. Van Gansbeke, J. J. Middelburg, K. Soetaert, M. Vincx, and J. Vanaverbeke. 2010. Role of macrofauna functional traits and density in biogeochemical fluxes and bioturbation. Mar. Ecol. Prog. Ser. **399**: 173–186. doi:10.3354/meps08336

Braeckman, U., M. Y. Foshtomi, D. Van Gansbeke, F. Meysman, K. Soetaert, M. Vincx, and J. Vanaverbeke. 2014. Variable Importance of Macrofaunal Functional Biodiversity for Biogeochemical Cycling in Temperate Coastal Sediments. Ecosystems **17**: 720–737. doi:10.1007/s10021-014-9755-7

Brakenhoff, L., R. Schrijvershof, J. van der Werf, B. Grasmeijer, G. Ruessink, and M. van der Vegt. 2020. From Ripples to Large-Scale Sand Transport: The Effects of Bedform-Related Roughness on Hydrodynamics and Sediment Transport Patterns in Delft3D. J. Mar. Sci. Eng. **8**: 25. doi:10.3390/jmse8110892

Breine, N. T., A. De Backer, C. Van Colen, T. Moens, K. Hostens, and G. Van Hoey. 2018. Structural and functional diversity of soft-bottom macrobenthic communities in the Southern North Sea. Estuar. Coast. Shelf Sci. **214**: 173–184. doi:10.1016/j.ecss.2018.09.012

Brown, K. M. 1992. Site specific constraints on shell selection behavior in the hermit crab, Clibanarius vittatus. Mar. Behav. Physiol. **21**: 239–254. doi:10.1080/10236249209378829

Bruno, J. F., J. J. Stachowicz, and M. D. Bertness. 2003. Inclusion of facilitation into ecological theory. Trends Ecol. Evol. **18**: 119–125. doi:10.1016/S0169-5347(02)00045-9

Brusca, R., R. Wetzer, and S. France. 1995. Cirolanidae (Crustacea: Isopoda: Flabellifera) of the Tropical Eastern Pacific. San Diego Int. Law J. **30**: 1–96.

Burdige, D. J. 2007. Preservation of Organic Matter in Marine Sediments: Controls, Mechanisms, and an Imbalance in Sediment Organic Carbon Budgets? Chem. Rev. **107**:

467–485. doi:10.1021/cr050347q

Burdon, D., S. Barnard, S. J. Boyes, and M. Elliott. 2018. Oil and gas infrastructure decommissioning in marine protected areas: System complexity, analysis and challenges. Mar. Pollut. Bull. **135**: 739–758. doi:10.1016/j.marpolbul.2018.07.077

Cadée, G. C. 1976. Sediment reworking by arenicola marina on tidal flats in the Dutch Wadden Sea. Netherlands J. Sea Res. **10**: 440–460. doi:10.1016/0077-7579(76)90020-X

Callender, W. R., E. N. Powell, G. M. Staff, and D. J. Davies. 1992. Distinguishing Autochthony, Parautochthony and Allochthony Using Taphofacies Analysis: Can Cold Seep Assemblages Be Discriminated from Assemblages of the Nearshore and Continental Shelf? Palaios **7**: 409–421. doi:10.2307/3514826

Cardinale, B., J. Duffy, A. Gonzalez, and others. 2012. Biodiversity loss and its impact on humanity. Nature **486**: 59–67. doi:10.1038/nature11148

Chandler, J., D. White, E. J. Techera, S. Gourvenec, and S. Draper. 2017. Engineering and legal considerations for decommissioning of offshore oil and gas infrastructure in Australia. Ocean Eng. **131**: 338–347. doi:10.1016/j.oceaneng.2016.12.030

Cheel, R. J. 2005. Bedforms and stratification under unidirectional flows, p. 129. *In* Introduction to Clastic Sedimentology.

Cheng, C. H., K. Soetaert, and B. W. Borsje. 2020. Sediment Characteristics over Asymmetrical Tidal Sand Waves in the Dutch North Sea. J. Mar. Sci. Eng. **8**: 1–16. doi:https://www.mdpi.com/2077-1312/8/6/409

Cheng, C. H., B. W. Borsje, O. Beauchard, S. O'Flynn, T. Ysebaert, and K. Soetaert. 2021. Small-scale macrobenthic community structure along asymmetrical sand waves in an underwater seascape. Mar. Ecol. **42**: e12657. doi:10.1111/maec.12657

Chessel, D., A.-B. Dufour, and J. Thioulouse. 2004. The ade4 package - I : One-table methods. R News **4**.

Clough, L., and G. Lopez. 1993. Potential carbon sources for the head-down deposit-feeding polychaete Heteromastus filiformis</I. J. Mar. Res. **51**: 595–616. doi:10.1357/0022240933224052

Coates, D., Y. Deschutter, M. Vincx, and J. Vanaverbeke. 2013. Enrichment and shifts in macrobenthic assemblages in an offshore wind farm area in the Belgian part of the North Sea. Mar. Environ. Res. **95**. doi:10.1016/j.marenvres.2013.12.008

Coleman, F., and S. Williams. 2002. Overexploiting marine ecosystem engineers: Potential consequences for biodiversity. Trends Ecol. Evol. **17**: 40–44. doi:10.1016/S0169-

5347(01)02330-8

Crain, C., and M. Bertness. 2005. Community impacts of a tussock sedge: Is ecosystem engineering important in benign habitats? Ecology **86**: 2695–2704. doi:10.1890/04-1517

Crain, C., and M. D. Bertness. 2006. Ecosystem Engineering across Environmental Gradients : Implications for Conservation and Management. **56**: 211–218.

Creutzberg, F., P. Wapenaar, G. Duineveld, and N. Lopez Lopez. 1984. Distribution and density of the benthic fauna in the southern North Sea in relation to bottom characteristics and hydrographic conditions. Rapp. Procès-Verbaux des Réunions du Cons. Perm. Int. pour l'Exploration la Mer **183**: 101–110.

Crouzy, B., F. Baerenbold, P. D'Odorico, and P. Perona. 2015. Ecomorphodynamic approaches to river anabranching patterns. Adv. Water Resour. **93**: 1–10. doi:10.1016/j.advwatres.2015.07.011

Curran, J. C. 2010. An investigation of bed armoring process and the formation of microclusters. *2nd Joint Federal Interagency Conference*. 1–12.

Cutler, E. B. 1994. The Sipuncula: Their Systematics, Biology, and Evolution, Comstock Pub. Associates.

Dalrymple, R. W. 1984. Morphology and internal structure of sandwaves in the Bay of Fundy. Sedimentology **31**: 365–382. doi:10.1111/j.1365-3091.1984.tb00865.x

Damen, J. M., T. A. G. P. Dijk, and S. J. M. H. Hulscher. 2018. Spatially Varying Environmental Properties Controlling Observed Sand Wave Morphology. J. Geophys. Res. Earth Surf. **123**: 262–280. doi:10.1002/2017JF004322

Damveld, J. H., K. J. Reijden, C. Cheng, and others. 2018. Video transects reveal that tidal sand waves affect the spatial distribution of benthic organisms and sand ripples. Geophys. Res. Lett. **0**. doi:10.1029/2018GL079858

Damveld, J. H., P. C. Roos, B. W. Borsje, and S. J. M. H. Hulscher. 2019. Modelling the two-way coupling of tidal sand waves and benthic organisms: A linear stability approach. Environ. Fluid Mech. doi:10.1007/s10652-019-09673-1

Damveld, J., B. W. Borsje, P. Roos, and S. J. M. H. Hulscher. 2020a. Horizontal and vertical sediment sorting in tidal sand waves: modeling the finite-amplitude stage. J. Geophys. Res. **125**. doi:10.1029/2019JF005430

Damveld, J. H., B. W. Borsje, P. C. Roos, and S. J. M. H. Hulscher. 2020b. Biogeomorphology in the marine landscape: Modelling the feedbacks between patches of the polychaete worm Lanice conchilega and tidal sand waves. Earth Surf. Process. Landforms **45**: 2572–

2587. doi:10.1002/esp.4914

De Borger, E., J. Tiano, U. Braeckman, T. Ysebaert, and K. Soetaert. 2020. Biological and biogeochemical methods for estimating bioirrigation: a case study in the Oosterschelde estuary. Biogeosciences **17**: 1701–1715. doi:10.5194/bg-17-1701-2020

de Jong, M., A. Stolk, S. Jong, and others. 2014a. First Interim Report of the Working Group on the Effects of Extraction of Marine Sediments on the Marine Ecosystem,.

de Jong, M. F., M. J. Baptist, R. van Hal, I. J. de Boois, H. J. Lindeboom, and P. Hoekstra. 2014b. Impact on demersal fish of a large-scale and deep sand extraction site with ecosystem-based landscaped sandbars. Estuar. Coast. Shelf Sci. **146**: 83–94. doi:10.1016/j.ecss.2014.05.029

de Jong, M. F., M. J. Baptist, H. J. Lindeboom, and P. Hoekstra. 2015a. Short-term impact of deep sand extraction and ecosystem-based landscaping on macrozoobenthos and sediment characteristics. Mar. Pollut. Bull. **97**: 294–308. doi:10.1016/j.marpolbul.2015.06.002

de Jong, M. F., M. J. Baptist, H. J. Lindeboom, and P. Hoekstra. 2015b. Relationships between macrozoobenthos and habitat characteristics in an intensively used area of the Dutch coastal zone. ICES J. Mar. Sci. J. du Cons. **72**: 2409–2422. doi:10.1093/icesjms/fsv060

de Jong, M. F., B. W. Borsje, M. J. Baptist, J. T. van der Wal, H. J. Lindeboom, and P. Hoekstra. 2016. Ecosystem-based design rules for marine sand extraction sites. Ecol. Eng. **87**: 271–280. doi:/10.1016/j.ecoleng.2015.11.053

De Mesel, I., F. Kerckhof, A. Norro, B. Rumes, and S. Degraer. 2015. Succession and seasonal dynamics of the epifauna community on offshore wind farm foundations and their role as stepping stones for non-indigenous species. Hydrobiologia **756**. doi:10.1007/s10750-014-2157-1

de Vrees, L. 2019. Adaptive marine spatial planning in the Netherlands sector of the North Sea. Mar. Policy 103418. doi:10.1016/j.marpol.2019.01.007

Decho, A. W., and T. Gutierrez. 2017. Microbial Extracellular Polymeric Substances (EPSs) in Ocean Systems. Front. Microbiol. **8**: 922. doi:10.3389/fmicb.2017.00922

Degraer, S., J. Wittoeck, W. Appeltans, and others. 2006. The Macrobenthos Atlas of the Belgian Part of the North Sea,.

Degraer, S., R. Brabant, B. Rumes, and L. Vigin. 2019. Environmental Impacts of Offshore Wind Farms in the Belgian Part of the North Sea: Marking a Decade of Monitoring, Research and Innovation,.

Deltacommissie. 2008. Working Together with Water. A living land builds for its future.

Findings of the Deltacommissie 2008 [Samen werken met water. Een land dat leeft, bouwt aan zijn toekomst. Bevindingen van de Deltacommissie 2008], Hollandia Printing.

Denny, M. W., and C. A. Blanchette. 2000. Hydrodynamics, shell shape, behavior and survivorship in the owl limpet Lottia gigantea. J. Exp. Biol. **203**: 2623–2639.

Dey, S. 2003. Incipient Motion of Bivalve Shells on Sand Beds under Flowing Water. J. Eng. Mech. **129**: 232–240. doi:10.1061/(ASCE)0733-9399(2003)129:2(232)

Dietrich, W., J. Kirchner, H. Ikeda, and F. Iseya. 1989. Sediment Supply and Development of Coarse Surface Layer in Gravel Bedded Rivers. Nature **340**. doi:10.1038/340215a0

Dillon, R. T. 2000. The Ecology of Freshwater Molluscs, Cambridge University Press.

Dodd, N., P. Blondeaux, D. Calvete Manrique, A. Falqués, H. de Swart, S. Hulscher, G. Różyński, and G. Vittori. 2003. Understanding Coastal Morphodynamics Using Stability Methods. J. Coast. Res. **19**.

Dolan, M., T. Thorsnes, J. Leth, Z. Al-Hamdani, J. Guinan, and V. Van Lancker. 2012. Terrain characterization from bathymetry data at various resolutions in European waters - experiences and recommendations.

Dolédec, S. successions and spatial variables in freshwater environments. I. D. of a complete two-way layout by projection of variables[Rythmes saisonniers et composantes stationnelles en milieu aquatique. I. D. d'un plan d'observati, and D. Chessel. 1987. Seasonal successions and spatial variables in freshwater environments. I. Description of a complete two-way layout by projection of variables [Rythmes saisonniers et composantes stationnelles en milieu aquatique. I. Description d'un plan d'observation com. Acta Oecologica/Oecologia Gen. **8**: 403–426.

Duineveld, G. C. A., P. A. W. J. De Wilde, and A. Kok. 1990. A synopsis of the macrobenthic assemblages and benthic ETS activity in the Dutch sector of the North Sea. Netherlands J. Sea Res. **26**: 125–138. doi:10.1016/0077-7579(90)90062-L

Dunn, O. J. 1964. Multiple Comparisons Using Rank Sums. Technometrics **6**: 241–252. doi:10.2307/1266041

Earle, S. 2020. Sea-Floor Sediments.

Eigaard, O., F. Bastardie, N. Hintzen, and others. 2016. The footprint of bottom trawling in European waters: Distribution, intensity, and seabed integrity. ICES J. Mar. Sci. **74**. doi:10.1093/icesjms/fsw194

Elliott, S. A. M., L. Guérin, R. Pesch, and others. 2018. Integrating benthic habitat indicators: Working towards an ecosystem approach. Mar. Policy **90**: 88–94.

doi:10.1016/j.marpol.2018.01.003

Ellis, J., T. Maxwell, M. Schratzberger, and S. I. Rogers. 2011. The benthos and fish of offshore sandbank habitats in the southern North Sea. J. Mar. Biol. Assoc. United Kingdom **91**: 1319–1335. doi:10.1017/S0025315410001062

Emmerson, M. C., and D. Raffaelli. 2000. Detecting the effects of diversity on measures of ecosystem function: experimental design, null models and empirical observations. Oikos **91**: 195–203. doi:10.1034/j.1600-0706.2000.910119.x

Escobar, C. A., R. Mayerle, and D. Restrepo. 2019. Estimation of sediment grain sizes in a mesotidal area, Dithmarschen Bight, German North Sea. Mar. Geol. **417**: 106006. doi:10.1016/j.margeo.2019.106006

Eshel, G., G. Levy, U. Mingelgrin, and M. Singer. 2004. Critical Evaluation of the Use of Laser Diffraction for Particle-Size Distribution Analysis. Reprod. from Soil Sci. Soc. Am. Journal. Publ. by Soil Sci. Soc. Am. All copyrights Reserv. **68**. doi:10.2136/sssaj2004.0736

Fang, X., S. Mestdagh, T. Ysebaert, T. Moens, K. Soetaert, and C. Van Colen. 2019. Spatio-temporal variation in sediment ecosystem processes and roles of key biota in the Scheldt estuary. Estuar. Coast. Shelf Sci. **222**: 21–31. doi:10.1016/j.ecss.2019.04.001

Fogel, B. N., C. M. Crain, and M. D. Bertness. 2004. Community level engineering effects of Triglochin maritima (seaside arrowgrass) in a salt marsh in northern New England, USA. J. Ecol. **92**: 589–597. doi:10.1111/j.0022-0477.2004.00903.x

Forster, S., R. N. Glud, J. K. Gundersen, and M. Huettel. 1999. In situ Study of Bromide Tracer and Oxygen Flux in Coastal Sediments. Estuar. Coast. Shelf Sci. **49**: 813–827. doi:10.1006/ecss.1999.0557

Forster, S., A. Khalili, and J. Kitlar. 2003. Variation of nonlocal irrigation in a subtidal benthic community. J. Mar. Res. **61**: 335–357. doi:10.1357/002224003322201223

Franco, M., J. Vanaverbeke, D. Oevelen, K. Soetaert, M. Costa, M. Vincx, and T. Moens. 2010. Respiration partitioning in contrasting subtidal sediments: Seasonality and response to a spring phytoplankton deposition. Mar. Ecol. **31**: 276–290. doi:10.1111/j.1439-0485.2009.00319.x

Fredsøe, J., and R. Deigaard. 1992. Mechanics of Coastal Sediment Transport, World Scientific.

Friedrichs, M., G. Graf, and B. Springer. 2000. Skimming flow induced over a simulated polychaete tube lawn at low population densities. Mar. Ecol. Prog. Ser. **192**: 219–228. doi:10.3354/meps192219

Friedrichs, M., T. Leipe, F. Peine, and G. Graf. 2009. Impact of macrozoobenthic structures on near-bed sediment fluxes. J. Mar. Syst. **75**: 336–347. doi:10.1016/j.jmarsys.2006.12.006

Friend, P. L., C. H. Lucas, P. M. Holligan, and M. B. Collins. 2008. Microalgal mediation of ripple mobility. Geobiology **6**: 70–82. doi:10.1111/j.1472-4669.2007.00108.x

Gabas, N., N. Hiquily, and C. Laguérie. 1994. Response of Laser Diffraction Particle Sizer to Anisometric Particles. Part. Part. Syst. Charact. **11**: 121–126. doi:10.1002/ppsc.19940110203

Gee, J. H. R., and P. S. Giller. 1987. Organization of communities past and present., p. 1–576. *In* Journal of Tropical Ecology. Blackwell Scientific Publications.

Gee, K., and B. Burkhard. 2010. Cultural ecosystem services in the context of offshore wind farming: A case study from the west coast of Schleswig-Holstein. Ecol. Complex. **7**: 349–358. doi:10.1016/j.ecocom.2010.02.008

Gerbersdorf, S. U., R. Bittner, H. Lubarsky, W. Manz, and D. M. Paterson. 2008. Microbial assemblages as ecosystem engineers of sediment stability. J. Soils Sediments **9**: 640–652. doi:10.1007/s11368-009-0142-5

Gerino, M., G. Stora, F. Carcaillet, F. Gilbert, J.-C. Poggiale, F. Mermillod-Blondin, G. Desrosiers, and P. Vervier. 2003. Macro- invertebrate functional groups in freshwater and marine sediments: A common mechanistic classification. Vie Milieu **53**: 221–232.

Giblin, A., C. Hopkinson, and J. Tucker. 1997. Benthic Metabolism and Nutrient Cycling in Boston Harbor, Massachusetts. Estuaries **20**: 346–364. doi:10.2307/1352349

Glud, R. N., J. K. Gundersen, N. P. Revsbech, B. B. Jorgensen, and M. Huettel. 1995. Calibration and performance of the stirred flux chamber from the benthic lander Elinor. Deep Sea Res. Part I Oceanogr. Res. Pap. **42**: 1029–1042. doi:/10.1016/0967-0637(95)00023-Y

Glud, R. N., S. Forster, and M. Huettel. 1996. Influence of radial pressure gradients on solute exchange in stirred benthic chambers. Mar. Ecol. Prog. Ser. **141**: 303–311. doi:10.3354/meps141303

Glud, R. N. 2008. Oxygen dynamics of marine sediments. Mar. Biol. Res. **4**: 243–289. doi:10.1080/17451000801888726

Gonzalez-Ortiz, V., L. G. Egea, R. Jimemez-Ramos, F. Moreno-Marin, J. L. Perez-Llorens, T. J. Bouma, and F. G. Brun. 2014. Interactions between seagrass complexity, hydrodynamic flow and biomixing alter food availability for associated filter-feeding organisms. PLoS One **9**. doi:10.1371/journal.pone.0104949

Gornitz, V. 2008. Encyclopedia of Paleoclimatology and Ancient Environments,.

Graf, G. 1992. Benthic-pelagic coupling: a benthic view, p. 149–190. *In* Oceanography and Marine Biology: An Annual Review.

Grant, W. D., L. F. Boyer, and L. . Sandford. 1982. The effect of bioturbation on the initiation of motion of intertidal sands. J. Mar. Res. **40**: 659–677. doi:10.1016/0077-7579(94)90028-0

Grant, W. D., and O. S. Madsen. 1986. The Continental-Shelf Bottom Boundary Layer. Annu. Rev. Fluid Mech. **18**: 265–305. doi:10.1146/annurev.fl.18.010186.001405

Grant, J., C. W. Emerson, and S. E. Shumway. 1993. Orientation, passive transport, and sediment erosion features of the sea scallop Placopecten magellanicus in the benthic boundary layer. Can. J. Zool. **71**: 953–959. doi:10.1139/z93-125

Grassle, J., and J. F. Grassle. 1976. Sibling species in the marine pollution indicator Capitella (polychaeta). Science **192**: 567–569. doi:10.1126/science.1257794

Gray, J. S. 1997. Gradients of marine biodiversity, p. 18–34. *In* Marine Biodiversity: Patterns and Processes. Cambridge University Press.

Gray, J., and M. Elliott. 2009. Ecology of Marine Sediments: From Science to Management,.

Gregr, E. J., and K. M. Bodtker. 2007. Adaptive classification of marine ecosystems: Identifying biologically meaningful regions in the marine environment. Deep Sea Res. Part I Oceanogr. Res. Pap. **54**: 385–402. doi:10.1016/j.dsr.2006.11.004

Gutiérrez, J., C. Jones, D. Strayer, and O. Iribarne. 2003. Mollusks as ecosystem engineers: The role of shell production in aquatic habitats. Oikos **101**: 79–90. doi:10.1034/j.1600-0706.2003.12322.x

Halpern, B. S., M. Frazier, J. Potapenko, and others. 2015. Spatial and temporal changes in cumulative human impacts on the world's ocean. Nat. Commun. **6**: 7615. doi:10.1038/ncomms8615

Hanes, D. M. 2012. The genesis of an inter-field marine sandwave and the associated anti-asymmetry migration of neighboring crests. Geophys. Res. Lett. **39**: 1–7. doi:10.1029/2011GL050641

Hatfield, R. G., M. T. Cioppa, and A. S. Trenhaile. 2010. Sediment sorting and beach erosion along a coastal foreland: Magnetic measurements in Point Pelee National Park, Ontario, Canada. Sediment. Geol. **231**: 63–73. doi:10.1016/j.sedgeo.2010.09.007

Hedges, J. I., and R. G. Keil. 1995. Sedimentary organic matter preservation: an assessment and speculative synthesis. Mar. Chem. **49**: 81–115. doi:10.1016/0304-4203(95)00008-F

Heip, C., D. Basford, J. A. Craeymeersch, and others. 1992. Trends in biomass, density and

diversity of north sea macrofauna. ICES J. Mar. Sci. **49**: 13–22. doi:10.1093/icesjms/49.1.13

Heip, C., and J. Craeymeersch. 1995. Benthic community structures in the North Sea. Helgoländer Meeresuntersuchungen **328**: 313–328. doi:10.1007/BF02368359

Heip, C. H. R., G. Duineveld, E. Flach, and others. 2001. The role of the benthic biota in sedimentary metabolism and sediment-water exchange processes in the Goban Spur area (NE Atlantic). Deep. Res. Part II Top. Stud. Oceanogr. **48**: 3223–3243. doi:10.1016/S0967-0645(01)00038-8

Hendriks, H. C. M., B. C. van Prooijen, S. G. J. Aarninkhof, and J. C. Winterwerp. 2020. How human activities affect the fine sediment distribution in the Dutch Coastal Zone seabed. Geomorphology **367**: 107314. doi:10.1016/j.geomorph.2020.107314

Herman, P. M. J., J. J. Middelburg, J. van de Koppel, and C. H. R. Heip. 1999. Ecology of Estuarine Macrobenthos,.

Herman, P., J. Middelburg, and C. Heip. 2001. Benthic community structure and sediment processes on an intertidal flat: Results from the ECOFLAT project. Cont. Shelf Res. **21**: 2055–2071. doi:10.1016/S0278-4343(01)00042-5

Hijmans, R. J. 2017. raster: Geographic Data Analysis and Modeling. R package version 2.6-7.

Hinrichsen, D. 2010. Ocean and Planet in Decline.

Hooper, D. U., F. S. Chapin III, J. J. Ewel, and others. 2005. Effects of biodiversity on ecosystem functioning: A consensus of current knowledge. Ecol. Monogr. **75**: 3–35. doi:10.1890/04-0922

Huettel, M., and G. Gust. 1992. Solute release mechanisms from confined sediment cores in stirred benthic chambers and flume flows. Mar. Ecol. Prog. Ser. **82**: 187–197. doi:10.3354/meps082187

Huettel, M., S. Forster, S. Kloser, and H. Fossing. 1996. Vertical Migration in the Sediment-Dwelling Sulfur Bacteria Thioploca spp. in Overcoming Diffusion Limitations. Appl. Environ. Microbiol. **62**: 1863–1872. doi:10.1128/AEM.62.6.1863-1872.1996

Huettel, M., and A. Rusch. 2000. Transport and degradation of phytoplankton in permeable sediment. Limnol. Oceanogr. **45**: 534–549. doi:10.4319/lo.2000.45.3.0534

Huettel, M., and I. T. Webster. 2001. Porewater flow in permeable sediments, p. 144–179. *In* Bernard P Boudreau and Bo Barker Jørgensen [eds.], The benthic boundary layer : transport processes and biogeochemistry. Oxford University Press.

Huettel, M., P. Berg, and J. E. Kostka. 2014. Benthic exchange and biogeochemical cycling in

permeable sediments. Ann. Rev. Mar. Sci. **6**: 23–51. doi:10.1146/annurev-marine-051413-012706

Hulscher, S. J. M. H. 1996. Tidal-induced large-scale regular bed form patterns in a three-dimensional shallow water model. J. Geophys. Res. Ocean. **101**: 20727–20744. doi:10.1029/96JC01662

Huntley, D. A., J. M. Huthnance, M. B. Collins, and others. 1993. Hydrodynamics and sediment dynamics of North Sea sand waves and sand banks. Philos. Trans. R. Soc. London. Ser. A Phys. Eng. Sci. **343**: 461–474. doi:10.1098/rsta.1993.0059

Ian.umces.edu/media-library. Integration and Application Network.

ICES. 2014. First Interim Report of the Working Group on the Effects of Extraction of Marine Sediments on the Marine Ecosystem (WGEXT). Rijswijk**,**: 1–67.

Idier, D., D. Astruc, and S. J. M. H. Hulscher. 2004. Influence of bed roughness on dune and megaripple generation. Geophys. Res. Lett. **31**: 1–5. doi:10.1029/2004GL019969

Ieno, E., M. Solan, P. Batty, and G. Pierce. 2006. How biodiversity affects ecosystem functioning: Roles of infaunal species richness, identity and density in the marine benthos. Mar. Ecol. Prog. Ser. **311**: 263–271. doi:10.3354/meps311263

IHO-IOC. 2014. General Bathymetric Chart of the Oceans. Available online: https://www.gebco.net/data_and_products/gridded_bathymetry_data/ (accessed on 08 February 2018). GEBCO Compil. Gr. GEBCO 2014 Grid. doi:10.5285/a29c5465-b138-234d-e053-6c86abc040b9

Janssen, F., P. Faerber, M. Huettel, V. Meyer, and U. Witte. 2005. Pore-water advection and solute fluxes in permeable marine sediments (II): Benthic respiration at three sandy sites with different permeabilities (German Bight, North Sea). Limnol. Oceanogr. **50**: 779–792. doi:10.4319/lo.2005.50.3.0768

Janssen, F., M. Bayani Cardenas, A. Sawyer, T. Dammrich, J. Krietsch, and D. de Beer. 2012. A comparative experimental and multiphysics computational fluid dynamics study of coupled surface-subsurface flow in bed forms. Water Resour. Res. **48**: 1–16. doi:10.1029/2012WR011982

Jenness, M. I., and G. C. A. Duineveld. 1985. Effects of tidal currents on chlorophyll a content of sandy sediments in the southern North Sea. Mar. Ecol. Prog. Ser. Oldend. **21**: 283–287. doi:10.3354/meps021283

Jennings, S., J. Pinnegar, N. Polunin, and K. Randall. 2001. Impacts of Trawling Disturbance on the Trophic Structure of Benthic Invertebrate Communities. Mar. Ecol. Prog. Ser. **213**:

127–142. doi:10.3354/meps213127

Jones, C. G., J. H. Lawton, and M. Shachak. 1994. Organisms as Ecosystem Engineers. Oikos **69**: 373–386. doi:10.2307/3545850

Jones, C. G., J. H. Lawton, and M. Shachak. 1997. Positive and Negative Effects of Organisms as Physical Ecosystem Engineers. America (NY). **78**: 1946–1957. doi:10.1890/0012-9658(1997)078[1946:PANEOO]2.0.CO;2

Jones, C. G. 2012. Ecosystem engineers and geomorphological signatures in landscapes. Geomorphology **157**–**158**: 75–87. doi:10.1016/j.geomorph.2011.04.039

Jongbloed, R. H., J. T. van der Wal, and H. J. Lindeboom. 2014. Identifying space for offshore wind energy in the North Sea. Consequences of scenario calculations for interactions with other marine uses. Energy Policy **68**: 320–333. doi:/10.1016/j.enpol.2014.01.042

Kaiser, M. J., J. S. Collie, S. J. Hall, S. Jennings, and I. R. Poiner. 2002. Modification of marine habitats by trawling activities: prognosis and solutions. Fish Fish. **3**: 114–136. doi:10.1046/j.1467-2979.2002.00079.x

Kannen, A., and B. Burkhard. 2009. Integrated Assessment of Coastal and Marine Changes Using the Example of Offshore Wind Farms: the Coastal Futures Approach. GAIA - Ecol. Perspect. Sci. Soc. **18**: 229–238. doi:10.14512/gaia.18.3.9

Katoh, K., H. Kume, K. Kuroki, and J. Hasegawa. 1998. The Development of Sand Waves and the Maintenance of Navigation Channels in the Bisanseto Sea, p. 3490–3502. *In* Coastal Engineering 1998.

Kaye, B. H., D. Alliet, L. Switzer, and C. Turbitt-Daoust. 1997. The Effect of Shape on Intermethod Correlation of Techniques for Characterizing the Size Distribution of Powder. Part 1: Correlating the Size Distribution Measured by Sieving, Image Analysis, and Diffractometer Methods. Part. Part. Syst. Charact. **14**: 219–224. doi:10.1002/ppsc.199700048

Kidwell, S. M. 1985. Palaeobiological and sedimentological implications of fossil concentrations. Nature **318**: 457–460. doi:10.1038/318457a0

Kidwell, S. M. 2013. Time-averaging and fidelity of modern death assemblages: building a taphonomic foundation for conservation palaeobiology. Palaeontology **56**: 487–522. doi:10.1111/pala.12042

Kleinhans, M. G. The Relation between Bedform Type, Vertical Sorting in Bedforms and Bedload Transport During Subsequent Discharge Waves in Large Sand Gravel Bed Rivers with Fixed Banks.

Kleinhans, M. G., F. Schuurman, W. Bakx, and H. Markies. 2009. Meandering channel dynamics in highly cohesive sediment on an intertidal mud flat in the Westerschelde estuary, the Netherlands. Geomorphology **105**: 261–276. doi:/10.1016/j.geomorph.2008.10.005

Kleyer, M., S. Dray, F. Bello, J. Lepš, R. J. Pakeman, B. Strauss, W. Thuiller, and S. Lavorel. 2012. Assessing species and community functional responses to environmental gradients: which multivariate methods? J. Veg. Sci. **23**: 805–821. doi:10.1111/j.1654-1103.2012.01402.x

Knaapen, M. A. F. 2005. Sandwave migration predictor based on shape information. J. Geophys. Res. Earth Surf. **110**. doi:10.1029/2004JF000195

Knowlton, N. 2003. Knowlton N. Sibling species in the sea. Ann Rev Ecol Syst, 24: 189-216. Annu. Rev. Ecol. Syst. **24**: 189–216. doi:10.1146/annurev.es.24.110193.001201

Koop, L., A. Amiri-Simkooei, K. J. van der Reijden, S. O'Flynn, M. Snellen, and D. G. Simons. 2019. Seafloor Classification in a Sand Wave Environment on the Dutch Continental Shelf Using Multibeam Echosounder Backscatter Data. Geosciences **9**: 1–24. doi:10.3390/geosciences9030142

Kösters, F., and C. Winter. 2014. Exploring German Bight coastal morphodynamics based on modelled bed shear stress. Geo-Marine Lett. **34**: 21–36. doi:10.1007/s00367-013-0346-y

Krasnow, L., and G. Taghon. 1997. Rate of Tube Building and Sediment Particle Size Selection during Tube Construction by the Tanaid Crustacean, Leptochelia dubia. Estuaries and Coasts **20**: 534–546. doi:10.2307/1352612

Krebs, C. J., and C. J. Krebs. 1985. Ecology: The Experimental Analysis of Distribution and Abundance, Harper & Row.

Kristensen, E. 2000. Organic matter diagenesis at the oxic/anoxic interface in coastal marine sediments, with emphasis on the role of burrowing animals. Hydrobiologia **426**: 1–24. doi:10.1023/A:1003980226194

Kristensen, E., G. Penha-Lopes, M. Delefosse, T. Valdemarsen, C. O. Quintana, and G. T. Banta. 2012. What is bioturbation? the need for a precise definition for fauna in aquatic sciences. Mar. Ecol. Prog. Ser. **446**: 285–302. doi:10.3354/meps09506

Kröncke, I., and C. Bergfeld. 2003. North Sea benthos: A Review. Senckenbergiana Maritima **33**: 205–268. doi:10.1007/BF03043049

Kröncke, I., H. Reiss, and J. W. Dippner. 2013. Effects of cold winters and regime shifts on macrofauna communities in shallow coastal regions. Estuar. Coast. Shelf Sci. **119**: 79–90.

doi:/10.1016/j.ecss.2012.12.024

Kruskal, W. H., and W. A. Wallis. 1952. Use of Ranks in One-Criterion Variance Analysis. J. Am. Stat. Assoc. **47**: 583–621. doi:10.2307/2280779

Künitzer, A., D. Basford, J. A. Craeymeersch, and others. 1992. The benthic infauna of the North Sea: species distribution and assemblages. ICES J. Mar. Sci. J. du Cons. **49**: 127–143. doi:10.1093/icesjms/49.2.127

Lancelot, C., Y. Spitz, N. Gypens, K. Ruddick, S. Becquevort, V. Rousseau, G. Lacroix, and G. Billen. 2005. Modelling diatom and Phaeocystis blooms and nutrient cycles in the Southern Bight of the North Sea: The MIRO model. Mar. Ecol. Prog. Ser. **289**: 63–78. doi:10.3354/meps289063

Langlois, V., and A. Valance. 2007. Initiation and evolution of current ripples on a flat sand bed under turbulent water flow. Eur. Phys. J. E **22**: 201–208. doi:10.1140/epje/e2007-00023-0

Lapôtre, M., M. Lamb, and B. McElroy. 2017. What sets the size of current ripples? Geology **45**: G38598.1. doi:10.1130/G38598.1

Lefebvre, A., A. J. Paarlberg, V. B. Ernstsen, and C. Winter. 2014. Flow separation and roughness lengths over large bedforms in a tidal environment: A numerical investigation. Cont. Shelf Res. **91**: 57–69. doi:10.1016/j.csr.2014.09.001

Lefebvre, A., A. J. Paarlberg, and C. Winter. 2016. Characterising natural bedform morphology and its influence on flow. Geo-Marine Lett. **36**: 379–393. doi:10.1007/s00367-016-0455-5

Lenth, R. V. 2016. Least-Squares Means: The R Package lsmeans. J. Stat. Softw. **69**: 1–33. doi:10.18637/jss.v069.i01

Levinton, J. 1970. The paleoecological significance of opportunistic species. Lethaia **3**: 69–78. doi:10.1111/j.1502-3931.1970.tb01264.x

Liao, H. R., and H. S. Yu. 2005. Morphology, hydrodynamics and sediment characteristics of the Changyun sand ridge offshore western Taiwan. Terr. Atmos. Ocean. Sci. **16**: 621–640. doi:10.3319/TAO.2005.16.3.621(T)

Lichtman, I. D., J. H. Baas, L. O. Amoudry, and others. 2018. Bedform migration in a mixed sand and cohesive clay intertidal environment and implications for bed material transport predictions. Geomorphology **315**: 17–32. doi:10.1016/j.geomorph.2018.04.016

Ligges, U., T. Short, P. Kienzle, and others. 2015. signal: Signal Processing.

Lindeboom, H., S. Degraer, J. Dannheim, A. B. Gill, and D. Wilhelmsson. 2015. Offshore wind park monitoring programmes, lessons learned and recommendations for the future. Hydrobiologia **756**. doi:10.1007/s10750-015-2267-4

Lobo, F. J., F. J. Hernández-Molina, L. Somoza, J. Rodero, A. Maldonado, and A. Barnolas. 2000. Patterns of bottom current flow deduced from dune asymmetries over the Gulf of Cadiz shelf (southwest Spain). Mar. Geol. **164**: 91–117. doi:/10.1016/S0025-3227(99)00132-2

Lohrer, A. A. M., S. S. F. Thrush, and M. Gibbs. 2004. Bioturbators enhance ecosystem function through complex biogeochemical interactions. Nature **431**: 1092–1095. doi:10.1038/nature03042

Maar, M., K. Bolding, J. Petersen, J. Hansen, and K. Timmermann. 2009. Local effects of blue mussels around turbine foundations in an ecosystem model of Nysted off-shore wind farm, Denmark. J. Sea Res. **62**: 159–174. doi:10.1016/j.seares.2009.01.008

Malarkey, J., J. H. Baas, J. A. Hope, and others. 2015. The pervasive role of biological cohesion in bedform development. Nat. Commun. **6**: 6257. doi:10.1038/ncomms7257

Manly, B. F. J. 1991. Randomization and Monte Carlo methods in Biology, Chapman and Hall.

Marinelli, R. L., and T. J. Williams. 2003. Evidence for density-dependent effects of infauna on sediment biogeochemistry and benthic–pelagic coupling in nearshore systems. Estuar. Coast. Shelf Sci. **57**: 179–192. doi:10.1016/S0272-7714(02)00342-6

Markert, E., I. Kröncke, and A. Kubicki. 2015. Small scale morphodynamics of shoreface-connected ridges and their impact on benthic macrofauna. J. Sea Res. **99**: 47–55. doi:10.1016/j.seares.2015.02.001

Martin, W. R., and G. T. Banta. 1992. The measurement of sediment irrigation rates: A comparison of the BR- tracer and 222Rn/226Ra disequilibrium techniques. J. Mar. Res. **50**: 125–154. doi:10.1357/002224092784797737

Martinius, A. W., and J. H. van den Berg. 2011. Atlas of sedimentary structures in estuarine and tidally-influenced river deposits of the Rhine-Meuse-Scheldt system : their application to the interpretation of analogous outcrop and subsurface depositional systems, EAGE.

Matisoff, G. 1982. Mathematical Models of Bioturbation, *In* Animal-Sediment Relations: The Biogenic Alteration of Sediments.

Mayer, L. M. 1993. Organic Matter at the Sediment-Water Interface BT - Organic Geochemistry: Principles and Applications, p. 171–184. *In* M.H. Engel and S.A. Macko [eds.]. Springer US.

McCarron, C., N. Howard, K. J. J. Van Landeghem, J. Baas, and L. Amoudry. 2016. Sediment transport and bedform morphodynamics in sand-gravel mixtures,.

McCave, I. N., R. J. Bryant, H. F. Cook, and C. A. Coughanowr. 1986. Evaluation of a laser-

diffraction-size analyzer for use with natural sediments. J. Sediment. Res. **56**: 561–564. doi:10.1306/212F89CC-2B24-11D7-8648000102C1865D

McDonald, J., and M. Kreitman. 1991. McDonald JH, Kreitman M... Adaptive evolution at the Adh locus in Drosophila. Nature 351: 652-654. Nature **351**: 652–654. doi:10.1038/351652a0

Meadows, P. S., A. Meadows, and J. M. H. Murray. 2012. Biological modifiers of marine benthic seascapes: Their role as ecosystem engineers. Geomorphology **157**–**158**: 31–48. doi:10.1016/j.geomorph.2011.07.007

Mehta, A. J., E. J. Hayter, W. R. Parker, R. B. Krone, and A. M. Teeter. 1989. Cohesive Sediment Transport. I: Process Description. J. Hydraul. Eng. **115**: 1076–1093. doi:10.1061/(ASCE)0733-9429(1989)115:8(1076)

Menge, B. A., and J. P. Sutherland. 1987. Community Regulation: Variation in Disturbance, Competition, and Predation in Relation to Environmental Stress and Recruitment. Am. Nat. **130**: 730–757.

Mestdagh, S., L. Bagaço, U. Braeckman, T. Ysebaert, B. De Smet, T. Moens, and C. Van Colen. 2018. Functional trait responses to sediment deposition reduce macrofauna-mediated ecosystem functioning in an estuarine mudflat. Biogeosciences **15**: 2587–2599. doi:10.5194/bg-15-2587-2018

Mestdagh, S., A. Amiri-Simkooei, K. J. van der Reijden, and others. 2020. Linking the morphology and ecology of subtidal soft-bottom marine benthic habitats: A novel multiscale approach. Estuar. Coast. Shelf Sci. **238**: 106687. doi:10.1016/j.ecss.2020.106687

Meysman, F. J. R., J. J. Middelburg, and C. H. R. Heip. 2006. Bioturbation: a fresh look at Darwin's last idea. Trends Ecol. Evol. **21**: 688–695. doi:10.1016/j.tree.2006.08.002

Miedema, S., and R. Ramsdell. 2011. Hydraulic transport of sand/shell mixtures in relation with the critical velocity. Terra Aqua **122**: 18–27.

Mietta, F., C. Chassagne, A. J. Manning, and J. C. Winterwerp. 2009. Influence of shear rate, organic matter content, pH and salinity on mud flocculation. Ocean Dyn. **59**: 751–763. doi:10.1007/s10236-009-0231-4

Miles, J., A. Thorpe, P. Russell, and G. Masselink. 2014. Observations of bedforms on a dissipative macrotidal beach. Ocean Dyn. **64**: 225–239. doi:10.1007/s10236-013-0677-2

Miller, A. I. 1988. Spatial resolution in subfossil molluscan remains: Implications for paleobiological analyses. Paleobiology **14**: 91–103. doi:10.1017/S0094837300011829

Mohr, H., S. Draper, L. Cheng, and D. White. 2016. Predicting the rate of scour beneath subsea pipelines in marine sediments under steady flow conditions. Coast. Eng. **110**: 111–126. doi:10.1016/j.coastaleng.2015.12.010

Montserrat, F., C. Van Colen, S. Degraer, T. Ysebaert, and P. Herman. 2008. Benthic community-mediated sediment dynamics. Mar. Ecol. Prog. Ser. **372**: 43–59. doi:10.3354/meps07769

Morelissen, R., S. J. M. H. Hulscher, M. A. F. Knaapen, A. A. Németh, and R. Bijker. 2003. Mathematical modelling of sand wave migration and the interaction with pipelines. Coast. Eng. **48**: 197–209. doi:10.1016/S0378-3839(03)00028-0

Murray, A. B., and E. R. Thieler. 2004. A new hypothesis and exploratory model for the formation of large-scale inner-shelf sediment sorting and "rippled scour depressions." Cont. Shelf Res. **24**: 295–315. doi:10.1016/j.csr.2003.11.001

Myers, A. C. 1977a. Sediment processing in a marine subtidal sandy bottom community. I. Physical aspects. J. Mar. Res. **35**: 609–632.

Myers, A. C. 1977b. Sediment processing in a marine subtidal sandy bottom community. II. biological consequences.

Nelson, T. R., G. Voulgaris, and P. Traykovski. 2013. Predicting wave-induced ripple equilibrium geometry. J. Geophys. Res. Ocean. **118**: 3202–3220. doi:10.1002/jgrc.20241

Németh, A. A., S. J. M. H. Hulscher, and H. J. de Vriend. 2002. Modelling sand wave migration in shallow shelf seas. Cont. Shelf Res. **22**: 2795–2806. doi:/10.1016/S0278-4343(02)00127-9

Neumann, A., J. Möbius, H. C. Hass, W. Puls, and J. Friedrich. 2016. Empirical model to estimate permeability of surface sediments in the German Bight (North Sea). J. Sea Res. **127**: 36–45. doi:10.1016/j.seares.2016.12.002

Newell, R. I. E. 1988. Ecological Changes in Chesapeake Bay: Are they the result of overharvesting the American Oyster, Crassostrea virginica? *Understanding the Estuary: Advances in Chesapeake Bay Research*. 1–11.

Nieuwenhuize, J., Y. E. M. Maas, and J. J. Middelburg. 1994. Rapid analysis of organic carbon and nitrogen in particulate materials. Mar. Chem. **45**: 217–224. doi:10.1016/0304-4203(94)90005-1

Nizzoli, D., G. Castaldelli, M. Bartoli, D. Welsh, P. Gomez, E. Fano, and P. Viaroli. 2002. Benthic Fluxes of Dissolved Inorganic Nitrogen in a Coastal Lagoon of the Northern Adriatic Sea: an Interpretation of Spatial Variability Based on Sediment Features and

Infauna Activity. Mar. Ecol. **23**. doi:10.1111/j.1439-0485.2002.tb00028.x

Nowell, A. R. M., and P. A. Jumars. 1984. Flow Environments of Aquatic Benthos. Annu. Rev. Ecol. Syst. **15**: 303–328. doi:10.1146/annurev.es.15.110184.001511

Olivera, A. M., and W. L. Wood. 1997. Hydrodynamics of bivalve shell entrainment and transport. J. Sediment. Res. **67**: 514–526. doi:10.1306/D42685B8-2B26-11D7-8648000102C1865D

Olsgard, F., M. Schaanning, S. Widdicombe, M. Kendall, and M. Austen. 2008. Effects of bottom trawling on ecosystem functioning. J. Exp. Mar. Bio. Ecol. **366**: 123–133. doi:10.1016/j.jembe.2008.07.036

Osorno, J.-L., L. Fernández-Casillas, and C. Rods4 guez-Juárez. 1998. Are hermit crabs looking for light and large shells? evidence from natural and field induced shell exchanges. J. Exp. Mar. Bio. Ecol. **222**: 163–173. doi:10.1016/S0022-0981(97)00155-X

Paarlberg, A. J., C. M. Dohmen-Janssen, S. J. M. H. Hulscher, and P. Termes. 2009. Modeling river dune evolution using a parameterization of flow separation. J. Geophys. Res. Earth Surf. **114**: 1–17. doi:10.1029/2007JF000910

Passchier, S., and M. G. Kleinhans. 2005. Observations of sand waves, megaripples, and hummocks in the Dutch coastal area and their relation to currents and combined flow conditions. J. Geophys. Res. Earth Surf. **110**: 1–15. doi:10.1029/2004JF000215

Paterson, D. M. 1989. Short-term changes in the erodibility of intertidal cohesive sediments related to the migratory behavior of epipelic diatoms. Limnol. Oceanogr. **34**: 223–234. doi:10.4319/lo.1989.34.1.0223

Paterson, A., T. Hume, and T. Healy. 2001. River Mouth Morphodynamics on a Mixed Sand-Gravel Coast. J. Coast. Res. 288–294.

Pearson, T. H., and R. Rosenberg. 1977. Macrobenthic succession in relation to organic enrichment and pollution of the marine environment. *Oceanography and Marine Biology*.

Pearson, T. H. 1978. Macrobenthic succession in relation to organic enrichment and pollution of the marine environment. Oceanogr. Mar. Biol. - An Annu. Rev. **16**: 229–311.

Pearson, T. H. 2001. Functional group ecology in soft-sediment marine benthos: The role of bioturbation, p. 233–267. *In* Oceanography and Marine Biology: An Annual Review.

Pianka, E. R. 2011. Evolutionary Ecology, Eric R. Pianka.

Piet, G. J., R. H. Jongbloed, A. M. Knights, J. E. Tamis, A. J. Paijmans, M. T. van der Sluis, P. de Vries, and L. A. Robinson. 2015. Evaluation of ecosystem-based marine management strategies based on risk assessment. Biol. Conserv. **186**: 158–166.

doi:10.1016/j.biocon.2015.03.011

Piet, G. J., A. M. Knights, R. H. Jongbloed, J. E. Tamis, P. de Vries, and L. A. Robinson. 2017. Ecological risk assessments to guide decision-making: Methodology matters. Environ. Sci. Policy **68**: 1–9. doi:10.1016/j.envsci.2016.11.009

Pilditch, C. A., C. W. Emerson, and J. Grant. 1997. Effect of scallop shells and sediment grain size on phytoplankton flux to the bed. Cont. Shelf Res. **17**: 1869–1885. doi:10.1016/S0278-4343(97)00050-2

Pope, N., J. Widdows, and M. Brinsley. 2006. Estimation of bed shear stress using the turbulent kinetic energy approach—A comparison of annular flume and field data. Cont. Shelf Res. **26**: 959–970. doi:10.1016/j.csr.2006.02.010

Powell, E. N., R. J. Stanton, D. Davies, and A. Logan. 1986. Effect of a large larval settlement and catastrophic mortality on the ecologic record of the community in the death assemblage. Estuar. Coast. Shelf Sci. **23**: 513–525. doi:10.1016/0272-7714(86)90007-7

Powell, E. N., and G. M. Staff. 1989. Macrobenthic death assemblages in modern marine environments: formation, interpretation, and application, *In* Reviews in Aquatic Sciences.

Powell, D. M. 1998. Patterns and processes of sediment sorting in gravel-bed rivers. Prog. Phys. Geogr. Earth Environ. **22**: 1–32. doi:10.1177/030913339802200101

Powell, E., K. Kuykendall, and P. Moreno. 2017. The Death Assemblage as a Marker for Habitat and an Indicator of Climate Change: Georges Bank, Surfclams and Ocean Quahogs. Cont. Shelf Res. **142**. doi:10.1016/j.csr.2017.05.008

Precht, E., and M. Huettel. 2003. Advective pore-water exchange driven by surface gravity waves and its ecological implications. Limnol. Oceanogr. **48**: 1674–1684. doi:10.4319/lo.2003.48.4.1674

Provoost, P., S. van Heuven, K. Soetaert, R. W. P. M. Laane, and J. Middelburg. 2010. Seasonal and long-term changes in pH in the Dutch coastal zone. Biogeosciences **7**. doi:10.5194/bg-7-3869-2010

Puig, P., M. Canals, J. B. Company, J. Martín, D. Amblas, G. Lastras, A. Palanques, and A. M. Calafat. 2012. Ploughing the deep sea floor. Nature **489**: 286–289. doi:10.1038/nature11410

Queiros, A., S. Birchenough, J. Bremner, and others. 2013. A bioturbation classification of European marine infaunal invertebrates. Ecol. Evol. **3**: 3958–3985. doi:10.1002/ece3.769

R Core Team. 2020. R: A language and environment for statistical computing. R Foundation for Statistical Computing,.

Rabaut, M., K. Guilini, G. Van Hoey, M. Vincx, and S. Degraer. 2007. A bio-engineered soft-bottom environment: The impact of Lanice conchilega on the benthic species-specific densities and community structure. Estuar. Coast. Shelf Sci. **75**: 525–536. doi:10.1016/j.ecss.2007.05.041

Rabaut, M., L. Van de Moortel, M. Vincx, and S. Degraer. 2010. Biogenic reefs as structuring factor in Pleuronectes platessa (Plaice) nursery. J. Sea Res. **64**: 102–106. doi:10.1016/j.seares.2009.10.009

Ramey-Balci, P., J. Grassle, J. Grassle, and R. Petrecca. 2009. Small-scale, patchy distributions of infauna in hydrodynamically mobile continental shelf sands: Do ripple crests and troughs support different communities? Cont. Shelf Res. **29**: 2222–2233. doi:10.1016/j.csr.2009.08.020

Ramírez-Ortega, D. B., L. A. Soto, A. Estradas-Romero, and F. E. Hernández-Sandoval. 2019. Photosynthetic Pigments Contained in Surface Sediments from the Hydrothermal System of Guaymas Basin, Gulf of California H. Felbeck [ed.]. J. Mar. Biol. **2019**: 1–8. doi:10.1155/2019/7484983

Ramsdell, R., and S. Miedema. 2010. Hydraulic transport of sand/shell mixtures. *WODCON XIX*. 1–21.

Reed, M. S., K. Hubacek, A. Bonn, and others. 2013. Anticipating and Managing Future Trade-offs and Complementarities between Ecosystem Services. Ecol. Soc. **18**. doi:10.5751/ES-04924-180105

Reed, M. S., K. Allen, A. Attlee, and others. 2017. A place-based approach to payments for ecosystem services. Glob. Environ. Chang. **43**: 92–106. doi:10.1016/j.gloenvcha.2016.12.009

Rees, H. L., J. D. Eggleton, E. Rachor, and others. 2007. The ICES North Sea Benthos Project 2000: aims, outcomes and recommendations. *Ices Cm 2007/a:21*. 1–22.

Regnier, P., P. Friedlingstein, P. Ciais, and others. 2013. Anthropogenic perturbation of the carbon fluxes from land to ocean. Nat. Geosci. **6**: 597–607. doi:10.1038/ngeo1830

Reiss, H., S. Degraer, G. C. A. Duineveld, and others. 2010. Spatial patterns of infauna, epifauna, and demersal fish communities in the North Sea. ICES J. Mar. Sci. J. du Cons. **67**: 278–293. doi:10.1093/icesjms/fsp253

Reubens, J. T., S. Degraer, and M. Vincx. 2014. The ecology of benthopelagic fishes at offshore wind farms: a synthesis of 4 years of research. Hydrobiologia **727**: 121–136. doi:10.1007/s10750-013-1793-1

Rhoads, D. C., and D. K. Young. 1970. The influence of deposit-feeding organisms on sediment stability and community trophic structure. J. Mar. Res. **28**: 150–178.

Rhoads, D. C. 1974. Organism-sediment relations on the muddy sea floor, Aberdeen University Press.

Rijks, D., M. de Jong, M. Baptist, and S. Aarninkhof. 2014. Utilizing the Full Potential of Dredging Works: Ecologically Enriched Extraction Sites. Terra aqua **136**: 5–15.

Ritchie, R. J. 2006. Consistent sets of spectrophotometric chlorophyll equations for acetone, methanol and ethanol solvents. Photosynth. Res. **89**: 27–41. doi:10.1007/s11120-006-9065-9

Rodil, I. F., P. Lucena-Moya, T. Tamelander, J. Norkko, and A. Norkko. 2020. Seasonal Variability in Benthic–Pelagic Coupling: Quantifying Organic Matter Inputs to the Seafloor and Benthic Macrofauna Using a Multi-Marker Approach. Front. Mar. Sci. **7**: 404. doi:10.3389/fmars.2020.00404

Roetert, T., T. Raaijmakers, and B. Borsje. 2017. Cable Route Optimization for Offshore Wind Farms in Morphodynamic Areas, p. 12. *In* The 27th International Ocean and Polar Engineering Conference. International Society of Offshore and Polar Engineers.

Roff, J., M. Taylor, and J. Laughren. 2003. Geophysical approaches to the classification, delineation and monitoring of marine habitats and their communities. Aquat. Conserv. Mar. Freshw. Ecosyst. **13**: 77–90. doi:10.1002/aqc.525

Romero, G., T. Gonçalves-Souza, C. Vieira, and J. Koricheva. 2014. Ecosystem engineering effects on species diversity across ecosystems: A Meta-analysis. Biol. Rev. Early View: 1–15. doi:10.1111/brv.12138

Roos, P. C., S. J. M. H. Hulscher, F. Van Der Meer, and I. G. M. Wientjes. 2007. Grain size sorting over offshore sandwaves : Observations and modelling. *5th IAHR Symposium on River, Coastal and Estuarine Morphodynamics*. 649–656.

Rossi, V., C. Lopez, J. Sudre, E. Hernández-García, and V. Garcon. 2008. Comparative study of mixing and biological activity of the Benguela and Canary upwelling systems. Geophys. Res. Lett. **35**: L11602. doi:10.1029/2008GL033610

Rouse, S., A. Kafas, R. Catarino, and H. Peter. 2018. Commercial fisheries interactions with oil and gas pipelines in the North Sea: considerations for decommissioning. ICES J. Mar. Sci. **75**: 279–286. doi:10.1093/icesjms/fsx121

Rumyantseva, A., S. Henson, A. Martin, A. F. Thompson, G. M. Damerell, J. Kaiser, and K. J. Heywood. 2019. Phytoplankton spring bloom initiation: The impact of atmospheric

forcing and light in the temperate North Atlantic Ocean. Prog. Oceanogr. **178**: 102202. doi:10.1016/j.pocean.2019.102202

Rusch, A., and M. Huettel. 2000. Advective particle transport into permeable sediments--evidence from experiments in an intertidal sandflat. Limnol. Oceanogr. **45**: 523–533. doi:10.4319/lo.2000.45.3.0525

Russell-Hunter, W. D. 1983. Overview: Planetary Distribution of and Ecological Constraints upon the Mollusca. Ecology 1–27. doi:10.1016/B978-0-12-751406-2.50008-8

Sanders, H. L. 1968. Marine Benthic Diversity: A Comparative Study. Am. Nat. **102**: 243–282.

Sandnes, J., T. Forbes, R. Hansen, and B. Sandnes. 2000. Influence of particle type and faunal activity on mixing of di(2-ethylhexyl)phthalate (DEHP) in natural sediments. Mar. Ecol. Prog. Ser. **197**: 151–167. doi:10.3354/meps197151

Santoro, V. C., E. Amore, L. Cavallaro, and M. De Lauro. 2004. Evolution of sand waves in the Messina Strait, Italy. Ocean Dyn. **54**: 392–398. doi:10.1007/s10236-003-0087-y

Santos, I. R., B. D. Eyre, and M. Huettel. 2012. The driving forces of porewater and groundwater flow in permeable coastal sediments: A review. Estuar. Coast. Shelf Sci. **98**: 1–15. doi:10.1016/j.ecss.2011.10.024

Sas, H., K. Didderen, T. van der Have, P. Kamermans, K. van den Wijngaard, and E. Reuchlin-Hugenholtz. 2019. Recommendations for flat oyster restoration in the North Sea.

Schall, J. J., and E. R. Pianka. 1978. Geographical Trends in Numbers of Species. Science (80-.). **201**: 679–686. doi:10.1126/science.201.4357.679

Schultze, M., and G. Nehls. 2017. Wadden Sea Quality Status Report Extraction and dredging.

Seibold, E., and W. Berger. 2017. Sources and Composition of Marine Sediments BT - The Sea Floor: An Introduction to Marine Geology, p. 45–61. *In* E. Seibold and W. Berger [eds.]. Springer International Publishing.

Serpetti, N., U. F. M. Witte, and M. R. Heath. 2016. Statistical Modeling of Variability in Sediment-Water Nutrient and Oxygen Fluxes. Front. Earth Sci. **4**: 1–17. doi:10.3389/feart.2016.00065

Serrano, O., P. Lavery, C. Duarte, G. Kendrick, A. Calafat, P. York, A. Steven, and P. Macreadie. 2016. Can mud (silt and clay) concentration be used to predict soil organic carbon content within seagrass ecosystems? Biogeosciences **13**: 4915–4926. doi:10.5194/bg-13-4915-2016

Shen, H. W., and J. Lu. 1983. Development and Prediction of Bed Armoring. J. Hydraul. Eng. **109**: 611–629. doi:10.1061/(ASCE)0733-9429(1983)109:4(611)

Shumway, S. W., and M. D. Bertness. 1994. Patch Size Effects on Marsh Plant Secondary Succession Mechanisms. Ecology **75**: 564–568. doi:10.2307/1939559

Slomp, C. P., S. J. Van der Gaast, and W. Van Raaphorst. 1996. Phosphorus binding by poorly crystalline iron oxides in North Sea sediments. Mar. Chem. **52**: 55–73. doi:10.1016/0304-4203(95)00078-X

Smyth, K., N. Christie, D. Burdon, J. P. Atkins, R. Barnes, and M. Elliott. 2015. Renewables-to-reefs? – Decommissioning options for the offshore wind power industry. Mar. Pollut. Bull. **90**: 247–258. doi:10.1016/j.marpolbul.2014.10.045

Snelder, T., K. Dey, and J. Leathwick. 2007. A Procedure for Making Optimal Selection of Input Variables for Multivariate Environmental Classifications. Conserv. Biol. **21**: 365–375. doi:10.1111/j.1523-1739.2006.00632.x

Snelgrove, P. V. R. 1998. The biodiversity of macrofaunal organisms in marine sediments. Biodivers. Conserv. **7**: 1123–1132. doi:10.1023/A:1008867313340

Soetaert, K., and J. J. Middelburg. 2009. Modeling eutrophication and oligotrophication of shallow-water marine systems: the importance of sediments under stratified and well-mixed conditions. Hydrobiologia **629**: 239–254. doi:10.1007/s10750-009-9777-x

Solan, M., B. Wigham, I. Hudson, R. Kennedy, C. Coulon, K. Norling, H. Nilsson, and R. Rosenberg. 2004. In situ quantification of bioturbation using time-lapse fluorescent sediment profile imaging (f-SPI), luminophore tracers and model simulation. Mar. Ecol. Prog. Ser. **271**: 1–12. doi:10.3354/meps271001

Soulsby, R. 1983. Chapter 5 The Bottom Boundary Layer of Shelf Seas, p. 189–266. *In* B.B.T.-E.O.S. Johns [ed.], Physical Oceanography of Coastal and Shelf Seas. Elsevier.

Soulsby, R. 1997. Dynamics of Marine Sands: A manual for Practical Applications, Thomas Telford Publishing.

Stephens, M. P., D. C. Kadko, C. R. Smith, and M. Latasa. 1997. Chlorophyll-a and pheopigments as tracers of labile organic carbon at the central equatorial Pacific seafloor. Geochim. Cosmochim. Acta **61**: 4605–4619. doi:10.1016/S0016-7037(97)00358-X

Stief, P. 2013. Stimulation of microbial nitrogen cycling in aquatic ecosystems by benthic macrofauna: mechanisms and environmental implications. Biogeosciences Discuss. **10**: 11785–11824. doi:10.5194/bgd-10-11785-2013

Stieglitz, T., P. Ridd, and P. Müller. 2000. Passive irrigation and functional morphology of crustacean burrows in a tropical mangrove swamp. Hydrobiologia **421**: 69–76. doi:10.1023/A:1003925502665

Stolk, A. 2000. Variation of sedimentary structures and grainsize over sandwaves. *Marine Sandwave Dynamics*. 23–24.

Stolk, A., and C. Dijkshoorn. 2009. Sand extraction Maasvlakte 2 Project: License, Environmental Impact Assessment and Monitoring. *European Marine Sand and Gravel Group - a wave of opportunities for the marine aggregates industry, EMSAGG Conference, 7-8 May 2009*. 7–8.

Stride, A. H., R. H. Belderson, N. Kenyon, and M. A. Johnson. 1982. Offshore tidal deposits: sand sheet and sand bank facies, p. 95–125. *In*.

Sugiyama, J., and K. Kobayashi. 2016. wvtool: Image Tools for Automated Wood Identification.

Svenson, C., V. B. Ernstsen, C. Winter, A. Bartholomä, and D. Hebbeln. 2009. Tide-driven Sediment Variations on a Large Compound Dune in the Jade Tidal Inlet Channel, Southeastern North Sea. J. Coast. Res. 361–365.

Szymczak-Żyła, M. 2016. Analysis of chloropigments in marine sediments using accelerated solvent extraction (ASE). Limnol. Oceanogr. Methods **14**: 477–489. doi:10.1002/lom3.10106

Terwindt, J. H. J. 1971. Sand waves in the southern bight of the North Sea. Mar. Geol. **10**: 51–67. doi:10.1016/0025-3227(71)90076-4

Thrush, S., J. Hewitt, M. Gibbs, C. Lundquist, and A. Norkko. 2006. Functional Role of Large Organisms in Intertidal Communities: Community Effects and Ecosystem Function. Ecosystems **9**: 1029–1040. doi:10.1007/s10021-005-0068-8

Tillin, H., J. Hiddink, S. Jennings, and M. Kaiser. 2006. Chronic bottom trawling alters the functional composition of benthic invertebrate communities on a sea basin scale. Mar. Ecol. Prog. Ser. **318**: 31–45. doi:10.3354/meps318031

Tilman, D. 1982. Resource competition and community structure.,.

Toussaint, E., E. De Borger, U. Braeckman, A. De Backer, K. Soetaert, and J. Vanaverbeke. 2021. Faunal and environmental drivers of carbon and nitrogen cycling along a permeability gradient in shallow North Sea sediments. Sci. Total Environ. **767**: 144994. doi:10.1016/j.scitotenv.2021.144994

Tuijnder, A. P., J. A. N. S. Ribberink, and S. J. M. H. Hulscher. 2009. An experimental study into the geometry of supply-limited dunes. Sedimentology **56**: 1713–1727. doi:10.1111/j.1365-3091.2009.01054.x

Urban-Malinga, B., T. Gheskiere, S. Degraer, S. Derycke, K. opaliński, and T. Moens. 2008.

Gradients in biodiversity and macroalgal wrack decomposition rate across a macrotidal, ultradissipative sandy beach. Mar. Biol. **155**. doi:10.1007/s00227-008-1009-9

van Bruggen, A. C., S. Wells, and T. C. M. Kemperman. 1995. Biodiversity and Conservation of the Mollusca: Proceedings of the Alan Solem Memorial Symposium on the Biodiversity and Conservation of the Mollusca at the Eleventh International Malacological Congress, Siena, Italy, 1992, Backhuys.

Van Colen, C., G. Meulepas, A. Backer, van D, M. Vincx, S. Degraer, and T. Ysebaert. 2010. Diversity, trait displacements and shifts in assemblage structure of tidal flat deposit feeders along a gradient of hydrodynamic stress. Mar. Ecol. Prog. Ser. **406**: 79–89. doi:10.3354/meps08529

Van Colen, C., F. Rossi, F. Montserrat, and others. 2012. Organism-Sediment Interactions Govern Post-Hypoxia Recovery of Ecosystem Functioning. PLoS One **7**: e49795. doi:10.1371/journal.pone.0049795

Van Colen, C., S. F. Thrush, M. Vincx, and T. Ysebaert. 2013. Conditional Responses of Benthic Communities to Interference from an Intertidal Bivalve. PLoS One **8**: e65861. doi:10.1371/journal.pone.0065861

van Dalfsen, J. A., K. Essink, H. T. Madsen, J. Birklund, J. Romero, and M. Manzanera. 2000. Differential response of macrozoobenthos to marine sand extraction in the North Sea and the Western Mediterranean. ICES J. Mar. Sci. J. du Cons. **57**: 1439–1445. doi:10.1006/jmsc.2000.0919

van Dalfsen, J. A. A., and K. Essink. 2001. Benthic Community Response to Sand Dredging and Shoreface Nourishment in Dutch Coastal Waters. Senckenbergiana Maritima **31**: 329–332. doi:10.1007/BF03043041

van den Berg, J. H., S. D. Nio, E. A. of Geoscientists, and E. Staff. 2010. Sedimentary Structures and Their Relation to Bedforms and Flow Conditions, EAGE Publications.

van Denderen, P. D., N. T. Hintzen, A. D. Rijnsdorp, P. Ruardij, and T. van Kooten. 2014. Habitat-Specific Effects of Fishing Disturbance on Benthic Species Richness in Marine Soft Sediments. Ecosystems **17**: 1216–1226. doi:10.1007/s10021-014-9789-x

van der Veen, H. H., S. J. M. H. Hulscher, and M. A. F. Knaapen. 2006. Grain size dependency in the occurrence of sand waves. Ocean Dyn. **56**: 228–234. doi:10.1007/s10236-005-0049-7

van der Wal, D., T. Ysebaert, and P. Herman. 2017. Response of intertidal benthic macrofauna to migrating megaripples and hydrodynamics. Mar. Ecol. Prog. Ser. **585**.

doi:10.3354/meps12374

van Dijk, T. A. G. P., and M. G. Kleinhans. 2005. Processes controlling the dynamics of compound sand waves in the North Sea, Netherlands. J. Geophys. Res. Earth Surf. **110**: 1–15. doi:10.1029/2004JF000173

van Dijk, T. A. G. P., R. C. Lindenbergh, and P. J. P. Egberts. 2008. Separating bathymetric data representing multiscale rhythmic bed forms: A geostatistical and spectral method compared. J. Geophys. Res. Earth Surf. **113**. doi:10.1029/2007JF000950

van Dijk, T. A. G. P., J. A. van Dalfsen, V. Van Lancker, R. A. van Overmeeren, S. van Heteren, and P. J. Doornenbal. 2012. Benthic Habitat Variations Over Tidal Ridges, North Sea, The Netherlands. Seafloor Geomorphol. as Benthic Habitat 241–249. doi:10.1016/B978-0-12-385140-6.00013-X

van Gerwen, W., B. W. Borsje, J. H. Damveld, and S. J. M. H. Hulscher. 2018. Modelling the effect of suspended load transport and tidal asymmetry on the equilibrium tidal sand wave height. Coast. Eng. **136**: 56–64. doi:/10.1016/j.coastaleng.2018.01.006

Van Lancker, V. R. M., and P. Jacobs. 2000. The dynamical behaviour of shallow-marine dunes. *International Workshop on Marine Sandwave Dynamics*. 213–220.

Van Lancker, V. R. M., G. Moerkerke, I. Du Four, E. Verfaillie, M. Rabaut, and S. Degraer. 2012. 14 - Fine-Scale Geomorphological Mapping of Sandbank Environments for the Prediction of Macrobenthic Occurrences, Belgian Part of the North Sea, p. 251–260. *In* Seafloor Geomorphology as Benthic Habitat: GeoHab Atlas of Seafloor Geomorphic Features and Benthic Habitats.

van Ledden, M., W. G. M. van Kesteren, and J. C. Winterwerp. 2004. A conceptual framework for the erosion behaviour of sand–mud mixtures. Cont. Shelf Res. **24**: 1–11. doi:10.1016/j.csr.2003.09.002

van Nugteren, P., P. Herman, L. Moodley, J. Middelburg, M. Vos, and C. Heip. 2009a. Spatial distribution of detrital resources determines the outcome of competition between bacteria and a facultative detritivorous worm. Limnol. Oceanogr. **54**: 1413–1419. doi:10.4319/lo.2009.54.5.1413

van Nugteren, P., L. Moodley, G.-J. Brummer, C. H. R. Heip, P. M. J. Herman, and J. J. Middelburg. 2009b. Seafloor ecosystem functioning: the importance of organic matter priming. Mar. Biol. **156**: 2277–2287. doi:10.1007/s00227-009-1255-5

van Nugteren, P., L. Moodley, G.-J. Brummer, C. Heip, P. Herman, and J. Middelburg. 2009c. Seafloor ecosystem functioning: The importance of organic matter priming. Mar. Biol.

156: 2277–2287. doi:10.1007/s00227-009-1255-5

Van Oyen, T., and P. Blondeaux. 2009a. Grain sorting effects on the formation of tidal sand waves. J. Fluid Mech. **629**: 311–342. doi:10.1017/S0022112009006387

Van Oyen, T., and P. Blondeaux. 2009b. Tidal sand wave formation: Influence of graded suspended sediment transport. J. Geophys. Res. Ocean. **114**: 1–18. doi:10.1029/2008JC005136

Van Oyen, T., H. E. de Swart, and P. Blondeaux. 2010. Bottom topography and roughness variations as triggering mechanisms to the formation of sorted bedforms. Geophys. Res. Lett. **37**: 1–5. doi:10.1029/2010GL043793

Van Oyen, T., H. de Swart, and P. Blondeaux. 2011. Formation of rhythmic sorted bed forms on the continental shelf: an idealised model. J. Fluid Mech. **684**: 475–508. doi:10.1017/jfm.2011.312

Van Oyen, T., P. Blondeaux, and D. Van den Eynde. 2013. Comparing field observations of sorting patterns along tidal sand waves with theoretical predictions. Mar. River Dune Dyn. 291–296. doi:10.1016/j.csr.2013.04.005

van Rijn, L. C. 1984. Sediment Transport, Part III: Bed forms and Alluvial Roughness. J. Hydraul. Eng. **110**: 1733–1754. doi:10.1061/(ASCE)0733-9429(1984)110:12(1733)

van Rijn, L. C. 1993. Principles of Sediment Transport in Rivers, Estuaries and Coastal Seas, Aqua Publications.

van Rijn, L. C., M. W. C. Nieuwjaar, T. van der Kaay, E. Nap, and A. van Kampen. 1993. Transport of Fine Sands by Currents and Waves. J. Waterw. Port, Coastal, Ocean Eng. **119**: 123–143. doi:10.1061/(ASCE)0733-950X(1993)119:2(123)

van Rijn, L. C. 2007. Manual Sediment Transport Measurements in Rivers, Estuaries and Coastal Seas, Aquapublications.

van Santen, R. B., H. E. de Swart, and T. A. G. P. van Dijk. 2011. Sensitivity of tidal sand wavelength to environmental parameters: A combined data analysis and modelling approach. Cont. Shelf Res. **31**: 966–978. doi:/10.1016/j.csr.2011.03.003

Vanni, M. 2002. Nutrient Cycling by Animals in Freshwater Ecosystems. Annu. Rev. Ecol. Syst **33**: 341–370. doi:10.1146/annurev.ecolsys.33.010802.150519

Venditti, J. G. 2013. 9.10 Bedforms in Sand-Bedded Rivers, p. 137–162. *In* J.F. Shroder [ed.], Treatise on Geomorphology. Academic Press.

Vericat, D., R. J. Batalla, and C. Garcia. 2006. Breakup and reestablishment of the armour layer in a large gravel-bed river below dams: The lower Ebro. Geomorphology **76**: 122–136.

doi:10.1016/j.geomorph.2005.10.005

Viles, H. A. 1988. Biogeomorphology, Blackwell.

Villnäs, A., J. Norkko, K. Lukkari, J. Hewitt, and A. Norkko. 2012. Consequences of Increasing Hypoxic Disturbance on Benthic Communities and Ecosystem Functioning. PLoS One **7**: e44920. doi:10.1371/journal.pone.0044920

Volkenborn, N., and K. Reise. 2006. Lugworm exclusion experiment: Responses by deposit feeding worms to biogenic habitat transformations. J. Exp. Mar. Bio. Ecol. **330**: 169–179. doi:10.1016/j.jembe.2005.12.025

Volkenborn, N., S. I. C. Hedtkamp, J. E. E. van Beusekom, and K. Reise. 2007a. Effects of bioturbation and bioirrigation by lugworms (Arenicola marina) on physical and chemical sediment properties and implications for intertidal habitat succession. Estuar. Coast. Shelf Sci. **74**: 331–343. doi:10.1016/j.ecss.2007.05.001

Volkenborn, N., L. Polerecky, S. I. C. Hedtkamp, J. E. E. van Beusekom, and D. de Beer. 2007b. Bioturbation and bioirrigation extend the open exchange regions in permeable sediments. Limnol. Oceanogr. **52**: 1898–1909. doi:10.4319/lo.2007.52.5.1898

Volkenborn, N., C. Meile, L. Polerecky, and others. 2012. Intermittent bioirrigation and oxygen dynamics in permeable sediments: An experimental and modeling study of three tellinid bivalves. J. Mar. Res. **70**: 794–823. doi:10.1357/002224012806770955

Wan Hussin, W. M. R., K. M. Cooper, C. R. S. B. Froján, E. C. Defew, and D. M. Paterson. 2012. Impacts of physical disturbance on the recovery of a macrofaunal community: A comparative analysis using traditional and novel approaches. Ecol. Indic. **12**: 37–45. doi:10.1016/j.ecolind.2011.03.016

Watling, L., and E. A. Norse. 1998. Disturbance of the Seabed by Mobile Fishing Gear: A Comparison to Forest Clearcutting. Conserv. Biol. **12**: 1180–1197.

Watling, L., R. H. Findlay, L. M. Mayer, and D. F. Schick. 2001. Impact of a scallop drag on the sediment chemistry, microbiota, and faunal assemblages of a shallow subtidal marine benthic community. J. Sea Res. **46**: 309–324. doi:10.1016/S1385-1101(01)00083-1

Whitlatch, R. 2019. Patterns of resource utilization and coexistence in marine intertidal deposit-feeding communities.

Widdows, J., and M. Brinsley. 2002. Impact of biotic and abiotic processes on sediment dynamics and the consequences to the structure and functioning of the intertidal zone. J. Sea Res. **48**: 143–156. doi:10.1016/S1385-1101(02)00148-X

Wilber, T. P. 1990. Influence of size, species and damage on shell selection by the hermit

crabPagurus longicarpus. Mar. Biol. **104**: 31–39. doi:10.1007/BF01313154

Wilcock, P., and B. Detemple. 2005. Persistence of Armor Layers in Gravel-Bed Streams. Geophys. Res. Lett **32**. doi:10.1029/2004GL021772

Wilson, A. M., M. Huettel, and S. Klein. 2008. Grain size and depositional environment as predictors of permeability in coastal marine sands. Estuar. Coast. Shelf Sci. **80**: 193–199. doi:/10.1016/j.ecss.2008.06.011

Wilson, R. J., D. C. Speirs, A. Sabatino, and M. R. Heath. 2018. A synthetic map of the north-west European Shelf sedimentary environment for applications in marine science. Earth Syst. Sci. Data **10**: 109–130. doi:10.5194/essd-10-109-2018

Winterwerp, J. C., and W. G. M. van Kesteren. 2004. Introduction to the Physics of Cohesive Sediment Dynamics in the Marine Environment, Elsevier Science.

Witbaard, R., M. J. N. Bergman, E. van Weerlee, and G. C. A. Duineveld. 2016. An estimation of the effects of Ensis directus on the transport and burial of silt in the near-shore Dutch coastal zone of the North Sea. J. Sea Res. **127**: 95–104. doi:10.1016/j.seares.2016.12.001

Woulds, C., G. L. Cowie, L. A. Levin, and others. 2007. Oxygen as a control on sea floor biological communities and their roles in sedimentary carbon cycling. Limnol. Oceanogr. **52**: 1698–1709. doi:10.4319/lo.2007.52.4.1698

Woulds, C., S. Bouillon, G. L. Cowie, E. Drake, J. J. Middelburg, and U. Witte. 2016. Patterns of carbon processing at the seafloor: the role of faunal and microbial communities in moderating carbon flows. Biogeosciences **13**: 4343–4357. doi:10.5194/bg-13-4343-2016

Yalin, M. 1985. On the Determination of Ripple Geometry. J. Hydraul. Eng. **111**: 1148–1155. doi:10.1061/(ASCE)0733-9429(1985)111:8(1148)

Ybema, M. S., D. Gloe, and R. H. L. Lambers. 2009. OWEZ pelagic fish, progress report and progression after T1. IMARES Wageningen UR.

Zenetos, A. 1990. Discrimination of autochthonous vs. allochthonous assemblages in the Eden estuary, fife, Scotland, U.K. Estuar. Coast. Shelf Sci. **30**: 525–540. doi:10.1016/0272-7714(90)90071-X

Ziebis, W., S. Forster, M. Huettel, and B. B. Jorgensen. 1996. Complex burrows of the mud shrimp Callianassa truncata and their geochemical impact in the sea bed. Nature **382**: 619–622. doi:10.1038/382619a0

4TU. Centre for Research Data. Available online: https://data.4tu.nl/repository/uuid:0d7e016d-2182-46ea-bc19-cdfda5c20308 (accessed on 19 May 2020).

Abbreviations

ACC	Acceleration
ANOVA	Analysis of variance
BCA	Between-class analysis
BSS	Bottom shear stress
Chl *a*	Chlorophyll *a*
CUBE	Combined Uncertainty Bathymetric Estimator
D	Density
D_{10}	10% of particles with smaller diameters than this value
D_{50}	Median grain size
D_{90}	90% of particles with smaller diameters than this value
DP	Dynamic positioning
EPS	Extracellular polymeric substances
GNSS	Global Navigation Satellite System
MBES	Multibeam echo sounder
MWTL	Dutch long term monitoring of macrobenthos in the Dutch Continental Economical Zone of the North Sea
MU	Morphological unit
nMDS	Nonmetric multidimensional scaling
NSBS	North Sea Benthos Survey
OC	Organic carbon
OWF	Offshore wind farm
OM	Organic matter
PCA	Principal component analysis
RDA	Redundancy analysis
SD	Standard deviation
SWI	Sediment-water interface
TKE	Turbulent kinetic energy

Equations

Permeability:

$$k = \frac{K * \mu}{d * g} \tag{2.1}$$

where μ is water viscosity (Pa s) calculated from temperature and salinity, d is water density (g cm^{-3}), g is gravitational acceleration (9.81 m s^{-2}) and K is sediment hydraulic conductivity (cm s^{-1}).

Hydraulic conductivity:

$$K = \frac{V * L}{h * A * t}, \tag{2.2}$$

where V is water volume collected from the core (cm^3), L is sediment length (cm), h is the pressure difference between reservoir and outlet (pressure head; cm), A is the core cross-sectional area (cm^2) and t is the time to collect V (s).

Near-bed turbulent kinetic energy:

$$TKE = 1/2\left(\overline{u'_{b,x}}^2 + \overline{u'_{b,y}}^2 + \overline{u'_{b,z}}^2\right) \tag{4.1}$$

where $\overline{u'_{b,x}}$, $\overline{u'_{b,y}}$ and $\overline{u'_{b,z}}$ represent the root-mean-squares of the near-bed flow velocity fluctuations in the x, y and z directions, respectively.

Bottom shear stress:

$$BSS = 0.19\rho TKE \tag{4.2}$$

where ρ is the water density (1000 kg m^{-3} for freshwater).

BSS (calculated from the depth-averaged velocity):

$$BSS = \rho g u^2 / C^2 \tag{4.3}$$

where u is the depth-averaged velocity (m s^{-1}), g is the gravitational acceleration (9.81 m s^{-2}) and C is the Chézy roughness coefficient (m$^{0.5}$ s^{-1}).

Chézy roughness coefficient:

$$C = 18\log(12h/ks) \tag{4.4}$$

where *h* is the water depth (0.4 m in this flume experiment), and *ks* is the total bed roughness (m).

SUMMARY

Sandy environments form an enormous and important part of coastal shelf seas. Particularly in the shallow regions, the seabed is strongly shaped by the hydrodynamic forces. As a result, many of these systems are filled with different types of bedforms, which come in a variety of shapes and sizes, although some are more dynamic than others. One such bedform, which is very common in the Dutch part of the North Sea and other similar systems around the world, are tidal sand waves. These are mid-sized, sinusoidal features that typically range from 1-5 meters in height and 100 to 1000 meters in length. What makes them especially unique is their ability to migrate at moderately quick speeds, from several meters to tens of meters per year. Sand waves have been of much interest for physical and engineering applications, and investigations have been carried out to better-understand the sedimentary and hydrodynamic conditions shaping them. However, they also function as important habitats for a wide range of benthic organisms, yet have been far less studied in the ecological context.

Benthic macrofauna are invertebrate animals, typically larger than 1.0 mm in size, that reside on or within the many different types of sediments in the marine environments. They often comprise a diverse assemblage within a given benthic biological community, and are important for small-scale reworking of the sediment grains, pumping of fluids and particles into/out of the sediment, thereby enhancing many of the sedimentary biogeochemical processes. Both the "ecosystem engineering" roles and longevity of some of these species make them useful indicators for the overall health and functioning of a given environment. Thus, the aim of this PhD research work was to identify the two-way coupling between the benthic organisms and the sedimentary conditions within a sand wave field.

We conducted fieldwork at a sand wave location approximately 20 km to the west of the island Texel, the Netherlands (**Chapter 2**). Here, the sand waves are relatively asymmetrical in shape, with one side that is about twice as long as the other, steeper side. This phenomenon occurs here because, despite the tidal oscillation, the residual current is slightly stronger in the NNE direction. In addition to affecting the sand wave shape, this also has potential consequences for the sediment conditions and benthic community composition. By collecting sediment samples along four different sections of the sand waves, we were able to show that the sediment composition, permeability, organic matter and chl *a* content differed significantly depending on location.

During the same campaign at the sand wave field, we also collected benthic samples to quantify and characterize the benthic community composition (**Chapter 3**). Following the same approach of dividing the sand waves into four distinct sections, we were able to identify four unique habitats based on the significant differences observed in the community composition. The steep slope was the most species rich and contained the largest amount of animal biomass. The gentle slope had the lowest species richness, followed by the crest. These two habitats were more similar in terms of sediment characteristics and benthic assemblage, while the trough and steep slope were more similar in containing finer sediment, lower permeability and a higher number of species. Somewhat in contrast to the sediment characteristics, the benthic community exhibited more complexity, where the gentle slope-half of the crest displayed its own unique benthic community, while many of the samples from the steep slope-half of the crest shared commonality with the taxa found in the steep slope habitat.

During the sampling work, we also found significant quantities of dead shell valves and fragments in almost all of the samples. Although these biogenic materials are very common in the marine environment, their potential to influence the sediment dynamics is not well studied. Therefore, we believed it was important to determine the direct consequences of shell content within a sandy sediment mixture on the development of sand ripples, which are small bedforms that are very common in sandy environments and shown to be abundant on at least the crests of these sand waves. Using the NIOZ racetrack flume (**Chapter 4**), we measured the influence of shells on ripples. In one set of experiments, we quantified the differences in ripple dimensions and migration rate between fine sand and sand with increasing percentages of shells (from 2.5 up to 50% by volume) over relatively high flow rates for several hours. In a second set of experiments, the flow rate was gradually increased so that we could measure the onset of sand grain motion. As the shell content increased, both the ripple size and migration rate decreased. Under the initial flat bed condition, the flow alteration was more complex, with low percentages of shell drastically enhancing turbulence while higher percentages exhibited a shell-density-driven dampening effect.

The significance and potential implications of our findings are presented in the discussion (**Chapter 5**). We show how the position along asymmetrical sand waves largely determines both the sediment conditions and benthic community composition. As shown by previous field studies, we also know that the occurrence and regularity in the shape of sand ripples are highly contrasting between the crest and trough of sand waves. Given the large variability and high prevalence of shell material in our samples, these could pose potential consequences for sediment transport, the overall sediment characteristics and also the benthic community. In

addition, the differences found over a very small area demonstrates the importance of high-resolution, small-scale sampling for highly dynamic and contrasting environments as sand waves.

SAMENVATTING

Zandige omgevingen vormen een belangrijk deel van kust- en zeesystemen. Vooral in de ondiepe gebieden wordt de zeebodem sterk gevormd door hydrodynamische krachten, waardoor er sterke verschillen ontstaan in de ruwheidskenmerken van deze systemen. Bodemvormen komen in verschillende vormen en maten voor, hoewel ze niet allemaal even dynamisch zijn. Één van deze bodemvormen zijn zandgolven. Dit zijn vaak voorkomende bodemvormen in het Nederlandse deel van de Noordzee, maar ook in vergelijkbare systemen overal ter wereld. Zandgolven zijn middelgroot, typisch 1 tot 5 meter in hoogte en 100 tot 1000 meter in lengte. Maar wat bijzonder is aan deze systemen, is hun vermogen te migreren: meestal een paar meter tot tientallen meters per jaar. Dit is van belang voor zowel fysische als technische toepassingen, en veel onderzoek wordt verricht om beter te begrijpen hoe ze worden gevormd en beïnvloed door de sedimentaire en hydrodynamische processen. Alhoewel ze ook functioneren als belangrijke habitats voor een breed scala van organismen, wordt tot nu toe veel minder onderzoek verricht binnen een ecologische context.

Benthische macrofauna zijn ongewervelde dieren die ruim 1.0 millimeter groot zijn en in veel verschillende soorten sedimenten in mariene gebieden wonen. Deze dieren spelen een belangrijke rol in de kleinschalige verwerking van de sedimenten, en pompen vloeistoffen en deeltjes in of uit het sediment. Dit heeft gevolgen voor de biogeochemische processen in het sediment. Door hun rol als “ecosysteem ingenieurs” en hun relatief lange levensduur zijn ze nuttig als indicatoren voor de algehele gezondheid en het functioneren van een bepaalde omgeving. Het doel van dit doctoraatsonderzoek was dus om de tweeledige interactie tussen de benthische organismen en de sedimentaire omstandigheden in een zandgolfveld te identificeren.

We voerden veldwerk uit op een zandgolflocatie die ongeveer 20 km ten westen van het eiland Texel, Nederland, ligt (**Hoofdstuk 2**). In dit gebied zijn de zandgolven naar verhouding asymmetrisch van vorm, waarbij een kant ongeveer twee keer zo lang is als de andere, steilere kant. Dit verschijnsel komt voor omdat de reststroom iets sterker is in de NNO-richting ondanks de getijoscillatie. Dit heeft niet alleen gevolgen voor de zandgolfvorm maar heeft ook mogelijke gevolgen voor de sedimentcondities en de samenstelling van de benthische gemeenschap. Door sedimentmonsters te verzamelen langs vier verschillende secties van de zandgolven, konden we laten zien dat de sedimentsamenstelling, doorlaatbaarheid van het sediment, organische stof en chlorofyl *a* gehalte significant verschilden naargelang de locatie.

Tijdens het veldwerk op de zandgolflocatie verzamelden we ook benthische monsters om de benthische gemeenschap te kwantificeren en karakteriseren (**Hoofdstuk 3**). We identificeerden vier unieke habitats langs de zandgolven op basis van significante verschillen die werden waargenomen in de samenstelling van de gemeenschap. De steilste helling was de meest soortenrijke en bevatte de grootste hoeveelheid dierlijke biomassa. De minst steile helling had de laagste soortenrijkdom, gevolgd door de top (kam). Deze twee habitats leken meer op elkaar met betrekking tot sedimentkenmerken en benthische assemblage, terwijl de trog en de steile helling meer op elkaar leken omdat ze fijner sediment bevatten, een lagere doorlaatbaarheid en een groter aantal dierensoort hadden. In tegenstelling tot de sedimentkenmerken, vertoonde de benthische gemeenschap nabij de top meer complexiteit: de zachte helling-helft van de top had een eigen unieke benthische gemeenschap, die contrasteerde met die van de steile helling-helft van de top, die meer gemeen had met de taxa van de steile helling habitat.

Tijdens het bemonsteringswerk vonden we ook aanzienlijke hoeveelheden dode-schelphelften en -fragmenten in bijna alle monsters. Hoewel dit biogeen materiaal veel voorkomt in het mariene milieu, is hun potentieel om de sedimentdynamiek te beïnvloeden niet goed bestudeerd. Daarom waren we van mening dat het belangrijk was om de directe gevolgen te bepalen van het gehalte aan schelpen in een zandig sedimentmengsel op de ontwikkeling van zandribbels. Dit zijn kleine bodemvormen die veel voorkomen in zanderige omgevingen en waarvan is aangetoond dat ze overvloedig aanwezig zijn op ten minste de toppen van deze zandgolven. Met behulp van de NIOZ racebaangoot (**Hoofdstuk 4**) hebben we de invloed van schelpen op zandribbels onderzocht. In één reeks experimenten hebben we de verschillen in ribbelafmetingen en migratiesnelheid gemeten tussen kaal zand en zand verrijkt met toenemende percentages schelpen (van 2,5 tot 50% in volume) over relatief hoge stroomsnelheden gedurende enkele uren. In een tweede reeks experimenten werd de stroomsnelheid geleidelijk verhoogd, zodat we het begin van de beweging van zandkorrels konden meten. Naarmate de inhoud van de schelpen toenam, namen zowel de ribbelgrootte als de migratiesnelheid af. Bij een aanvankelijke vlakke bodem was de stroomverandering complex: bij lage percentages schelpen werd de turbulentie drastisch verhoogd bij toenemede stroomsnelheid, terwijl bij hogere percentages een verzwakkingseffect waargenomen werd.

De betekenis en mogelijke implicaties van onze bevindingen worden gepresenteerd in de discussie (**Hoofdstuk 5**). We laten zien hoe de positie langs asymmetrische zandgolven in grote mate bepalend is voor zowel de sedimentcondities als de samenstelling van de benthische gemeenschap. Zoals blijkt uit eerdere veldstudies, weten we ook dat het voorkomen en de

regelmaat in de vorm van zandribbels in hoge mate contrasteren tussen de top en de trog van zandgolven. Gezien de grote variabiliteit en hoge prevalentie van schelpen materiaal in onze monsters, zou dit mogelijke gevolgen kunnen hebben voor het sedimenttransport, de algehele sedimentkenmerken en ook voor de benthische gemeenschappen. Bovendien tonen de gevonden verschillen over een zeer klein gebied het belang aan van hoge resolutie en kleinschalige bemonstering voor zeer dynamische en contrasterende omgevingen zoals zandgolven.

ACKNOWLEDGMENTS

This PhD work would never have been possible without the help, support and advice from the many colleagues at NIOZ, and also my project collaborators from TUDelft and UTwente. I am grateful to have been able to work closely with my two colleagues, Erik and Johan, from the SANDBOX project. It has been a very enjoyable experience, and I have learned so much beyond my own area of expertise thanks largely to this collaboration. The campaigns, experiments and sample analyses would not have been possible without the support from Anton, Pieter, Peter, Yvonne, Jurian, Jeroen, Lennart, Daniel, Arne and Bert. The crew from the *RV – Pelagia* are also greatly acknowledged for their help with the seagoing research.

Also many thanks to my fellow American colleagues and friends, Justin and Greg, and also to Roeland. When I first moved to the Netherlands, it was a new environment and I did not know a single person. You guys were among the first to reach out to me and help me get settled. Living in De Keete for the first year or so brought about many interesting conversations and fun social activities. Special thanks also to Carlos, Rick, Laura and John for all the good times there, and to the many other colleagues that I have met over the years while working at the NIOZ.

I also want to really thank my friend and housemate, Jaco, for his immense support and encouragement. Although I try to maintain a healthy work/life balance, either one can really only be optimal when the other is as well. Having shared the apartment with you for almost 4 years has far exceeded any expectations I ever could have had. It has definitely made a very positive difference on my work, especially this past year with the lockdown. Thanks also to Esther, who moved in with us last March.

And a very special thanks to Rien and Inge for all of their support and for really being like a second family to me. Many thanks also to my friends, Jetze and Lisanne, for all their support and encouragement.

I would like to especially thank my co-promoters, Karline and Bas, for all their support throughout my PhD and really helping me to grow as a researcher. Karline, first and foremost, thank you for having given me the opportunity to work on the SANDBOX project. The road back to academia was long and arduous, and I had come very close to giving up. None of this would have been possible if you had not accepted me as one of your students. Bas, I also want to express my gratitude for all of your support and guidance, especially over the last couple of years. Given my background in the biological sciences, it was quite intimidating at times to venture into the

field of physical modeling and sediment dynamics. But with your help, I was able to overcome much of this.

Last but not least, I want to thank my mom, dad, sister and Ayla. To be living so far away has been especially difficult for them, but they have only expressed encouragement and confidence in my decision to live and work on the other side of the Atlantic. Finally, I would like to dedicate my entire PhD work to my grandfather, who had always hoped that I would one day be able to hold the title of "Dr.", and was a great inspiration for me.